REPORT DOCUMENTATION PAGE

Form Approved OMB No. 0704-0188

1. REPORT DATE *(DD-MM-YYYY)*	2. REPORT TYPE	3. DATES COVERED *(From – To)*
21-11-2002	Final Report	26 September 2001 - 26-Mar-02

4. TITLE AND SUBTITLE

Configuration Studies Supporting Design / Assessment of Sensor Craft

5a. CONTRACT NUMBER
F61775-01-WE087

5b. GRANT NUMBER

5c. PROGRAM ELEMENT NUMBER

6. AUTHOR(S)

Dr. Rajendar Kumar Nangia

5d. PROJECT NUMBER

5d. TASK NUMBER

5e. WORK UNIT NUMBER

7. PERFORMING ORGANIZATION NAME(S) AND ADDRESS(ES)
Nangia Aero Research Associates
West Point, 78-Queens Road
Bristol BS8 1QX
United Kingdom

8. PERFORMING ORGANIZATION REPORT NUMBER

N/A

9. SPONSORING/MONITORING AGENCY NAME(S) AND ADDRESS(ES)

EOARD
PSC 802 BOX 14
FPO 09499-0014

10. SPONSOR/MONITOR'S ACRONYM(S)

11. SPONSOR/MONITOR'S REPORT NUMBER(S)
SPC 01-4087

12. DISTRIBUTION/AVAILABILITY STATEMENT

Approved for public release; distribution is unlimited.

13. SUPPLEMENTARY NOTES

14. ABSTRACT This report results from a contract tasking Nangia Aero Research Associates as follows: The objective of the proposed work is to support on-going research at the Configuration Aerodynamics Branch (AFRL/VA) for design/assessment of a Sensor Craft configuration. The sensor aircraft is subject to challenging flight envelope (mission profile). The design at present is relatively "fluid". Box wings of different layouts arise. It has to cruise and loiter (very high L/D) for substantial periods and needs to carry a large percentage of its all-up-weight in fuel. The high aspect-ratio wings therefore need to be fairly thick. This implies emphasis on efficient aerodynamic and structural loading. A particularly critical aspect is the design of juncture and LE/TE design. Obviously there are many geometry parameters that arise implying substantial computation. It is proposed to commence work on this configuration. Suitable geometry parameters have been discussed with VA scientists. In the first phase with seed funding from EOARD, it is proposed to:
1. Set up the methodology of the design problem including flight envelope (Mach #, altitude & scale effects). Indicate important/critical design regimes.
2. Set up appropriate geometry with thick aerofoil sections including junctions.
3. Solve for design (under appropriate constraints) of the wings with mutual interference and allowance for juncture effects.
4. Two typical cases are to be done, showing the effects of main parametric variations.
5. Results will show the forces, moments and pressure distributions. Longitudinal behavior is the first interest. A restricted effort will be directed toward laterals also.
6. Compiling a report on the techniques used and results obtained with conclusions and suggestions for further work.
7. Draft report is to be sent for comments before issuing the final version, which is the main deliverable.
Parametric and optimization and further studies will be done when and if further funds are made available.

15. SUBJECT TERMS
EOARD, Sensor Technology, Aeronautics, Aircraft Design

16. SECURITY CLASSIFICATION OF:			17. LIMITATION OF ABSTRACT	18, NUMBER OF PAGES	19a. NAME OF RESPONSIBLE PERSON
a. REPORT	b. ABSTRACT	c. THIS PAGE	UL		Wayne A. Donaldson
UNCLAS	UNCLAS	UNCLAS			**19b. TELEPHONE NUMBER** *(Include area code)* +44 (0)20 7514 4299

Standard Form 298 (Rev. 8/98)
Prescribed by ANSI Std. Z39-18

CONFIGURATION & AERODYNAMIC DESIGN STUDIES OF JOINED-WING HIGH ASPECT RATIO SENSORCRAFT CONCEPT

Dr. R. K. Nangia

SUMMARY

Unmanned Sensor Craft air vehicles have been proposed as the air-breathing component of a future intelligence, surveillance, and reconnaissance (ISR) infrastructure to provide revolutionary capabilities. Such craft must take advantage of high aspect ratio (AR) wings for aerodynamic efficiency, and may also be required to enclose an antenna in a diamond aircraft planform. A large proportion of fuel must be carried, and "loiter" is at high altitudes for a few days in each flight. This implies that a wide C_l–altitude capability is required.

This report is concerned with configuration and design studies of high AR Sensor Craft. Implications of typical flight envelope on Wing Design aspects have been mentioned. Three different types of joined-wing layouts have been proposed. The configuration differences arise due to orientation of the outer wing tip, whether it is (conventional) aft-swept or forward-swept, and the dihedral of each wing.

Results are presented for wings with uncambered sections and then with designed camber and twist, trimmed for neutral stability. Layouts with forward-swept outer tips give spanwise loadings which are possibly more tolerant at off-design conditions over the wide flight envelope. Such configurations may have less tendency for wing-drop at high lift. Results of the inverse design application are shown here, and further work is proposed in several areas.

The Investigation which is the subject of this report was initiated by USAF - EOARD, 223/231 Old Marylebone Road, London, NW1 5TH, UK and was carried out under the terms of Contract SPC-01-4087

DISTRIBUTION LIST

1	Dr. W. Donaldson	USAF-EOARD, London NW1 5TH, UK
1	Mr. D. Multhopp	Chief, AFRL/VAAA Bldg 45
		2130 8th Street, WPAFB, Ohio, USA 45433-7542
1	Dr. C. P. Tilmann	Sr. Aerospace Engineer, AFRL/VAAA Bldg 45
		2130 8th Street, WPAFB, Ohio, USA 45433-7542
1	Dr. C. N. Raffoul	Propulsion, USAF-AFRL, WPAFB, Dayton, Ohio, USA
1	Mr. William Fields	Tech Area Lead, AFRL/VAAA Bldg 45
		2130 8th Street, WPAFB, Ohio, USA 45433-7542
1	Mr. Larry Leavitt	Head, Configuration Aerodynamics Branch
		NASA Langley Research Centre, Mail Stop 499
		Hampton, VA 23681-2199
1	Dr. James Luckring	Configuration Aerodynamics Branch
		NASA Langley Research Centre, Mail Stop 286
		Hampton, VA 23681-2199
1	Mr. John Perdzock	Head, SensorCraft Integrating Concept Office
		AFRL/VAC Bldg 45, 2130 8th Street, WPAFB, Ohio, USA 45433-7542
1	ILT Jennifer Schwartz	Portfolio Planner for UAVs, AFRL/XPA Bldg 15
		1864 4th Street, WPAFB, Ohio, USA 45433-6163
1	Dr. Michael OL	Research Engineer, AFRL/VAAA Bldg 45
		2130 8th Street, WPAFB, Ohio, USA 45433-7542
2	Dr. R.K. Nangia	Nangia Aero Research Associates
		WestPoint, 78-Queens Road, Clifton
		BRISTOL BS8 1QX

RESTRICTED DISTRIBUTION

ALL RECIPIENTS OF THIS REPORT ARE ADVISED THAT IT IS NOT TO BE COPIED IN PART OR IN WHOLE OR BE GIVEN FURTHER DISTRIBUTION, WITHOUT THE WRITTEN APPROVAL OF THE AUTHOR

RELATED FORMAL PUBLICATIONS

1. NANGIA, R.K., PALMER, M.E., TILMANN, C.P., "On Design and Optimisation of Unconventional High Aspect-Ratio "Joined-Wing" Type Aircraft", CEAS Aerospace Aerodynamics Research Conference (Royal Aeronautical Society), 10 - 12 June 2002, Cambridge, UK   (PAPER 85)

2. NANGIA, R.K., PALMER, M.E. & TILMANN, C.P., "On Design of Unconventional High Aspect Ratio "Joined-Wing" Type Aircraft", Paper 25R2, ICAS-2002, Toronto, Canada, September 2002.

3. NANGIA, R.K., PALMER, M.E. & TILMANN, C.P., "Unconventional High Aspect Ratio Joined-Wing Aircraft With Aft- & Forward- Swept Wing-Tips", Paper for 41st AIAA Aerospace Sciences Meeting & Exhibit, 6 - 9 January 2003, Reno NV, USA.

CONTRACTUAL DECLARATIONS

"The Contractor, Dr. R. K. Nangia, hereby delcares that, to the best of its knowledge and belief, the technical data delivered herewith under Contract No. F61775-01-WE087 is complete, accurate, and complies with all requirements of the contract.

DATE: __15 July 02__   Name and Title of Authorized Official: Dr. R. K. NANGIA"

"I certify that there were no subject inventions to declare as defined in FAR 52.227-13, during the performance of this contract."

DATE: __15 July 02__   Name and Title of Authorized Official: Dr R. K. NANGIA"

2

CONTENTS

SUMMARY

DISTRIBUTION LIST
RELATED FORMAL PUBLICATIONS

CONTENTS

1. INTRODUCTION, BACKGROUND, & WORK PROGRAMME

1.1. Background, Wider Context

Following the USAF-EOARD sponsored "Window-on-Science" (WOS) visit (Dec 2000) to the US Air Force Research Laboratory (AFRL) at Wright-Patterson Air Force Base, a programme of work to support the laboratory's programme was identified.

The AFRL (Ref.1) is actively engaged in fundamental and (more visible) applied issues that "spearhead" future advances in technology. Several projects are being undertaken, some in co-operation with industry. One of the primary AF organizations involved in such activities is the Aerodynamic Configuration Branch led by Mr. Dieter Multhopp. The projects include short-, mid- and longer- term "visions" e.g.

Current- & Short-term

- UAV, UCAV systems are being designed with the aim of suppressing enemy defences (not risking pilots). The designs are not necessarily highly manoeuvrable.

Current- & Mid-term

- The AWACS are to be replaced by ESR Sensor aircraft. Long endurance at high altitudes will require high t/c (15-25%) wings swept at 30 deg. The projected L/D is 30 for aspect ratio 20 to 30. This may imply joined wing configurations with appreciable laminar flow.
- Non-Planar Configurations, Winglets.
- Tilt-Wing, 4-Engined version.

Longer-term. Assessments Current. Priorities subject to Revision

- Further continued improvements to existing projects.
- UAV Wings, Oblique wings.
- Highly Manoeuvrable, Air-to-Air Vehicles.
- Supersonic Combat UAV's.
- SWARM of UAV's.
- Wing-in-Ground (WIG) Craft.
- Directed Energy Concepts.

1.2. A Brief Note on Our Work

The author has worked in Configuration Aerodynamics and related R & D for the best part of three decades. Clients include, British Aerospace, DERA / QinetiQ, Rolls Royce & AFRL. Projects include: Gnat (RAF advanced trainer), Concorde, Harrier, Euro-fighter, Advanced STOVL, Stealthy Wings, Advanced SST, Blended Wing Body (BWB) Aircraft, HSCT, UAV Wings, Oblique Wings and joined wings. More "fundamental" work relates to Inverse Design Methods, Vortex flows, high lift on 2-D & 3-D wings, and Store Separation (incl. STOVL jets).

Several special techniques have been developed for dealing with design & assessment of unusual advanced configurations. Propulsion issues have been addressed e.g. Intake Design, inclusion of ASTOVL Jets.

Aspects of work have been presented in contractor reports, at International (AIAA, RAeS, CEAS), NATO (AGARD & RTO) meetings and in Aerospace Journals (e.g. Refs.2-16).

1.3. Introduction to Present Work

The over-riding objective is to support the work programme of the Aerodynamic Configuration Branch in design / assessment of several types of configurations. Following communications with the laboratory, the first configuration of interest is the Sensor Craft with two joined wings (dihedral/anhedral "box-wing" with extensions in frontal view).

The Joined Wing concept conceived by Wolkovitch in the 1980's (Refs.17-18) features diamond-shapes in the plan and front views. Several aircraft applications were proposed (Fig.1.3.1). Some of the ideas were carried into experimental research aircraft and RPVs. These generally had a "mixed reception" but confirmed some of the advantages claimed over "equivalent" conventional aircraft in terms of aerodynamic (large AR feasibility) and structural efficiency. There are however some adverse problems also e.g. spanwise flows etc., lack of fuel volume, junction flows.

With advances in technologies related to controls, propulsion, and flow control, there is emphasis on re-visiting some of the older concepts and devising newer applications. Some have been publicized, Fig.1.3.2, e.g. Prandtl-Plane, Lockheed Fuel Tanker, Goldschmied (NASA), Sensor-craft etc. (Refs.19-20). Some shapes feature wings joined at the tips, others part way. The tip-wings can be appropriately aft- or forward-swept.

To replace the AWACS aircraft, a proposal is for remotely-controlled UAV sensor-craft. Such craft take advantage of high AR as well as enclosing an antenna in the aircraft diamond planform. Such aircraft carry a large proportion of fuel and are expected to "loiter" at high altitudes for a few days in each flight. This implies a wide C_L - altitude capability. The "diamond" shapes offer useful stealth "compliance". The aerofoil shapes need to be thick for fuel tankage. The cruise Mach number is expected to be "high" subsonic. The low-speed near-field performance is more akin to that of a (very) high aspect ratio wing glider. Take-off and landing phases are critical.

The design demands obviously "conflict" and this has led to a challenging work programme towards suitable layouts.

The sensor aircraft as envisaged in Fig.1.3.3, is subject to a challenging flight envelope (mission profile). At present, the design is relatively "fluid". "Box" wings of different layouts arise. The sensor craft has to cruise and loiter (very high L/D) for substantial periods and needs to carry a large percentage of its all-up-weight (AUW) in fuel. The high aspect-ratio wings (sweep about +/- 35°) therefore need to be fairly thick. This implies emphasis on efficient aerodynamic and structural loading. A particularly critical aspect is the design of the wing juncture and LE / TE design. Obviously there are many geometry parameters that arise implying substantial computations.

1.4. Present Work Programme

Suitable geometry parameters of the joined-wing configuration have been discussed with the AFRL together with some preliminary results.

In the first phase with "seed" funding by EOARD, the following aspects have been proposed (setting-up, Design & Solutions, Reporting & Presentation deliverables):

1. Set up the methodology of the design problem including flight envelope (Mach, altitude & Scale effects). Indicate important / Critical Design regimes.

2. Set up appropriate geometry with thick aerofoil sections including junctions.

3. Solve for design (under appropriate constraints) of the wings with mutual interference and allowance for juncture effects.

4. Two typical cases are to be done, showing the effects of the main parametric variations.

5. Results will show the forces, moments and pressure distributions. Longitudinal behaviour is of primary interest. A restricted effort will be directed toward laterals also.

6. Compiling a Report on the techniques used and results obtained with conclusions and suggestions for further work.

7. Draft report is to be sent for comments before issuing the final version, which is the main Deliverable.

8. Presentation on findings and future work possibilities at the AFRL laboratory during a WOS visit (this effectively constitutes another Deliverable).

In view of the relatively small financial scope of the present funding, more detailed and necessary parametric optimisation and other studies will be subject to further funds being sanctioned.

1.5. Layout of Report

The remainder of this report is in Sections 2 to 8 as follows:

Section 2 describes briefly the method and procedure for application.

Section 3 deals with the anticipated flight envelope and geometry aspects of configurations feasible (AT1 with aft-swept outer tips, and FT1 & FT2 both with forward-swept outer tips).

Section 4 refers to the calculations on configurations of the type AT1.

Section 5 refers to the calculations on configurations of the type FT1.

Section 6 refers to the calculations on configurations of the type FT2.

Section 7 describes the scope of further work and Development of Techniques.

Section 8 mentions Concluding Remarks.

2. COMPUTATIONAL & MODELLING ASPECTS, METHODS USED

On novel layouts, often, the experience is that the complexities "defy" an automated "hands-off" design process being used with confidence (unique solutions doubted). Therefore, we have chosen a process that allows a significant understanding to be gained with reasonable manual control over the design process (Refs.4-8).

Panel and Euler codes are being utilised that enable assessment of the aerodynamic performance over the range of low to high speeds. Most of the early work can be accomplished with a panel method. This is considered adequate for design work at this stage as flight Mach number is of the order of 0.6.

The Euler or Navier-Stokes solvers at subsonic speeds imply CPU hours rather than minutes for the panel codes. Their usage is appropriate when definitive configurations have been arrived at.

The camber and twist design, under force and moment constraints, is via previously validated attained suction design methods (Refs.2, 6, 7, 8, 9, 10, 11). In view of the very high aspect ratios involved, this process has been simplified and uses a restricted set of camber and twist modes.

An inverse design method using 3-D membrane analogy (Ref.3) can "tailor" and "fine-tune" aerofoil shapes for more optimum pressure distributions as required.

3. FLIGHT ENVELOPE, REYNOLDS NO. & CONFIGURATION CONSIDERATIONS

3.1. Flight Envelope, Reynolds Number Effects.

Previous work conducted at the AFRL indicated that the main sizing driver aspect is the integration of a "rhombic" antenna. This leads to very thick aerofoils. The payload and range performance demands lead to the design of thick aerofoils (t/c normal to the LE, between 15 and 21%) operating at high C_L values, Fig.3.1.1.

Mission Profile and Requirements are shown in Fig.3.1.2.

The AFRL studies indicated flight conditions as summarised in Fig.3.1.3.

Fig.3.1.4 gives an idea of Altitude and Weight relationships during a typical mission. The Reynolds number variation is also depicted. Fig.3.1.5 shows the Mach number and C_L relationships (C_L based on the front wing area, Section 3.2). Take-off is near C_L of 0.95 at Mach 0.2 (Re 1.414×10^6/ft), whilst landing is at C_L of 0.7 at Mach 0.15 (Re 1.06×10^6/ft). The Mach 0.6 cruise C_L varies from 1.58 to 0.88 (Re 0.44×10^6/ft to 0.345×10^6/ft).

It is interesting to reflect that on conventional aircraft the cruise C_L values are near 0.5 and take-off / landing C_L values near 0.8 to 1.2.

As the thick aerofoil sections give an appreciable range of C_L operation, we now have to focus on what C_L to chose for design. We need to have an idea of the "attained operation ranges (or bands)" for "attached" flow.

Fig.3.1.6 shows estimates of "attained operation ranges", for 15% t/c, 35° aft- and forward-swept wings, assuming a wing-span of 200 ft, chord of 6.640006 ft (dimensions are based on Section 3.2).

The curves corresponding to cruise conditions are more demanding. The aft-swept wing gives a bandwidth between 10.5° (root) - 8° (mid) - 10° (tip), whilst the forward swept wing gives a bandwidth of 6.5° (root) - 8.4° (mid) - 14° (tip).

Fig.3.1.7 refers to 17.2% t/c sections. The increasing t/c "expands" the bandwidths appreciably.

The minimum operating design α of about 4° would seem reasonable to start with at this stage. Once confidence is built up in the techniques, higher design angles can be attempted as well as maximising cruise L/D.

For maximising L/D, The lift-induced drag term C_{Di} must equal the profile drag term C_{D0} (comprising planar wing friction-drag and wave-drag (if any)). We will therefore eventually need to ascertain viscous effects.

It is interesting to reflect on how such a craft of very high AR could be tested in a wind tunnel. Because of large wing-span and small local chords, a large wind tunnel section would be ideally required. The popular tunnels range between 8 and 16 ft and these are thought to be rather on the small side for these configurations. Another associated problem is the stiffness of the model in aero-elastic sense. Bending and twisting modes are likely to be present.

So theoretical work needs to be pre-requisite before any large-scale experimental models are attempted.

3.2. Reference Configuration (AFRL) with Aft-Swept Tips - Config. AT1

Fig.3.2.1 shows the general arrangement of the sensor craft with 9° dihedral on the fore-wing and 9° anhedral on the aft-wing. The fuselage shape is essentially "notional" at this stage. Note the location of control surfaces. These are not supposed to interfere with the antenna.

Brief Reference Projected Planform Geometry

Fore-Wing of Aspect Ratio 30.12, Taper ratio 1.0, Sweep 35°
Wing Span 200 ft.
Fore-Wing Gross Area = 1320 ft^2
$c_{aero} = 6.640006$ ft = c_{av}

Aft-Wing of Aspect Ratio 21.97, Taper ratio 1.0, Sweep -35°
Wing Span 150 ft (joined to the fore-wing at between 140 & 150 ft)
Aft-Wing Gross Area = 957 ft^2
$c_{aero} = 6.640006$ ft = c_{av}

For ease of modelling we have chosen semi-span as 1.0 and the most leading-point (i.e. the forward wing apex) is chosen as the reference point for pitching moments and measurements. The reference area is the area of the forward wing. The reference length is the c_{av} (which is the same for both wings).

A basic super-critical aerofoil with t/c = 15% streamwise is the starting point. The camber and twist variations need to be designed.

A typical case with t/c 17.2% has also been run (Config. FT1 series).

Tilmann et al (Ref.21) mention the design of thick aerofoils and these can be incorporated, as and when required.

3.3. Two Possible Alternative Layouts with Forward-Swept Tips, Configs. FT1 & FT2

To improve handling and to reduce the "build-up" of loading on the swept tip, particularly during "off-design", the author has proposed (Fig.3.2.1) incorporation of a forward-swept wing tip. Two arrangements arise:

Config. FT1

The front wing has dihedral and the aft wing has anhedral. The wing-tip has dihedral, joined either to the fore-wing or the aft-wing with suitable "cranks".

Config. FT2

This variation implies that the front-wing will have anhedral and the aft-wing will have dihedral. This will ensure that the spar of the aft-wing will essentially remain "unbent". From a practical viewpoint, we will need to assess the fuselage and intake integration.

We now need to look at each configuration in turn and assess the relative merits of the various layouts.

For configurations that have a considerably large flight envelope, the off-design considerations become very important. It is desirable that, for a given pitch stability level, the tendency for flow separation does not increase with increasing angle of attack.

In each case, we need to assess angle of attack and camber effects prior to design.

The designs are essentially "first-cut" to demonstrate the major effects. Obviously the addition of fuselage and intakes will have localised effects and these can be introduced at a later stage. The pitching moment effects may be more significant.

9

4. BASIC PLANFORM EFFECTS, SPANWISE LOADINGS, STATIC STABILITY CONSIDERATIONS, Config. AT1, Mach 0.6

4.1. Basic Planform Effects, Uncambered Case

Fig.4.1.1 shows the general arrangement and a 3-D perspective. This has been modelled as 3 wing components: front, aft and the outer tip. Fig.4.1.2 shows the uncambered aerofoil shapes.

Fig.4.1.3 shows the C_L and C_m (about the most leading point) characteristics. Also shown are the contributions due to the 3 component wings. Note that the forward wing carries more lift than the second wing as might be expected from downwash considerations. The neutral point is located at $x/s = 0.552$ (as marked on Fig.4.1.1).

Fig.4.1.4 shows the spanwise lift loadings due to angle of attack, on the 3 wing components and their sum. The forward wing is more loaded towards the wing-juncture. At the centre-line, in spite of the downwash effects, the aft wing carries more loading and this is to be expected on a forward-swept wing. For minimum drag of the total configuration, a near elliptic lift loading is required, as shown. For this layout, however, relatively high loadings appear near the wing tip.

Fig.4.1.5(a-d) shows the chordwise loadings along various wing sections at $\alpha = 0°$, $3.25°$, $4.25°$ and $5.25°$. The corresponding C_L values are 0.0, 0.580, 0.759 and 0.936. Note the increase in LE loads as α increases.

At a given design condition (C_L and α), one could design camber and twist for minimum drag elliptic loading, but the tendency at off-design will be to depart from the elliptic loading. This will have implications on pitch stability.

4.2. Designed Case

The minimum C_L design point is related to landing. We have chosen $C_L = 0.768$ i.e. equivalent flat wing α of $4.25°$. We have tried to approach the elliptic loading for the design. In view of the thick sections and anticipated attached flow bandwidths, the operational range should extend to C_L of 1.5.

The twist and camber parameter variations along the wing-span (of the three wings) are shown in Fig.4.2.1. Note the characteristic twist and camber differences for the forward-swept and aft-swept wings. The front wing has less twist and camber, compared with the rear wing.

Fig.4.2.2 shows the aerofoil design shapes compared with the uncambered case.

Fig.4.2.3 shows the C_L - α and C_m - C_L characteristics. The CG for this design is located at $x/s = 0.546$. The CG position can be controlled easily, if required, by very small additional changes in twist. This is however not considered worthwhile in view of the preliminary nature of the study and considering that fuselage and intakes still need to incorporated.

Fig.4.2.4 shows the spanwise lift loadings due to angle of attack, on the 3 wing components and their sum. For minimum drag, a near elliptic lift loading is required, as shown. As angle of attack increases, the tips show higher loadings.

Fig.4.2.5(a-c) shows the chordwise loadings along various wing sections at $\alpha = 3.25°$, $4.25°$ and $5.25°$. The corresponding C_L values are 0.588, 0.768 and 0.946.

Note the upper surface flat-top nature of the chordwise pressure distributions (c.f. uncambered case, Fig.4.1.5). Geometry details near the wing juncture could do with some local improvements, if required.

4.3. Designed Case at Low Speed (Mach 0.15)

We have briefly examined the low speed capability of the designed layout of the previous section. LE and TE flaps remain to be included, however.

10

Fig.4.3.1 shows the C_L - α and C_m - C_L characteristics. The Mach 0.6 design has been evaluated at 0.15. The CG for this design at Mach 0.15 is located at x/s = 0.553, which is slightly aft of the comparable Mach 0.6 location at x/s = 0.546. The CG positions and resulting C_{m0} can be controlled easily, if required, by using LE / TE flaps at the lower speed condition. This work needs to be continued.

Fig.4.3.2 shows the spanwise lift loadings on the 3 wing components and their sum, arising due to angle of attack. For minimum drag, a near elliptic lift loading is required, as shown. As angle of attack increases, the tips show slightly higher loadings.

Fig.4.3.3(a-c) shows the chordwise loadings along various wing sections at α = 3.25°, 4.25° and 5.25°. The corresponding C_L values are 0.520, 0.677 and 0.833.

The process confirms the ability to pinpoint the main flow features and to tackle the design of high aspect ratio joined-wing layouts at high and low speeds.

5. BASIC PLANFORM EFFECTS, SPANWISE LOADINGS, STATIC STABILITY CONSIDERATIONS, Config. FT1, Mach 0.6

5.1. Basic Planform Effects, Uncambered Case, 15%t/c

Fig.5.1.1 shows the general arrangement and a 3-D perspective. This has been modelled as 3 wing components: front, aft and the outer tip. Fig.5.1.2 shows the uncambered aerofoil shapes.

Fig.5.1.3 shows the C_L and C_m (about the most leading point) characteristics. Also shown are the contributions due to the 3 component wings. As previously, the forward wing carries more lift than the second, due to downwash considerations. The neutral point is located at $x/s = 0.528$ (as marked on Fig.5.1.1).

Fig.5.1.4 shows the spanwise lift loadings due to angle of attack on the 3 wing components and their sum. The forward wing is more loaded towards the wing-juncture. At the centre-line, in spite of the downwash effects, the aft wing carries more loading and this is to be expected on a forward-swept wing. For minimum drag of the total configuration, a near elliptic lift loading is required, as shown. On this layout, relatively lower loadings appear near the wing tip and overall the lift loadings are near "elliptic" (except for a very small discontinuity near the juncture).

Fig.5.1.5(a-d) shows the chordwise loadings along various wing sections at $\alpha = 0°$, $3.25°$, $4.25°$ and $5.25°$. The corresponding C_L values are 0.0, 0.58, 0.759 & 0.936. Note the increase in LE loads as α increases.

For this configuration, the minimum drag, elliptic loading is more easily matched not only at a given design condition (C_L and α), but also over an "extended" off-design range.

5.2. Designed Case, 15%t/c

The minimum C_L design point is related to landing. We have chosen $C_L = 0.76$ i.e. equivalent flat wing α of $4.25°$. We have tried to keep the spanwise loadings similar to those for the planar case rather than perfectly elliptic. This implies neutral stability. In view of the thick sections and anticipated attached flow bandwidths, the operational range should extend to C_L of 1.5.

The twist and camber parameter variation along the wing-span is shown in Fig.5.2.1.

Fig.5.2.2 shows the aerofoil shapes compared with the uncambered case.

Fig.5.2.3 shows the C_L - α and C_m - C_L characteristics. The CG for this design is located at $x/s = 0.523$. The CG position can be controlled easily, if required, by very small additional changes in twist. This is, however, not considered worthwhile, in view of the preliminary nature of the study and considering that fuselage and intakes still need to incorporated.

Fig.5.2.4 shows the spanwise lift loadings due to angle of attack on the 3 wing components and their sum. For minimum drag, a near elliptic lift loading is required, as shown. As angle of attack increases, the tips show loadings lower than the elliptical shape. The small discontinuity at the wing juncture has been allowed to "persist".

Fig.5.2.5(a-c) shows the chordwise loadings along various wing sections at $\alpha = 3.25°$, $4.25°$ and $5.25°$. The corresponding C_L values are 0.582, 0.761 and 0.940.

Note the upper surface flat-top nature of the chordwise pressure distributions (c.f. uncambered case, Fig.5.1.5). Geometry details near the wing juncture could do with some local improvements, if required.

The process continues to confirm the ability to tackle the main flow features, design and detail design of high aspect ratio joined-wing layouts.

5.3. Basic Planform Effects, Uncambered Case, 17.2%t/c

Fig.5.3.1 shows the general arrangement and a 3-D perspective. This has been modelled as 3 wing components: front, aft and the outer tip. **Fig.5.3.2** shows the uncambered aerofoil shapes.

Fig.5.3.3 shows the C_L and C_m (about the most leading point) characteristics. Also shown are the contributions due to the 3 component wings. As previously, the forward wing carries more lift than the second, due to downwash considerations. The neutral point is located at $x/s = 0.528$ (as marked on **Fig.5.1.1**).

Fig.5.3.4 shows the spanwise lift loadings due to angle of attack on the 3 wing components and their sum. The forward wing is more loaded towards the wing-juncture. At the centre-line, in spite of the downwash effects, the aft wing carries more loading and this is to be expected on a forward-swept wing. For minimum drag of the total configuration, a near elliptic lift loading is required, as shown. On this layout, relatively lower loadings appear near the wing tip and overall the lift loadings are near "elliptic". The wing juncture loadings can be improved, if required.

Fig.5.3.5(a-d) shows the chordwise loadings along various wing sections at $\alpha = 0°$, $4°$, $5°$ and $6°$. The corresponding C_L values are 0.0, 0.719, 0.899 & 1.073. Note the increase in LE loads as α increases.

For this configuration, the minimum drag, elliptic loading is more easily matched, not only at a given design condition (C_L and α), but also over an "extended" off-design range.

5.4. Designed Case, 17.2%t/c

We have chosen $C_L = 0.711$ i.e. equivalent flat wing α of $4°$. We have tried to keep the loadings similar to those for the planar case rather than perfectly elliptic. This implies neutral stability. In view of the thick sections and anticipated attached flow bandwidths, the operational range should extend to C_L of 1.5+.

The twist and camber parameter variation along the wing-span is shown in **Fig.5.4.1**.

Fig.5.4.2 shows the aerofoil shapes compared with the uncambered case.

Fig.5.4.3 shows the C_L - α and C_m - C_L characteristics. The CG for this design is located at $x/s = 0.53$. The CG position can be easily controlled, if required, by very small additional changes in twist.

Fig.5.4.4 shows the spanwise lift loadings due to angle of attack on the 3 wing components and their sum. For minimum drag, a near elliptic lift loading is required, as shown. As angle of attack increases, the tips show loadings lower than the elliptical shape.

Fig.5.4.5(a-c) shows the chordwise loadings along various wing sections at $\alpha = 4°$, $5°$ and $6°$. The corresponding C_L values are 0.711, 0.891 and 1.071.

Note the upper surface flat-top nature of the chordwise pressure distributions (c.f. uncambered case, **Fig.5.1.5**). Geometry detail near the wing juncture could do with some local improvements, if required.

6. BASIC PLANFORM EFFECTS, SPANWISE LOADINGS, STATIC STABILITY CONSIDERATIONS, Config. FT2, Mach 0.6

6.1. Basic Planform Effects, Uncambered Case, 15% t/c

Fig.6.1.1 shows the general arrangement and a 3-D perspective. This has been modelled as 3 wing components: front, aft and the outer tip. Fig.6.1.2 shows the uncambered aerofoil shapes.

Fig.6.1.3 shows the C_L and C_m (about the most leading point) characteristics. Also shown are the contributions due to the 3 component wings. As previously, the forward wing carries more lift than the second, due to downwash considerations. The neutral point is located at $x/s = 0.529$ (as marked on Fig.6.1.1).

Fig.6.1.4 shows the spanwise lift loadings due to angle of attack on the 3 wing components and their sum. The forward wing is more loaded towards the wing-juncture. At the centre-line, in spite of the downwash effects, the aft wing carries more loading and this is to be expected on a forward-swept wing. For minimum drag of the total configuration, a near elliptic lift loading is required, as shown. For this layout, relatively lower loadings appear near the wing tip and, overall, the lift loadings are near "elliptic".

Fig.6.1.5(a-d) shows the chordwise loadings along various wing sections at $\alpha = 0°$, $3.25°$, $4.25°$ and $5.25°$. The corresponding C_L values are 0.0, 0.585, 0.764 and 0.942. Note the increase in LE loads as α increases.

For this configuration, the minimum drag, elliptic loading is more easily matched not only at a given design condition (C_L and α), but also over an "extended" off-design range.

6.2. Designed Case, 15% t/c

We have chosen $C_L = 0.754$ i.e. equivalent flat wing α of $4.25°$. We have tried to keep the loadings similar to those for the planar case rather than perfectly elliptic. This implies neutral stability. In view of the thick sections and anticipated attached flow bandwidths, the operational range should extend to C_L of 1.5.

The twist and camber parameter variation along the wing-span is shown in Fig.6.2.1. For simplicity, this has been taken as being the same as that for the case of Section 5.1.

Fig.6.2.2 shows the aerofoil shapes compared with the uncambered case.

Fig.6.2.3 shows the C_L - α and C_m - C_L characteristics. The CG for this design is located at $x/s = 0.572$. This represents a slightly statically unstable case. The CG position can be controlled easily, if required, by very small additional changes in twist.

Fig.6.2.4 shows the spanwise lift loadings due to angle of attack on the 3 wing components and their sum. For minimum drag, a near elliptic lift loading is required, as shown. As angle of attack increases, the tips show loadings approaching the elliptical shape.

Fig.6.2.5(a-c) shows the chordwise loadings along various wing sections at $\alpha = 3.25°$, $4.25°$ and $5.25°$. The corresponding C_L values are 0.575, 0.754, 0.932.

Note the upper surface flat-top nature of the chordwise pressure distributions (c.f. uncambered case, Fig.6.1.5). Geometry detail near the wing juncture could do with local improvements, if required.

The process continues to confirm the ability to pin-point the main flow features and to tackle the design of high aspect ratio joined-wing layouts.

7. FURTHER WORK

So far we have looked at Mach 0.6 design on three different types of sensor-craft, joined-wing layouts. Several interesting features have emerged. But there is more to do!

Further work is seen in a number of aspects and these are listed as follows:

- Lower speeds, field performance considerations.
- Parametric geometric studies.
- Appropriate method development.
- Different design C_L studies as required.
- Different aerofoils incorporation, if required, from the point of view of validation with CFD and transonic codes.
- Pitching moment, static margins control.
- LE / TE Flap, setting geometry restrictions, segmentation, effects separately and combined.
- Fuselage / Intake incorporation, additional effects on forces and moments.
- Inclusion of viscous effects, spanwise pressure gradients control.
- Drag prediction.
- Off-design performance.
- Include aero-elastics.
- Lateral and directional characteristics estimation.
- Creating full 3-D geometry model.
- Choice of type of configurations (AT or FT series).
- Experimental work (various aspects)

It is apparent that we are only at a starting post and a sizeable, interesting work programme remains!

8. CONCLUDING REMARKS

To replace the AWACS aircraft, a proposal is for remotely-controlled UAV sensor-craft. Such craft take advantage of high aspect ratio (AR) as well as enclosing an antenna in the aircraft diamond planform. The aircraft carry a large proportion of fuel and "loiter" at high altitudes for a few days in each flight, iimplying a wide C_L - altitude capability.

This report has been concerned with configuration and design studies of high AR sensor-craft. Implications of typical flight envelope on wing design aspects have been mentioned.

Three different types of joined-wing layouts have been proposed. The configuration differences arise due to the orientation of the outer wing tip whether it is conventionally aft-swept or forward-swept.

Results have been presented for wings with uncambered sections and then with designed camber and twisted sections.

Layouts with forward-swept outer tips give spanwise loadings which are possibly more tolerant at off-design conditions over the wide flight envelope. Such configurations may have less tendency for wing-drop at high lift. More loading occurs on the front-wing near the juncture, rather than at the outer wing tip.

Further work has been proposed in several areas.

ACKNOWLEDGEMENTS

REFERENCES

1. Discussions with AFRL, www.afrl.af.mil, & AFRL Brochure.

2. NANGIA, R.K., "The Design of "Manoeuvrable" Wings using Panel Methods, Attained Thrust & Euler Codes", ICAS-92.

3. NANGIA, R.K., "Development of an Inverse Design Technique using 3-D Membrane Analogy", Future Paper.

4. NANGIA, R.K. & GALPIN, S.A., "Towards Design of High-Lift Krueger Flap Systems with Mach & Reynolds No. Effects for Conventional & Laminar Flow Wings", CEAS European Forum, Bath, UK, 1995.

5. NANGIA, R.K. & GALPIN, S.A., "Prediction of LE & TE Devices Aerodynamics in High-Lift Configurations with Mach & Reynolds No. Effects", ICAS-96-2.7.6, 1996.

6. NANGIA, R.K. & GREENWELL, D.I., "Wing Design of an Oblique-Wing Combat Aircraft", ICAS-2000-1.6.1, 2000.

7. NANGIA, R.K., PALMER, M.E. & GREENWELL, D.I., "Design of Conventional and Unconventional Wings for UAV's", RTO - AVT Symposium, Turkey, October 2000.

8. NANGIA, R.K. & MILLER, A.S. "Vortex Flow Dilemmas & Control on Wing Planforms for High Speeds", RTO AVT Symposium, Loen, Norway, May 2001.

9. NANGIA, R.K., "Low Speed Performance Optimisation of Advanced Supersonic Civil Transport With Different Types of LE & TE Devices", 7th EAC'94, Toulouse, October 1994.

10. NANGIA, R.K., PALMER, M.E. & DOE, R.H., A study of Supersonic Aircraft with Thin Wings of Low Sweep, AIAA 2002-0709, Jan.2002.

11. NANGIA, R.K., Assessment of Low-Speed, High-Lift Capability of "Diamond" Planform wings with Mach & Reynolds Number Effects & Possible Improvements", RKN/Aero/Report/93-50, July 1993. (Sponsored by USAF-EOARD, SPC-93-4023).

12. NANGIA, R.K., PALMER, M.E. & MARTIN, P.G., "Flow Separation Prediction on Inlets with Mach & Reynolds Number Effects in Subsonic Flight", RAeS - IMechE Conference "Engine-Airframe integration", October 1996, Bristol, UK.

13. NANGIA, R.K., PALMER, M.E. & HODGES, J., "Modelling of 3-D Aircraft Inlets at "Zero" Speed (& Low Speeds with Cross-wind) & Flow Separation Prediction", RAeS - IMechE Conference "Verification of Design Methods by Test & Analysis", November 1998, London, UK.

14. NANGIA, R.K. & PALMER, M.E., "Negatively Scarfed Inlets for Acoustic Reduction, Aerodynamic Performance Assessment", AIAA 2000-0354, January 2000.

15. NANGIA, R.K. & PALMER, M.E., "Inlets with Negative Scarf for Acoustic Reduction, Aerodynamic Performance Assessment at Transonic Speeds", AIAA 2000-4409, August 2000.

16. NANGIA, R.K. & PALMER, M.E., "Application of Negative Scarf to Inlet Design for Acoustic Reduction, Aerodynamic Assessment At Subsonic & Transonic Speeds", ICAS 2000.

17. WOLKOVITCH, J., "The Joined Wing: An Overview", Jo. of. Air, pp 161-78, 1986.

18. WOLKOVITCH, J. & MONTALBO, R., "A Second Look at the Joined Wing", Book: "Unconventional Aircraft Concepts", Delft Uni. Press, 1987.

19. FREDIANI, A., "A New Large Aircraft with Box-Shaped Swept Wings", Symposium, Toulouse, 1999.

20. Several sources on www.

21. TILMANN, C.P. et al., "Development & Validation of Airfoils for Global Range Transports", AIAA-2000-4509, August 2000.

LIST OF SYMBOLS & ABBREVIATIONS

Only the general symbols are defined here. Other symbols are of local significance within the Section they arise in.

AR	Aspect Ratio
A	Axial Force along wing-plane x-axis (for definition of C_A)
b	$= 2\,s$, Wing span
BL	Boundary Layer
c	Local Wing Chord
c_{aero}	$= c$, Aerodynamic Wing Chord
c_{av}	$= c = c_{ref}$, Average Wing Chord
C_A	$= A/(q\,S)$, Axial Force Coefficient, measured in Wing plane
C_{AL}	= Local Axial Force Coefficient
C_D	$= D/(q\,S)$, Drag Coefficient
C_{D0}	Drag Coefficient at zero lift (see text)
C_{Di}	Lift Induced Drag
CG	Centre of Gravity
C_L	$= L/(q\,S)$, Lift Coefficient
C_{LL}	= Local Lift Coefficient
C_{Lmax}	Maximum Lift Coefficient
C_m	$= m/(q\,S\,c)$, Pitching Moment (Body Axis) defined about x_{CG} or Reference point
C_{m0}	C_m at zero lift
C_N	$= N/(q\,S)$, Normal Force Coefficient
C_p	Coefficient of Pressure
c_r	Wing Root chord
c_t	Wing Tip chord
D	Drag force
k	$= \Theta\,A\,C_{Di}/C_L^2$, Lift Induced Drag Factor
L	Lift Force
LE	Leading Edge
LEF	Leading Edge Flap
m	Pitching moment (Body Axis)
M	Mach Number
q	$= 0.5\,\rho\,V^2$, Dynamic Pressure
r	Aerofoil radius
r_n	Aerofoil radius normal to c
R	Reynolds Number, based on c_{av} (unless otherwise stated)
s	Wing semi-span
S	Wing Area, taken here as (front-wing + tip-wing) area
t	Aerofoil thickness
TE	Trailing Edge
TEF	Trailing Edge Flap
V	Airstream Velocity
x,y,z	Orthogonal Wing Co-ordinates, x along body axis
x_{ac}	Location of Aerodynamic Centre or Neutral point along x-axis.
	Note x_{ac} & x_{CG} coincide when static margin is zero.
x_{CG}	Location of Centre of Gravity or Moment reference Point along x-axis
x_{cp}	Location of Centre of pressure along x-axis
α	Angle of Attack, usually referred to the body axis
λ	Taper Ratio
Λ	LE Sweep Angle
ρ	Air Density
η	$= y/s$, Non-dimensional spanwise Distance

18
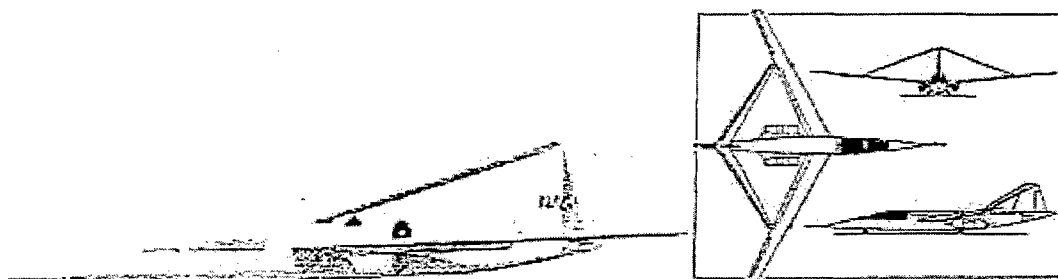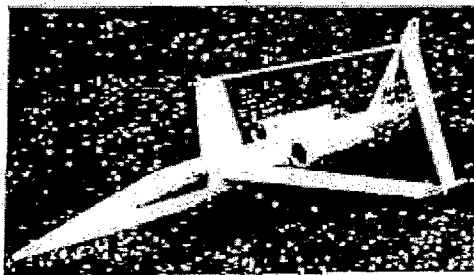
FIG. 1.3.1 JOINED-WING CRAFT (WOLKOVITCH)
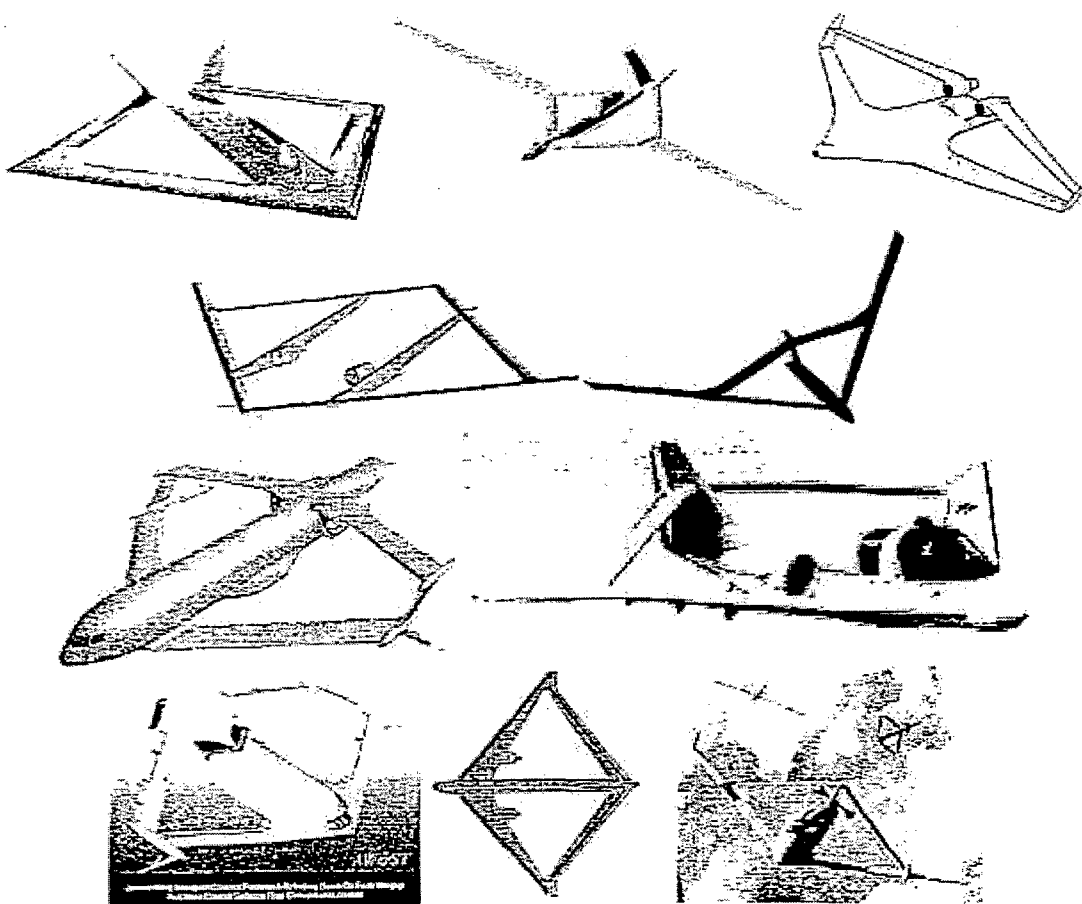
FIG. 1.3.2 SEVERAL RECENT JOINED-WING APPLICATIONS
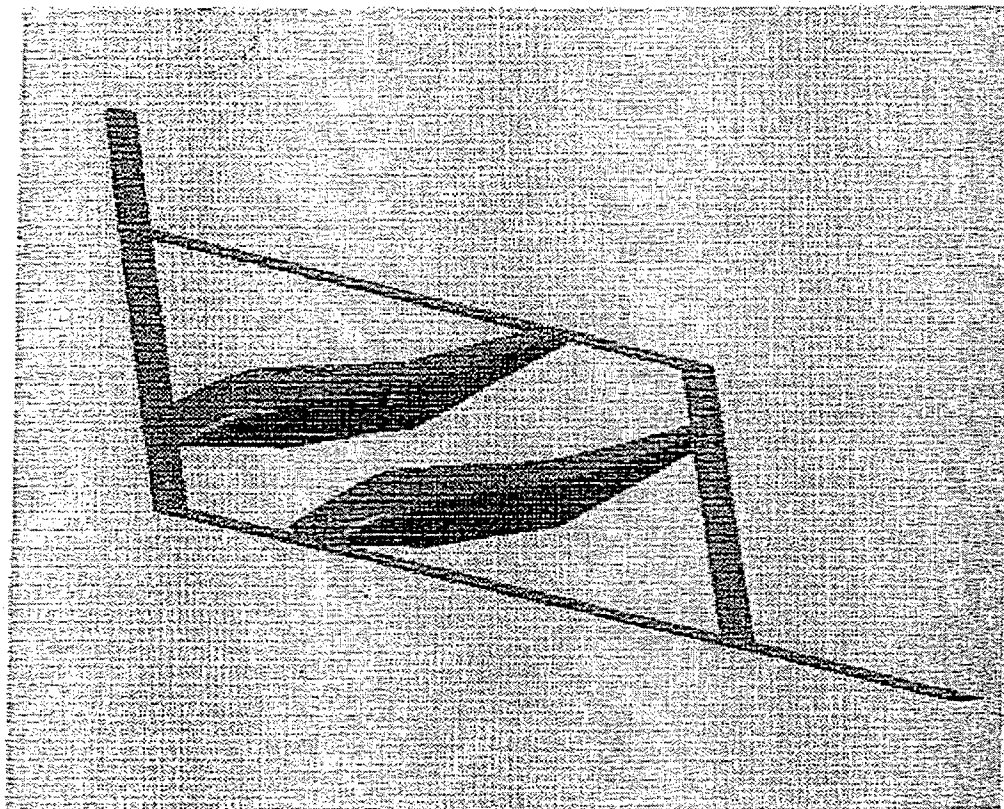
FIG. 1.3.3 SENSOR-CRAFT ENVISAGED FOR PRESENT WORK

Reference Configuration – Antenna Integration

Design Driver: Aero-Performance of Very Thick Airfoils

X – Band Antenna
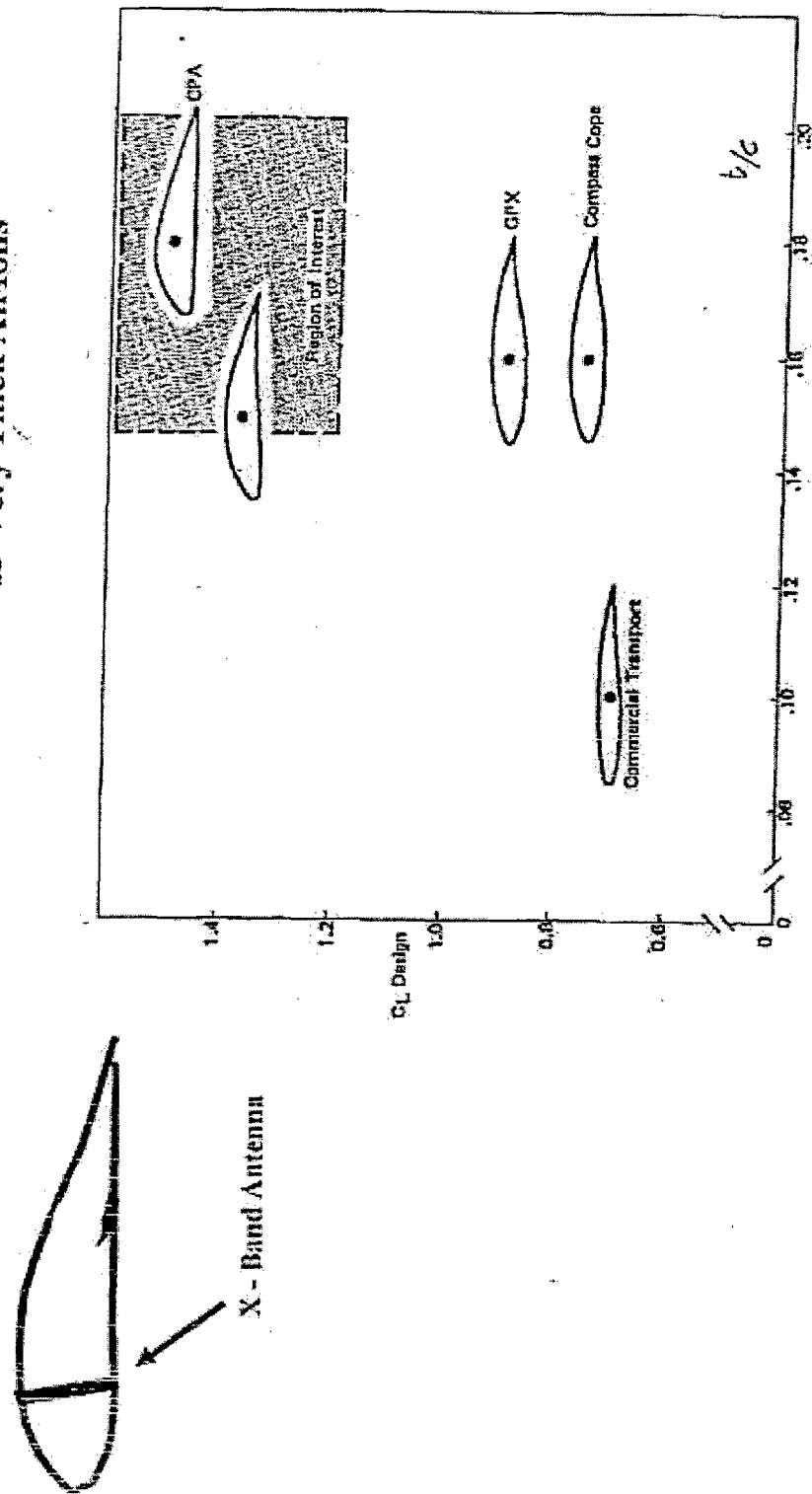
FIG. 3.1.1 THICK AEROFOIL REQUIREMENT (PREVIOUS AFRL WORK)

Mission profile and requirements

Loiter
40-80 hr 65 kft

Loiter
1 hr @ SL

3000 nm

3000 nm

W_{TO}
1 2 3

4

5

6

7

8

9

10
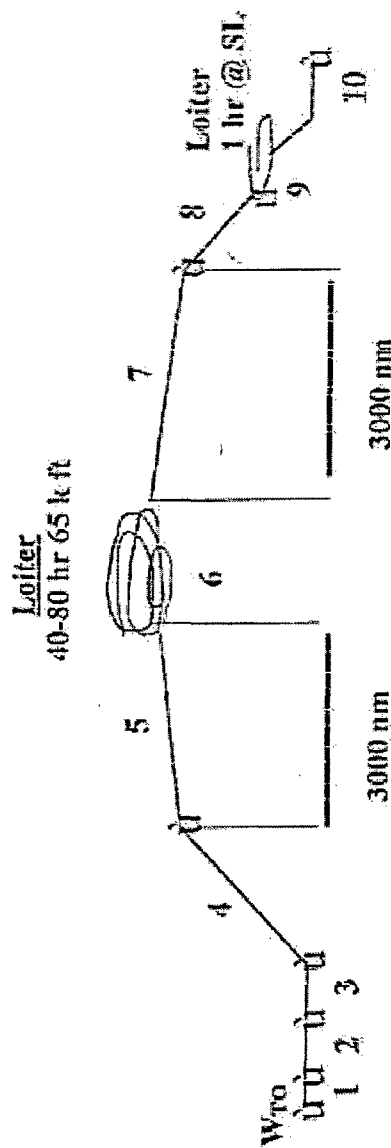
Mission Segments

1. Engine Start & Warm-up
2. Taxi
3. Takeoff
4. Climb & Accelerate to Cruise
5. Cruise out 3000
6. Loiter
7. Return Cruise
8. Descend
9. Loiter at Sea Level
10. Landing, Taxi, Shutdown

Cruise Radius: 3000 nm

Loiter: 65 Kft for 40 - 80 hr (at 3000 nm range)

Payload: 4000 lb **Field Length:** 5350 ft over 50 ft Obstacle (SLS)

Control: 20 kt cross-wind on takeoff and landing

W/S range of interest: 30 - 60

T/W range of interest: .30 - .50

FIG. 3.1.2 MISSION PROFILE & REQUIREMENTS (PREVIOUS AFRL WORK)
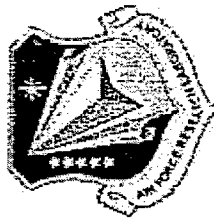
AFRL/VA ISR Study
Flight conditions

VAAA CASP analysis:

	Takeoff	Begin loiter	End loiter	Landing	Landing (abort)
Altitude	0	63,200	65,520	0	0
Weight	75,000	62,150	35,200	30,650	75,000
Speed	M=0.2	M=0.6	M=0.6	M=0.15	M=0.2
C.G.*	46.8	47.1	48.9	49.5	46.8

Moments of inertia calculated for each condition

Fuel loading revised from VAAA first cut:

	Wing	Nacelle	Tail	C.G. travel
May	22400 lb	17000 lb	0	4.2 ft
July	16200 lb	16200 lb	7000 lb	2.7 ft

* ft from nose, a.c. at 50.7 ft

FIG. 3.1.3 FLIGHT CONDITIONS (PREVIOUS AFRL WORK, 2000)

FIG. 3.1.5 - CL - Mach RELATIONSHIPS

FIG. 3.1.4 POSSIBLE DERIVED FLIGHT ENVELOPE

Aft-Swept Wing 35° sweep

Forward-Swept Wing -35° sweep

M=0.15, Re=7.04x10⁵

M=0.20, Re=9.39x10⁵

M=0.60, Re=2.92x10⁶

M=0.60, Re=2.29x10⁶
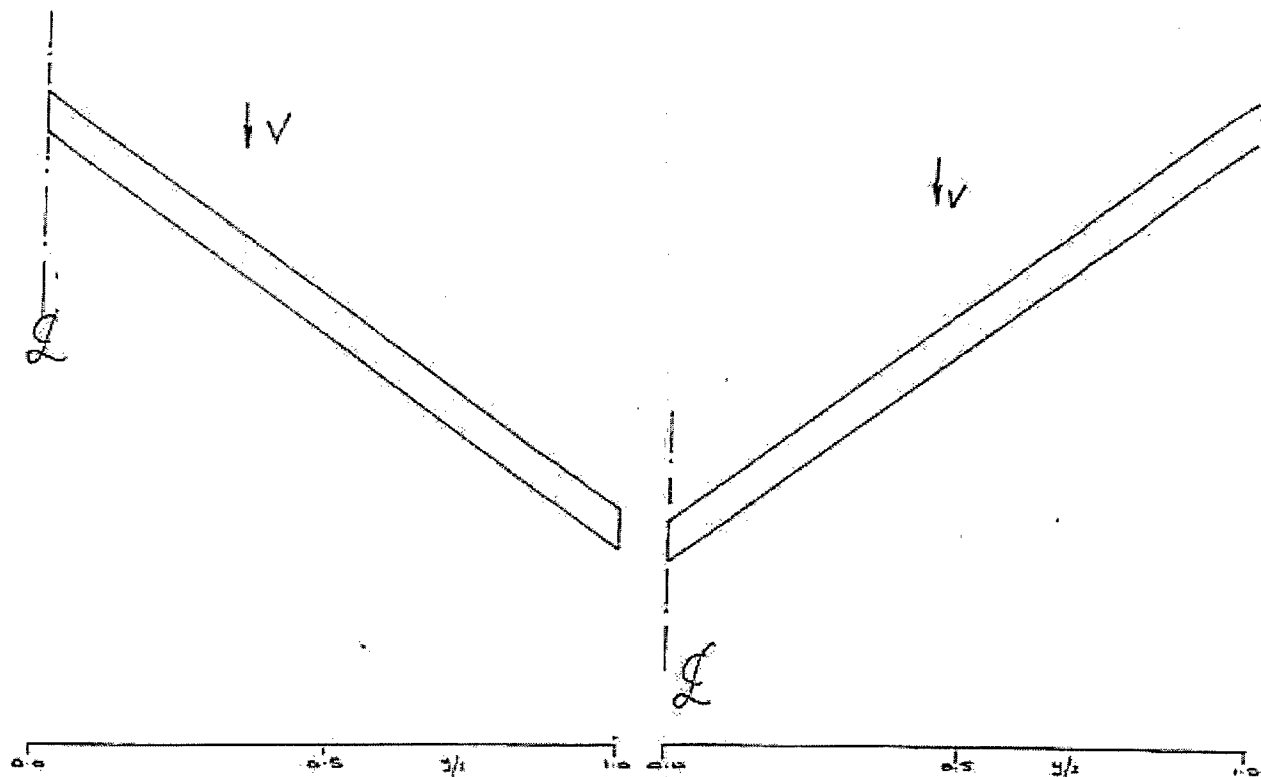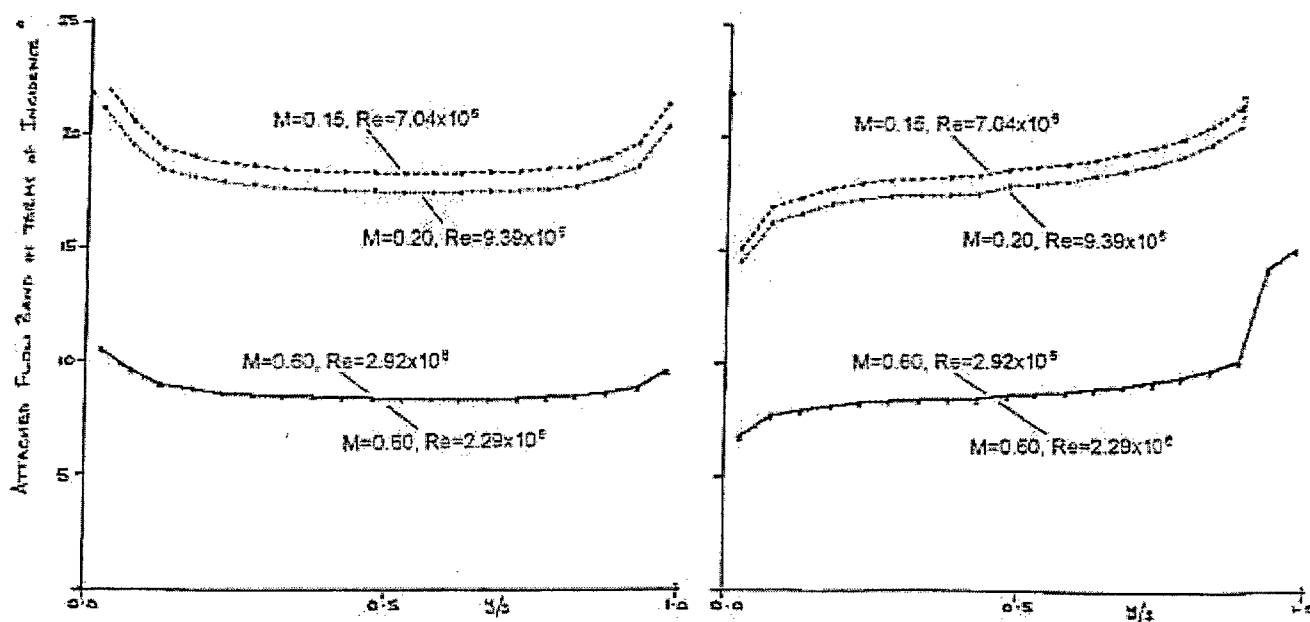
FIG. 3.1.6 15% t/c WINGS, ATTAINED α BANDS AT DIFFERENT MACH & Re COMBINATIONS
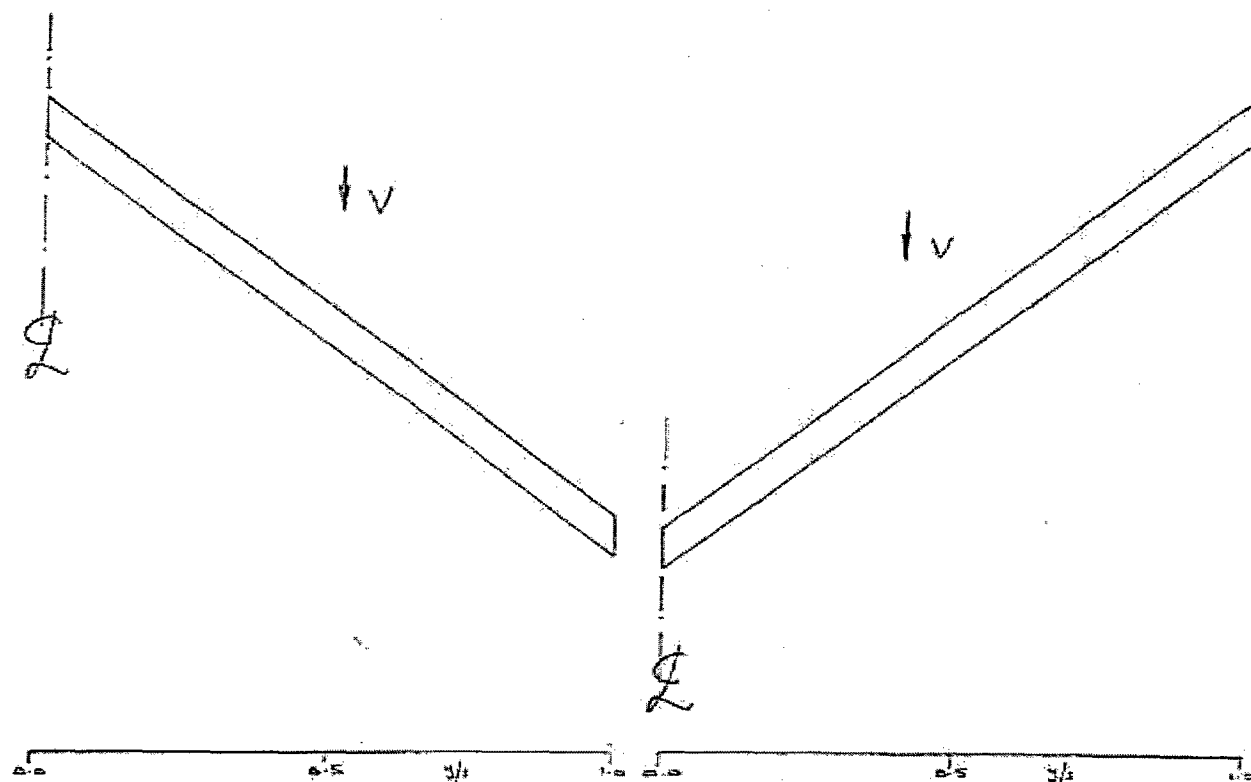
Aft-Swept Wing 35° sweep

Forward-Swept Wing -35° sweep
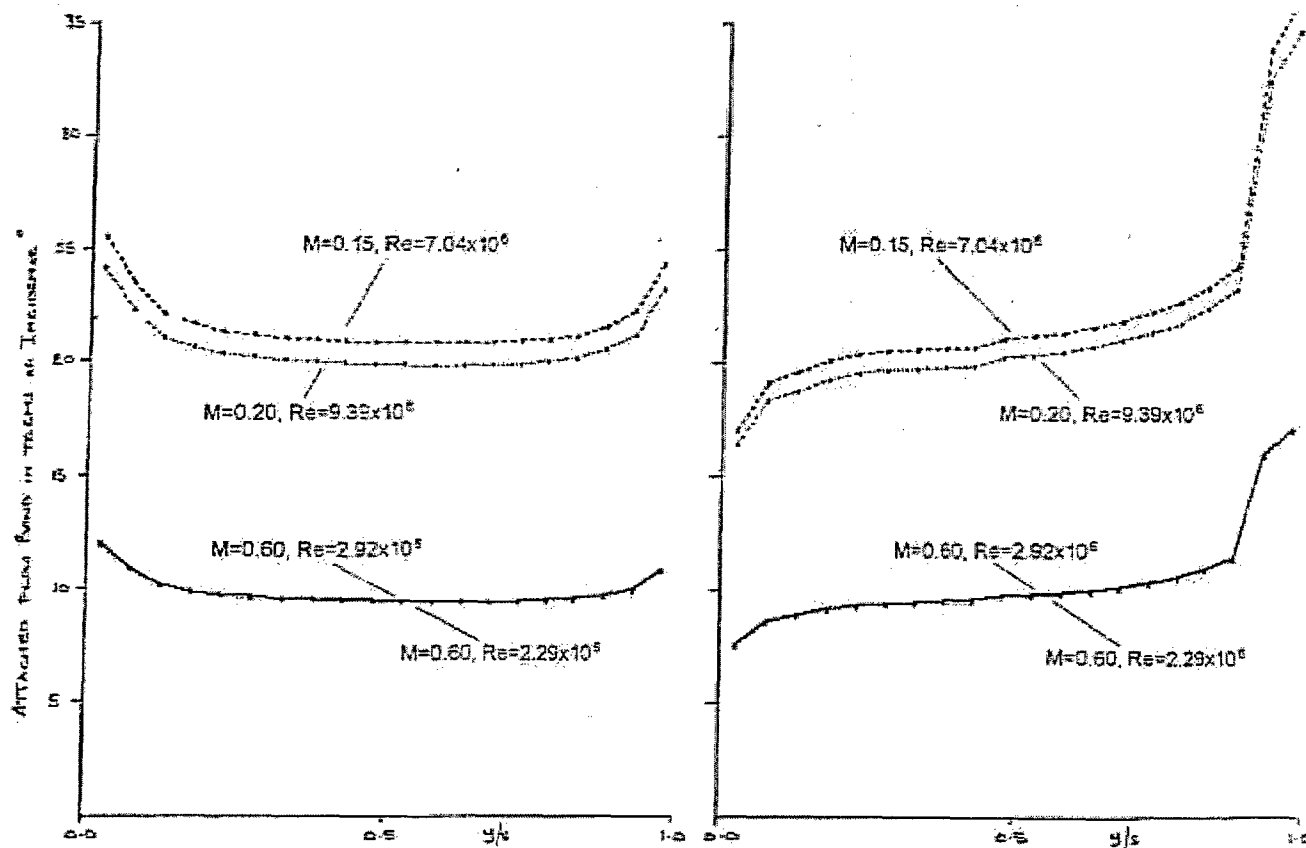
FIG. 3.1.7 17.2% t/c WINGS, ATTAINED α BANDS AT DIFFERENT MACH & Re COMBINATIONS

Reference Configuration

Sized Geometry

- (From W/S = 30) Wing Area (Gross): 2300 sq ft

  (From Antenna) Aspect Ratio (Gross): 17.4

Alternative Forward Swept Proposed

This would imply possibly
Front wing Anhedral
Aft wing Dihedral

AR wet = 5.5

Span = 200 ft

Sweep = 35 deg

Twin T-fans

X - Band Antenna

aft

tip

fwd
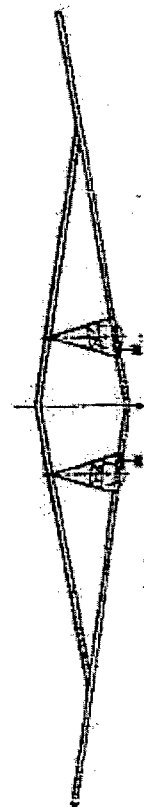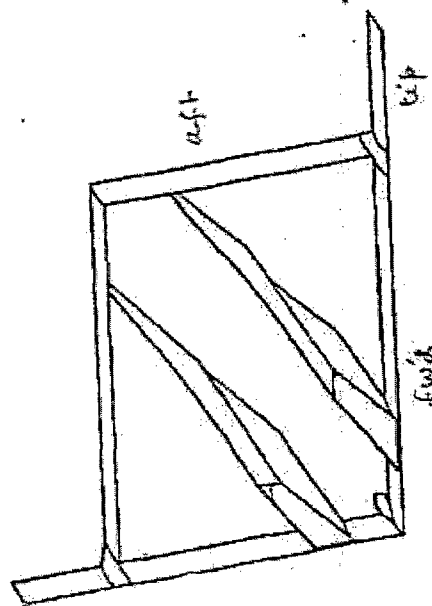
FIG. 3.2.1 SENSOR-CRAFT REFERENCE CONFIGURATION BASED ON PREVIOUS AFRL WORK
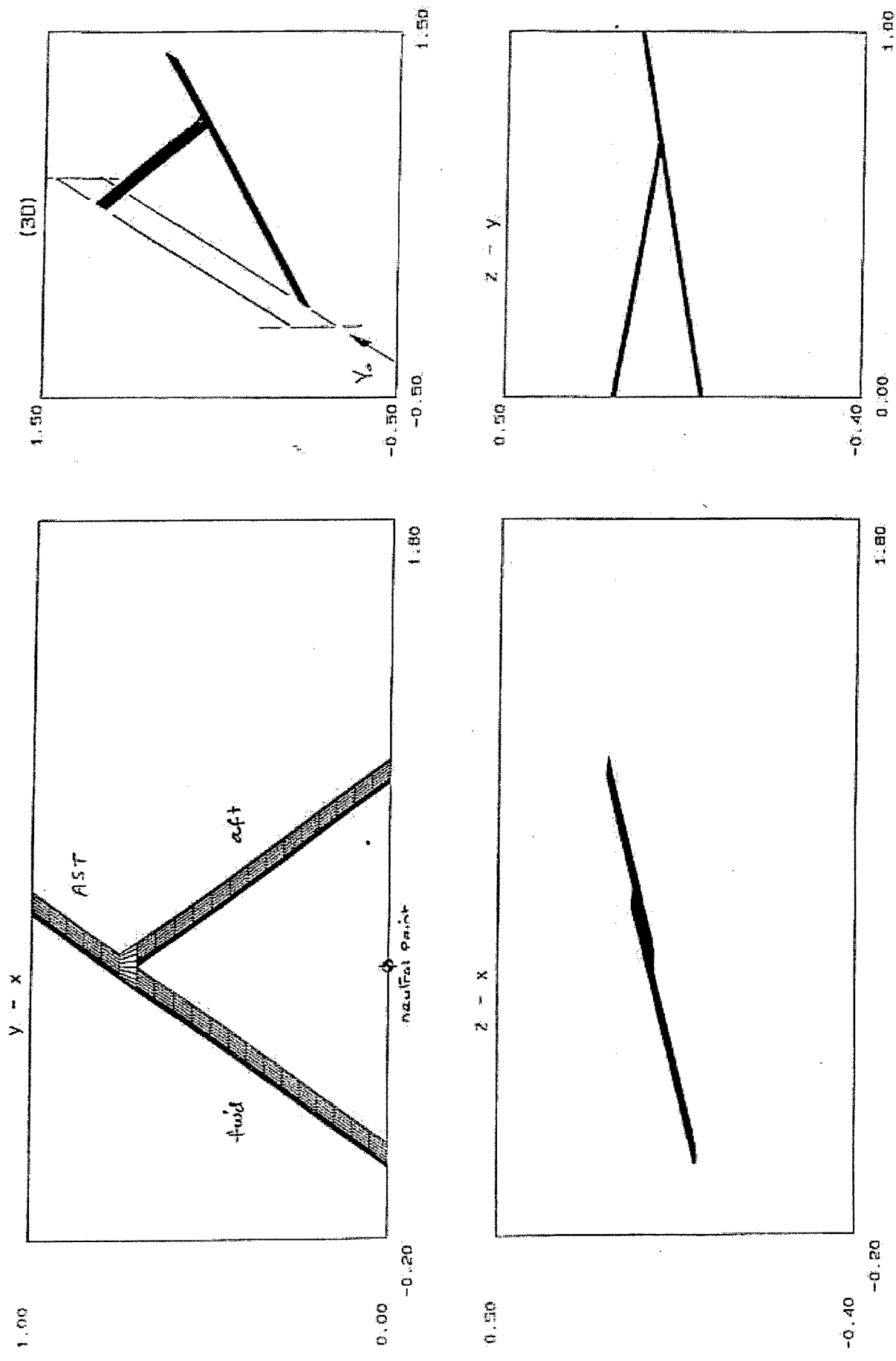
FIG. 4.1.1 CONFIG. AT1, GENERAL ARRANGEMENT (3 COMPONENTS).
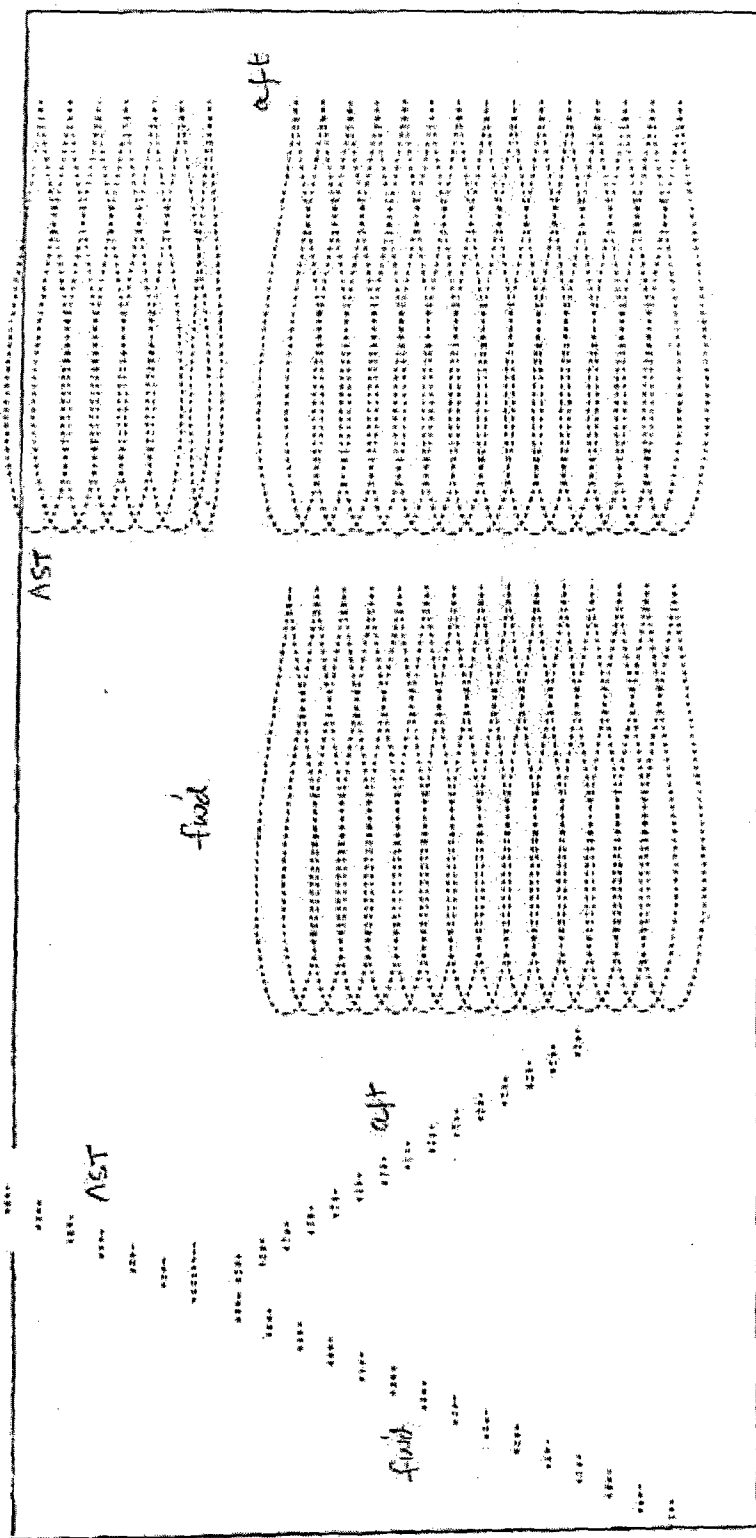
FIG. 4.1.2 CONFIG: AT1, UNCAMBERED AEROFOIL SHAPES
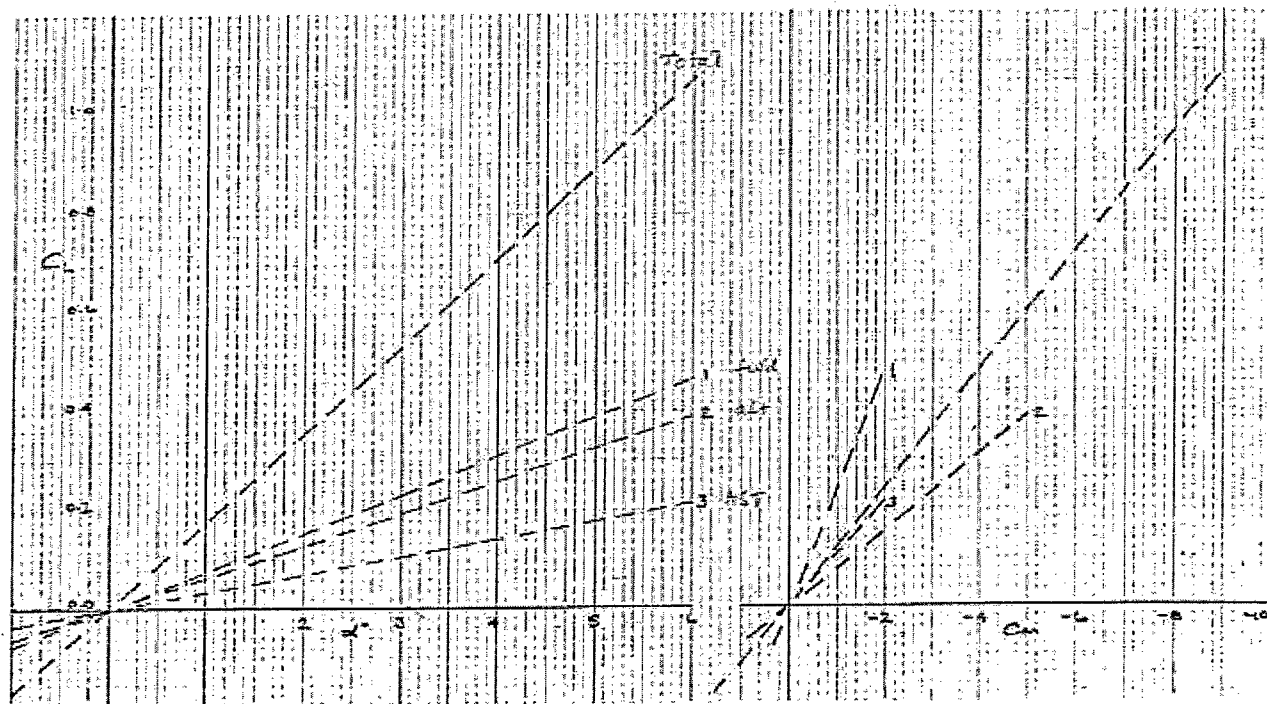
FIG. 4.1.3. CONFIG. AT1, UNCAMBERED WINGS, C_L & C_m CHARACTERISTICS & COMPONENT BREAKDOWN

$(\alpha, C_L) = (3.25°, 0.580)$

$(\alpha, C_L) = (4.25°, 0.759)$
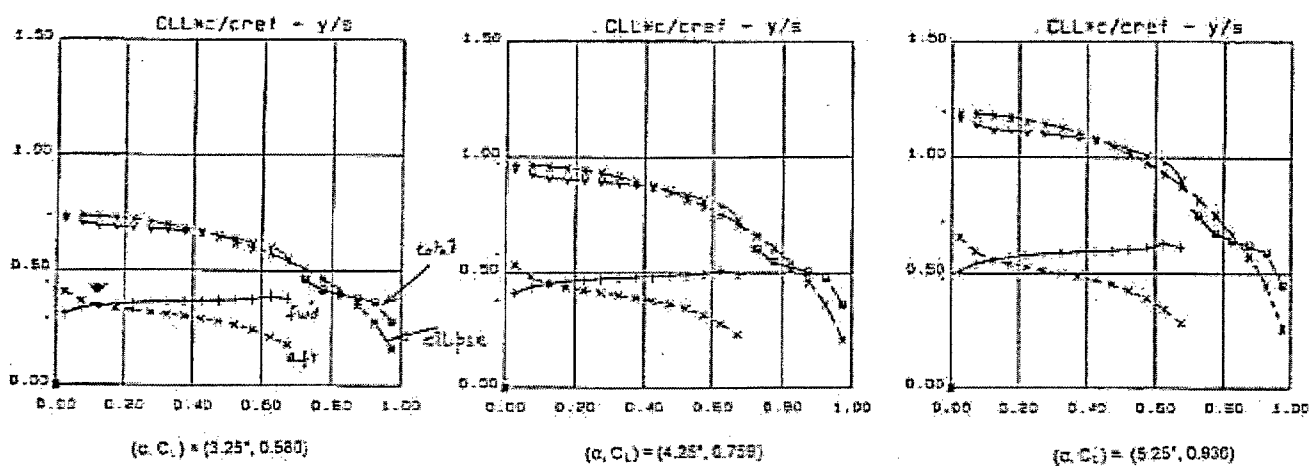
$(\alpha, C_L) = (5.25°, 0.936)$

FIG. 4.1.4 CONFIG. AT1, UNCAMBERED WINGS, C_{LL} SPANWISE LOADING

$(\alpha, C_L) = (3.25°, 0.580),\quad (4.25°, 0.759),\quad (5.25°, 0.936)$
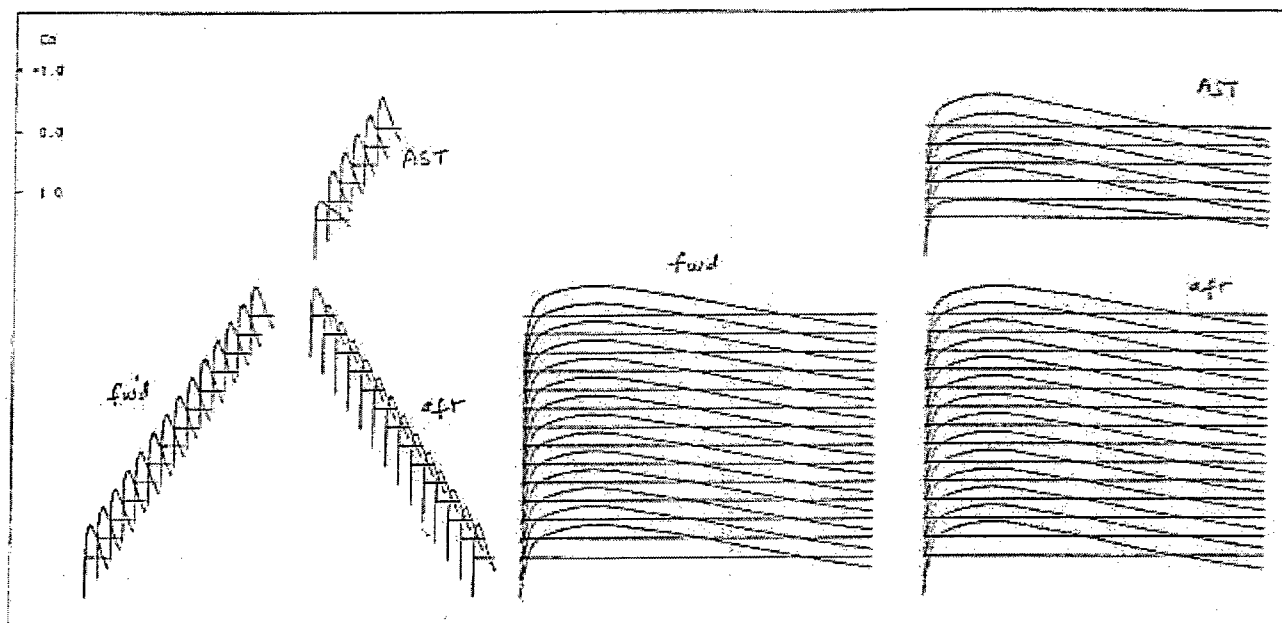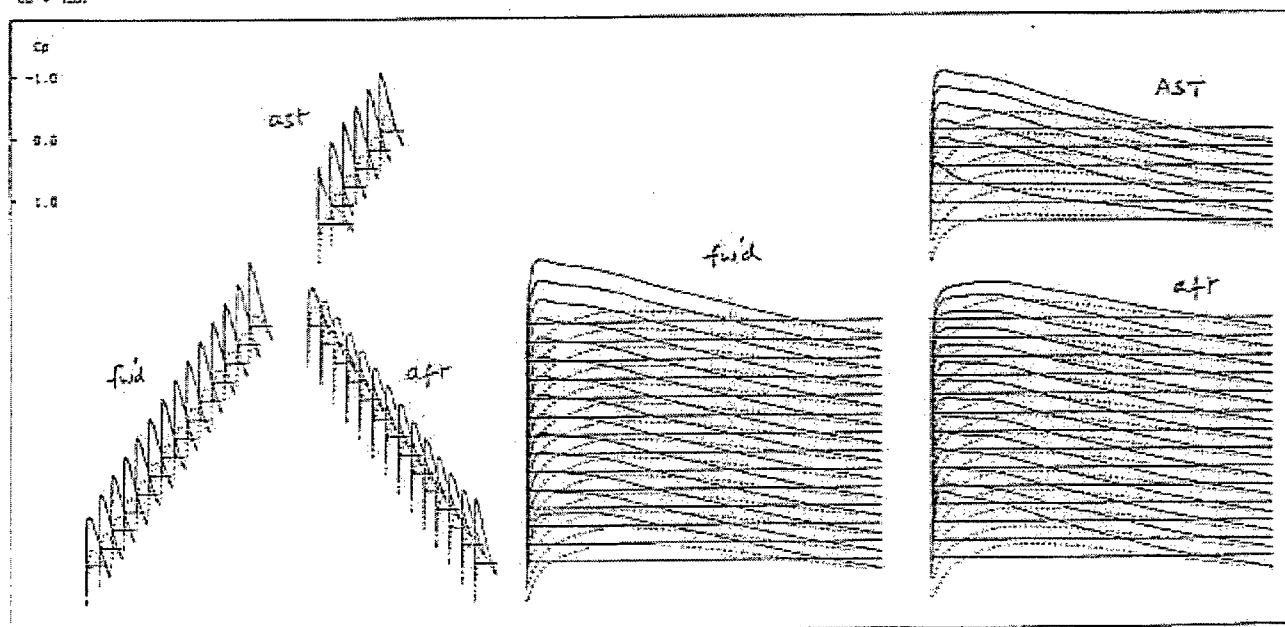
(a) $(\alpha, C_L) = (0.0°, 0.0)$

(b) $(\alpha, C_L) = (3.25°, 0.580)$

FIG. 4.1.5 CONFIG. AT1, UNCAMBERED WINGS, C_P DISTRIBUTIONS

$(\alpha, C_L) = (0.0°, 0.0), \quad (3.25°, 0.580), \quad (4.25°, 0.759), (5.25°, 0.936)$
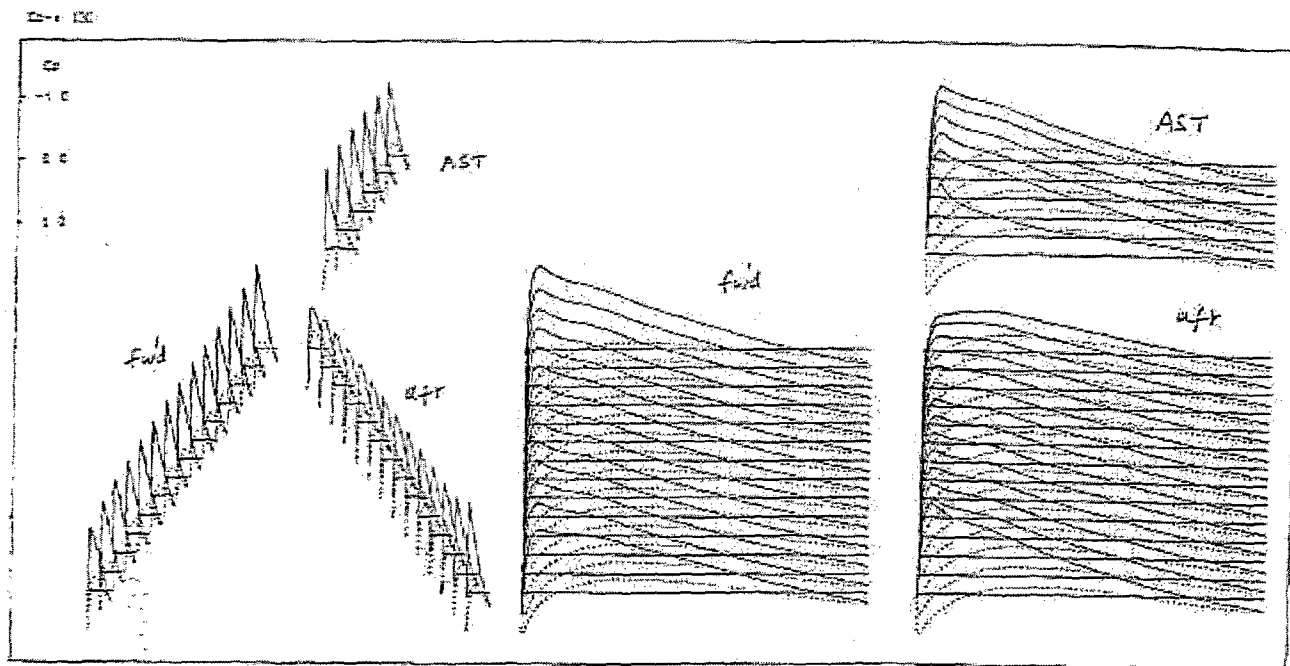
(c) $(\alpha, C_L) = (4.25°, 0.759)$
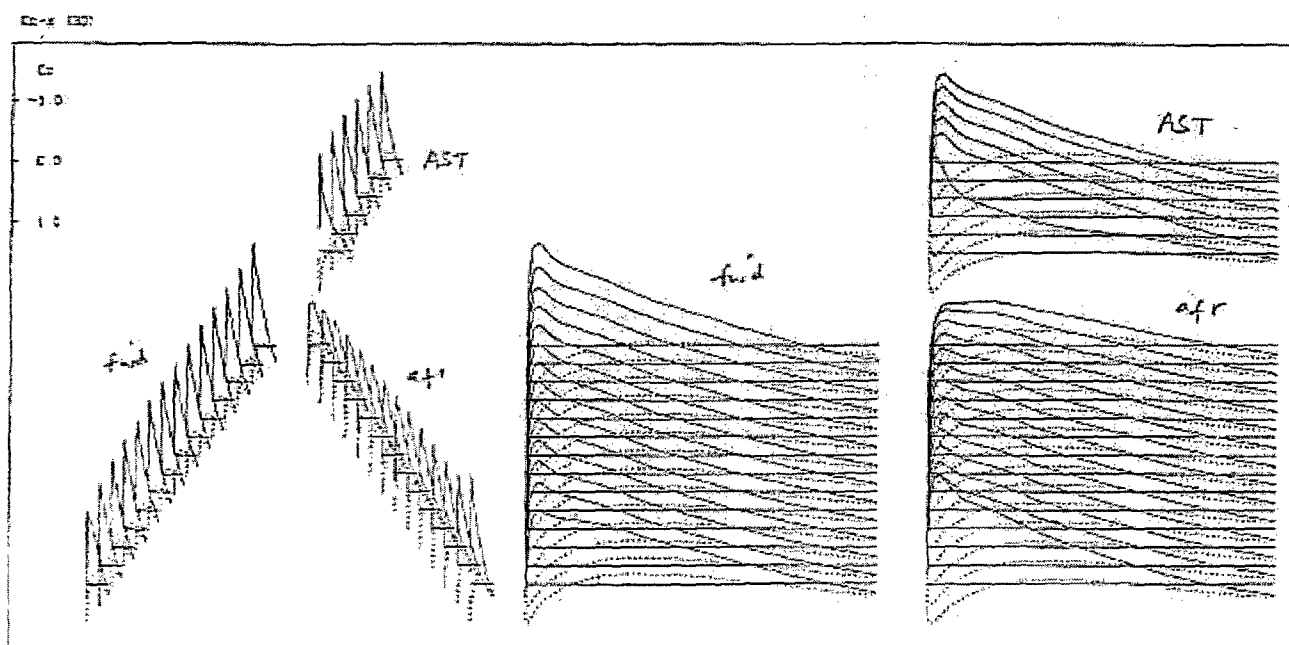
(d) $(\alpha, C_L) = (5.25°, 0.936)$

FIG. 4.1.5 (cont'd)
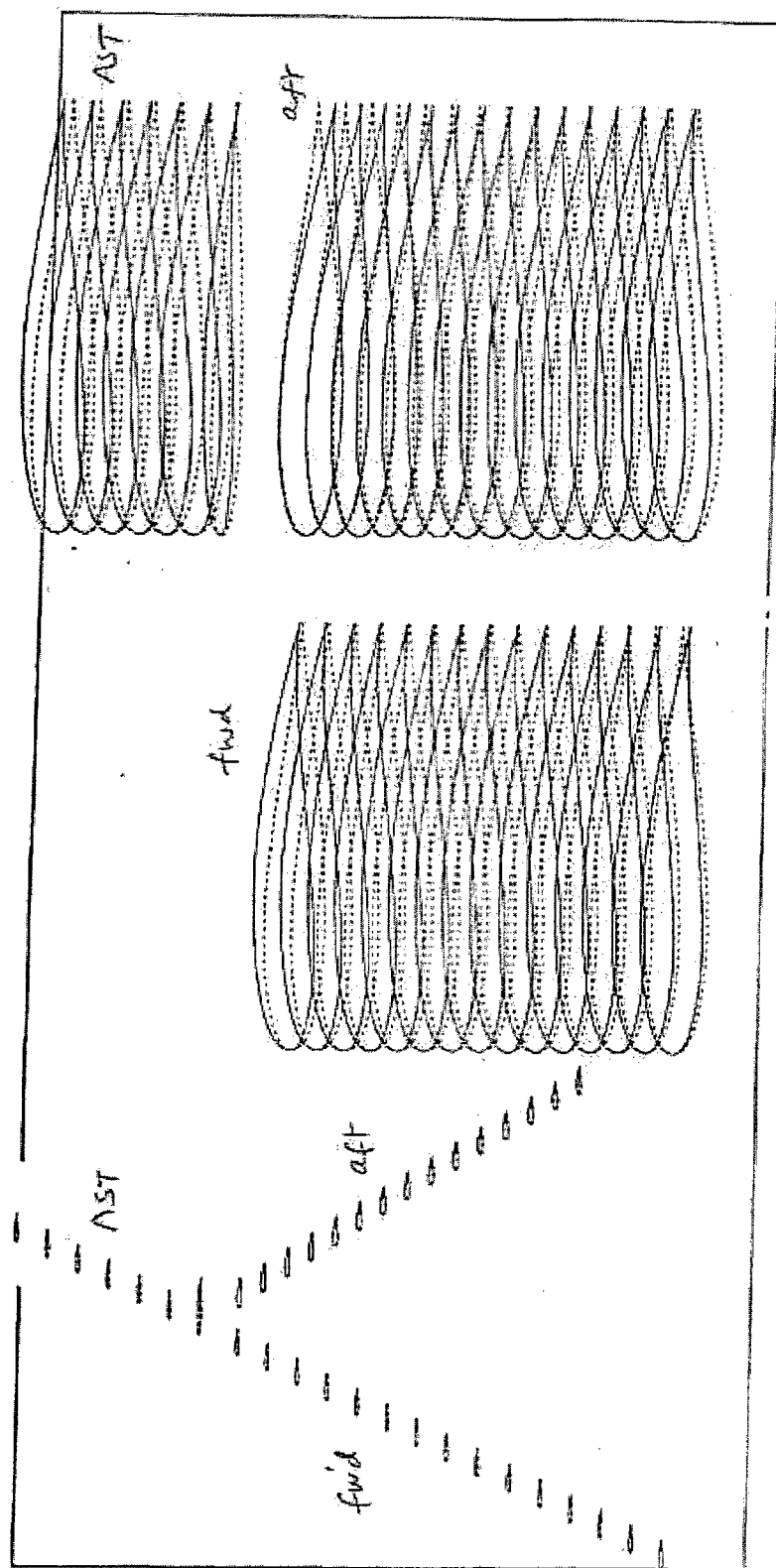
FIG. 4.2.2 CONFIG. AT1, DESIGNED CONFIGURATION, AEROFOIL SHAPES
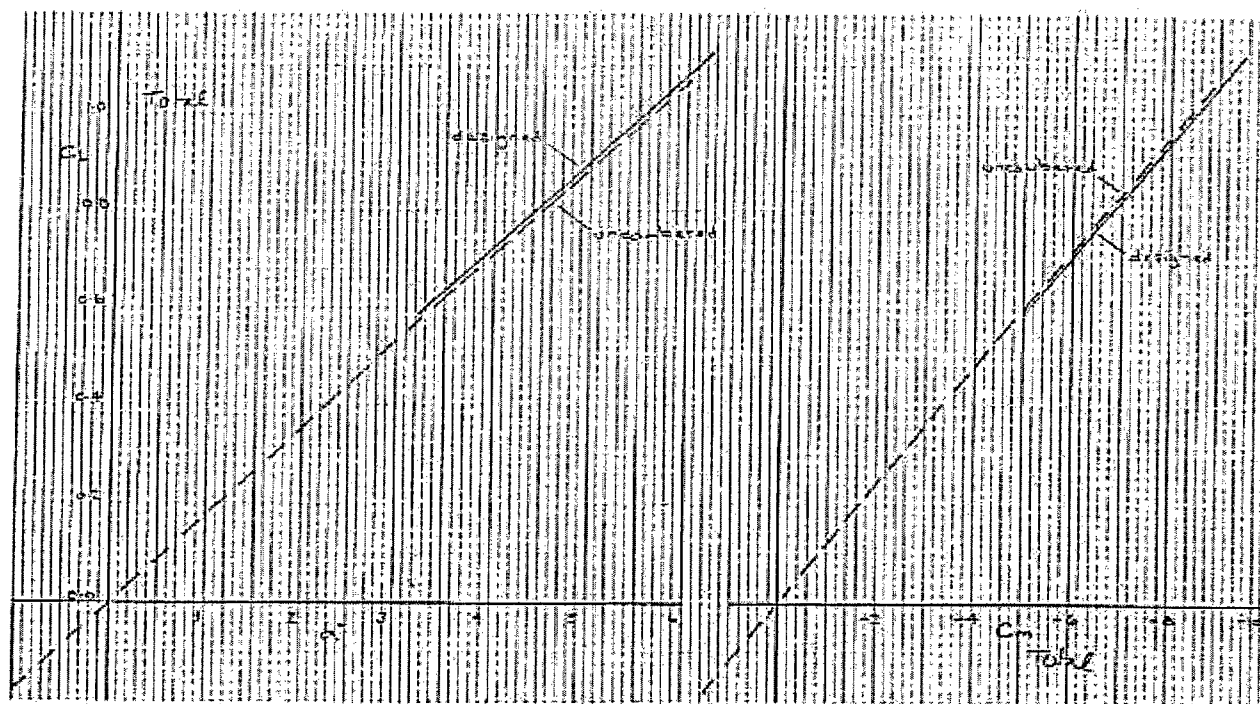
FIG. 4.2.3 CONFIG. AT1, COMPARING   CAMBERED & DESIGNED WINGS, C_L & C_m
CHARACTERISTICS

$(\alpha, C_L) = (3.25°, 0.588)$ $(\alpha, C_L) = (4.25°, 0.768)$ $(\alpha, C_L) = (5.25°, 0.946)$
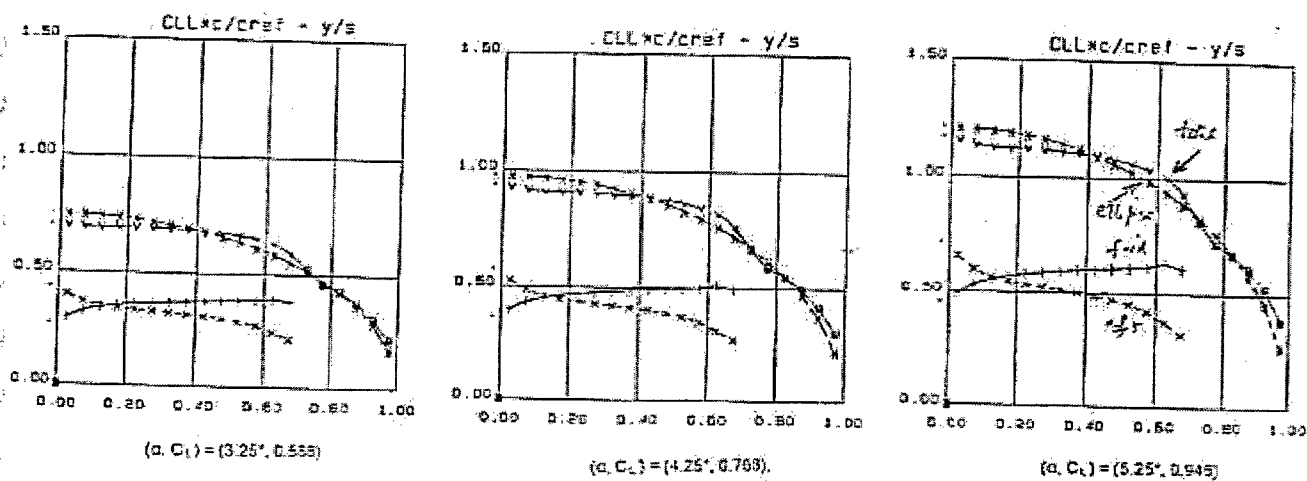
FIG. 4.2.4 CONFIG. AT1, DESIGNED WINGS, C_{LL} SPANWISE LOADING

$(\alpha, C_L) = (3.25°, 0.588)$, $(4.25°, 0.768)$, $(5.25°, 0.946)$
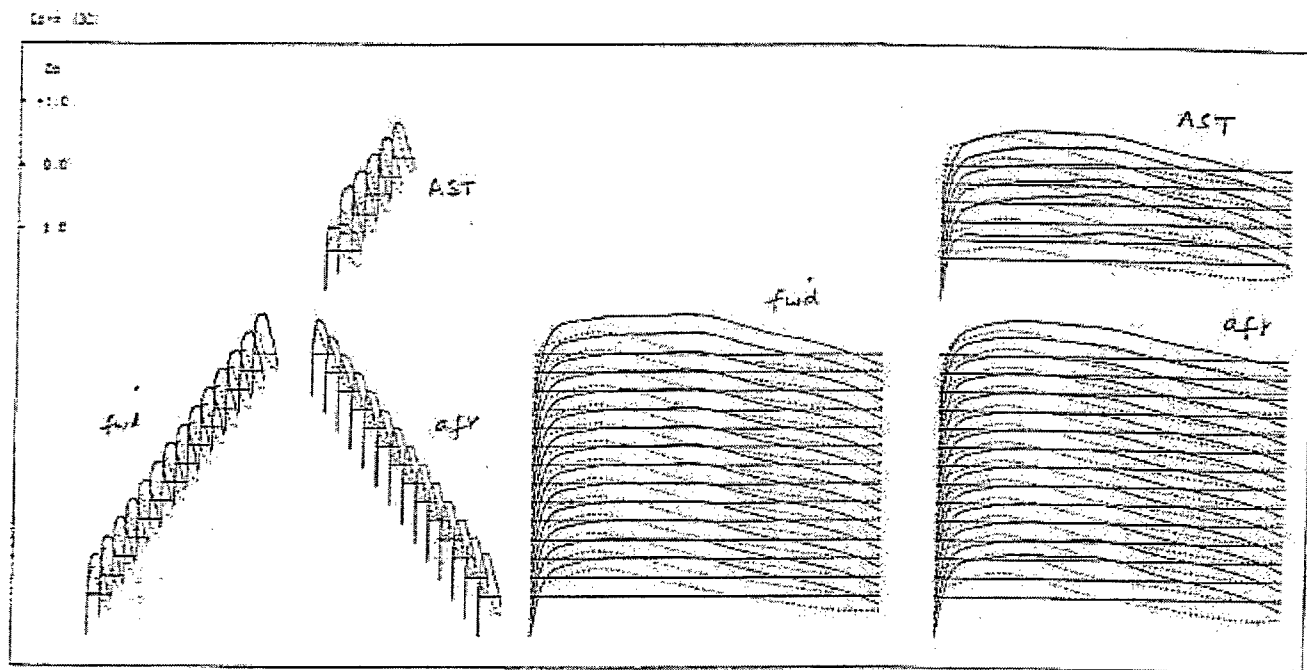
(a) $(\alpha, C_L) = (3.25°, 0.588)$
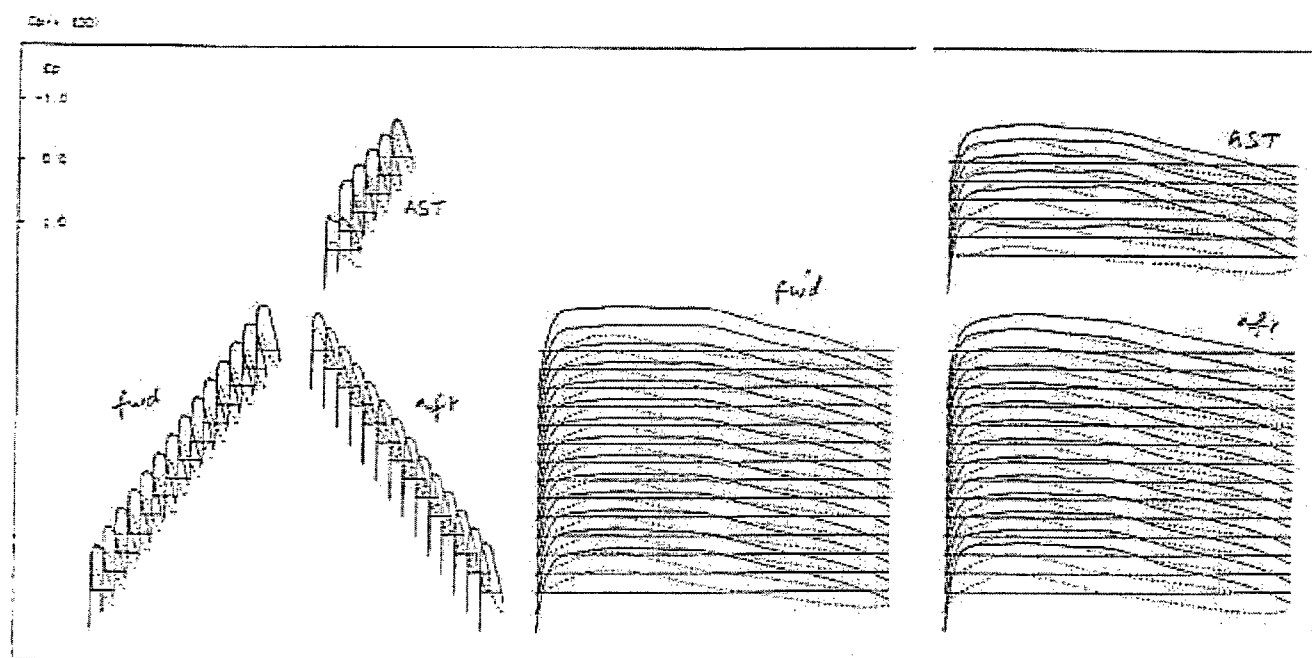
(b) $(\alpha, C_L) = (4.25°, 0.768)$

FIG. 4.2.5 CONFIG. AT1, CAMBERED WINGS, C_p DISTRIBUTIONS

$(\alpha, C_L) = (3.25°, 0.588), \quad (4.25°, 0.768), (5.25°, 0.946)$
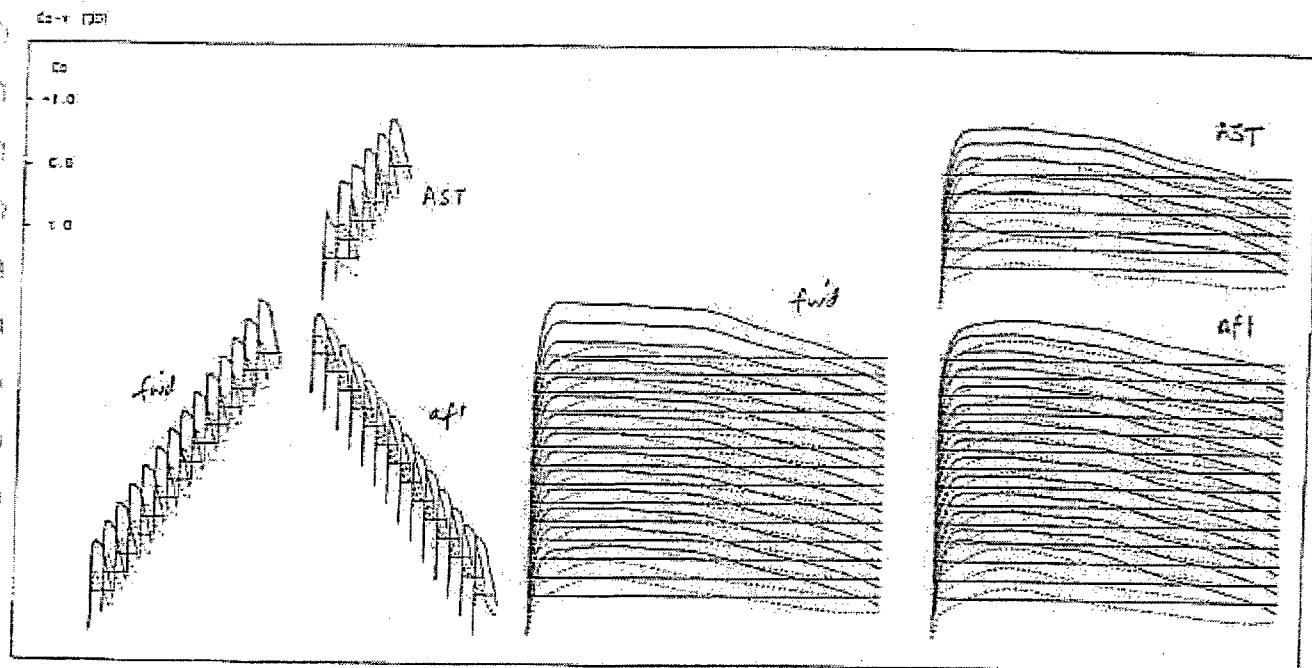
(c) $(\alpha, C_L) = (5.25°, 0.946)$

FIG. 4.2.5 (cont'd)
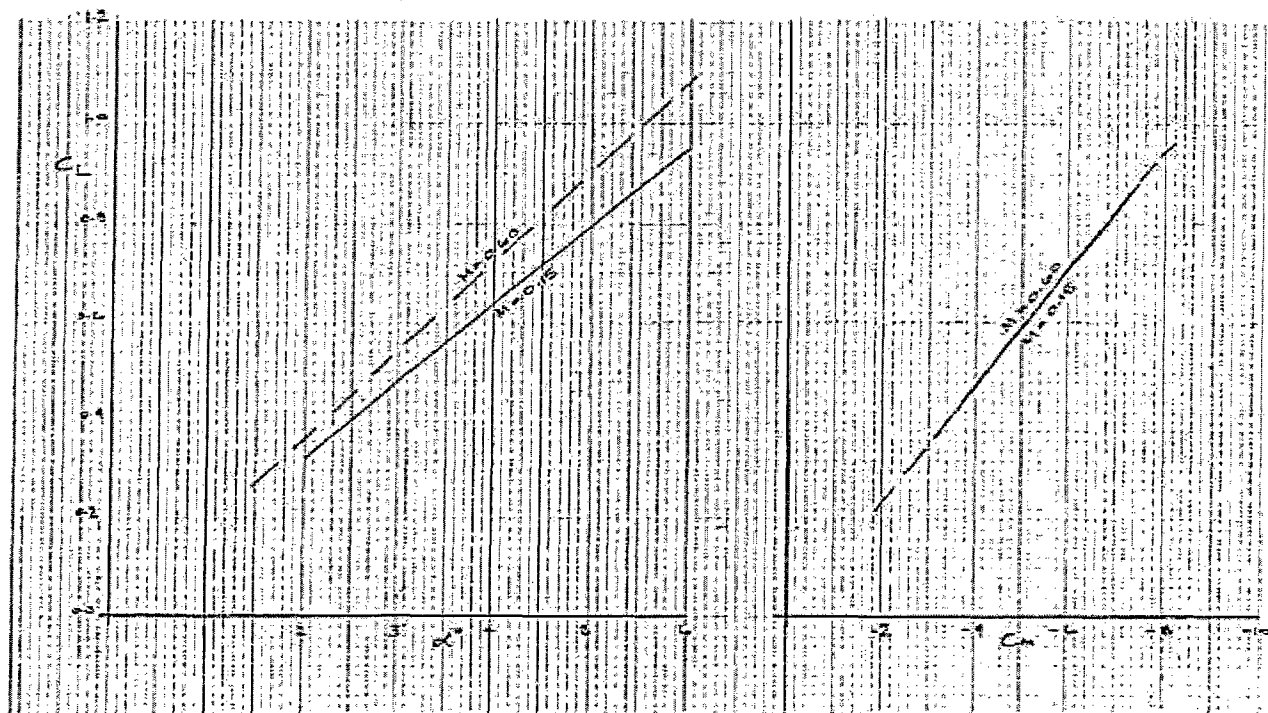
FIG. 4.3.1 CONFIG. AT1, MACH 0.6 DESIGNED WINGS EVALUATED AT MACH 0.15, C_L & C_m CHARACTERISTICS COMPARISONS

$(\alpha, C_L) = (3.25°, 0.520)$ $(\alpha, C_L) = (4.25°, 0.677)$ $(\alpha, C_L) = (5.25°, 0.833)$
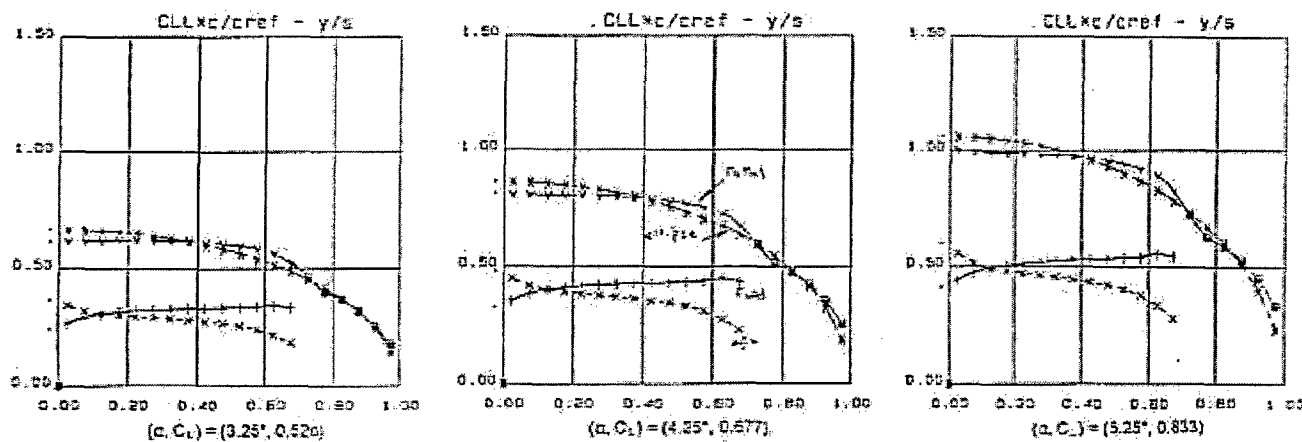
FIG. 4.3.2 CONFIG. AT1, DESIGNED WINGS EVALUATED AT MACH 0.15, C_{LL} SPANWISE LOADING

$(\alpha, C_L) = (3.25°, 0.520),$ $(4.25°, 0.677),$ $(5.25°, 0.833)$

(a) $(\alpha, C_L) = (3.25°, 0.520)$

(b) $(\alpha, C_L) = (4.25°, 0.677)$
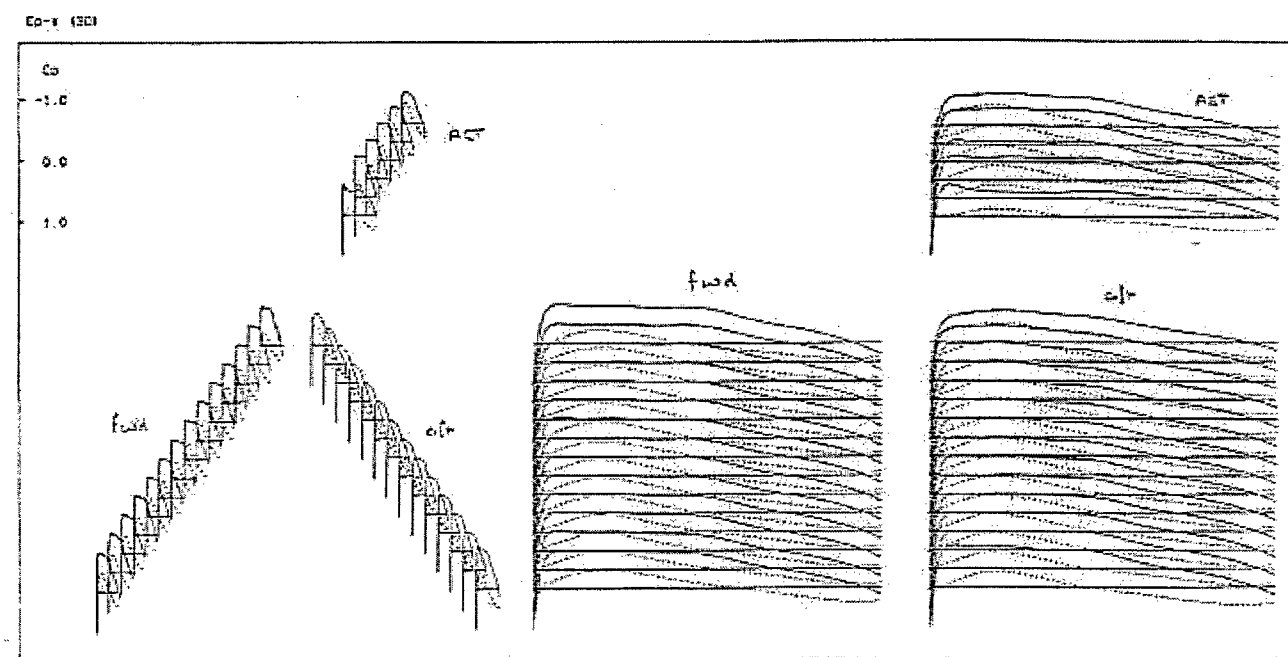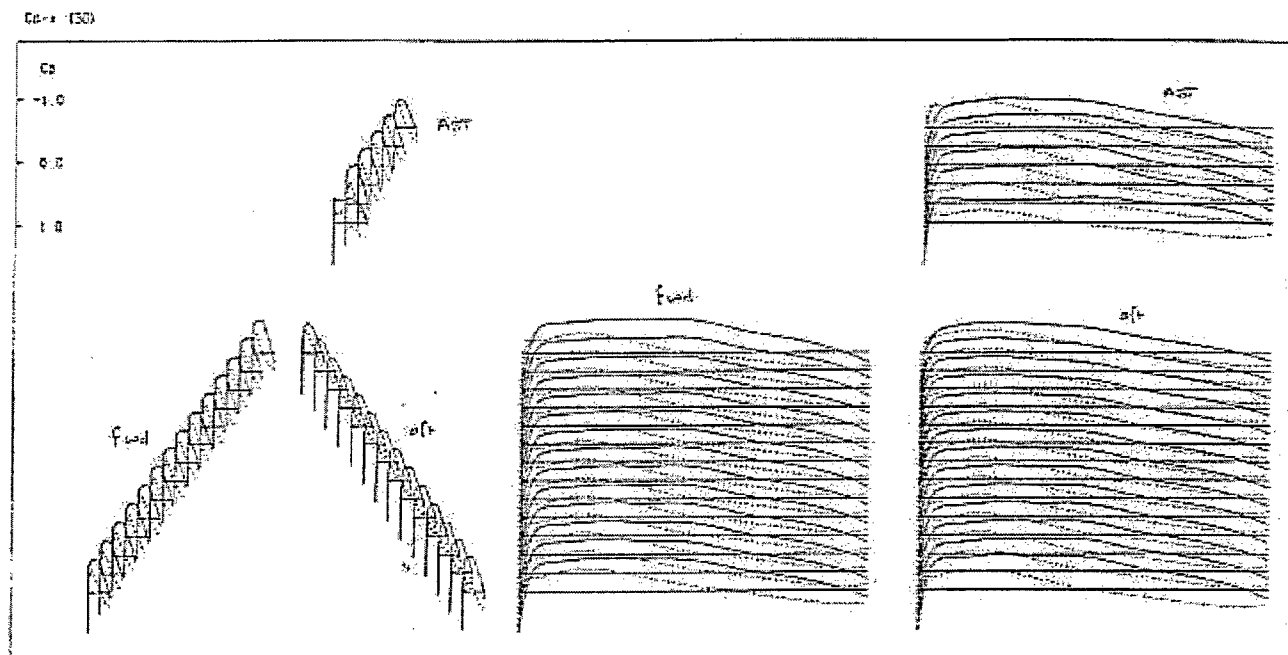
FIG. 4.3.3 CONFIG. AT1, CAMBERED WINGS EVALUATED AT MACH 0.15, C_F DISTRIBUTIONS

$(\alpha, C_L) = (3.25°, 0.520)$, $(4.25°, 0.677)$, $(5.25°, 0.833)$
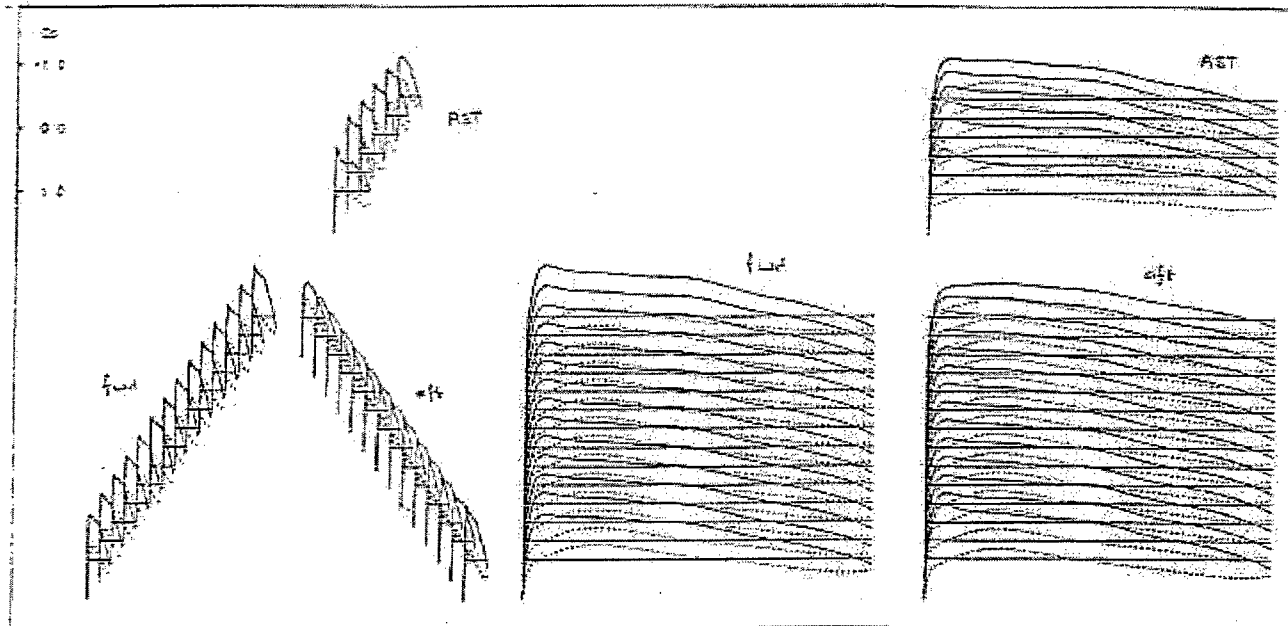
(c) $(\alpha, C_L) = (5.25°, 0.833)$

FIG. 4.3.3 (cont'd)
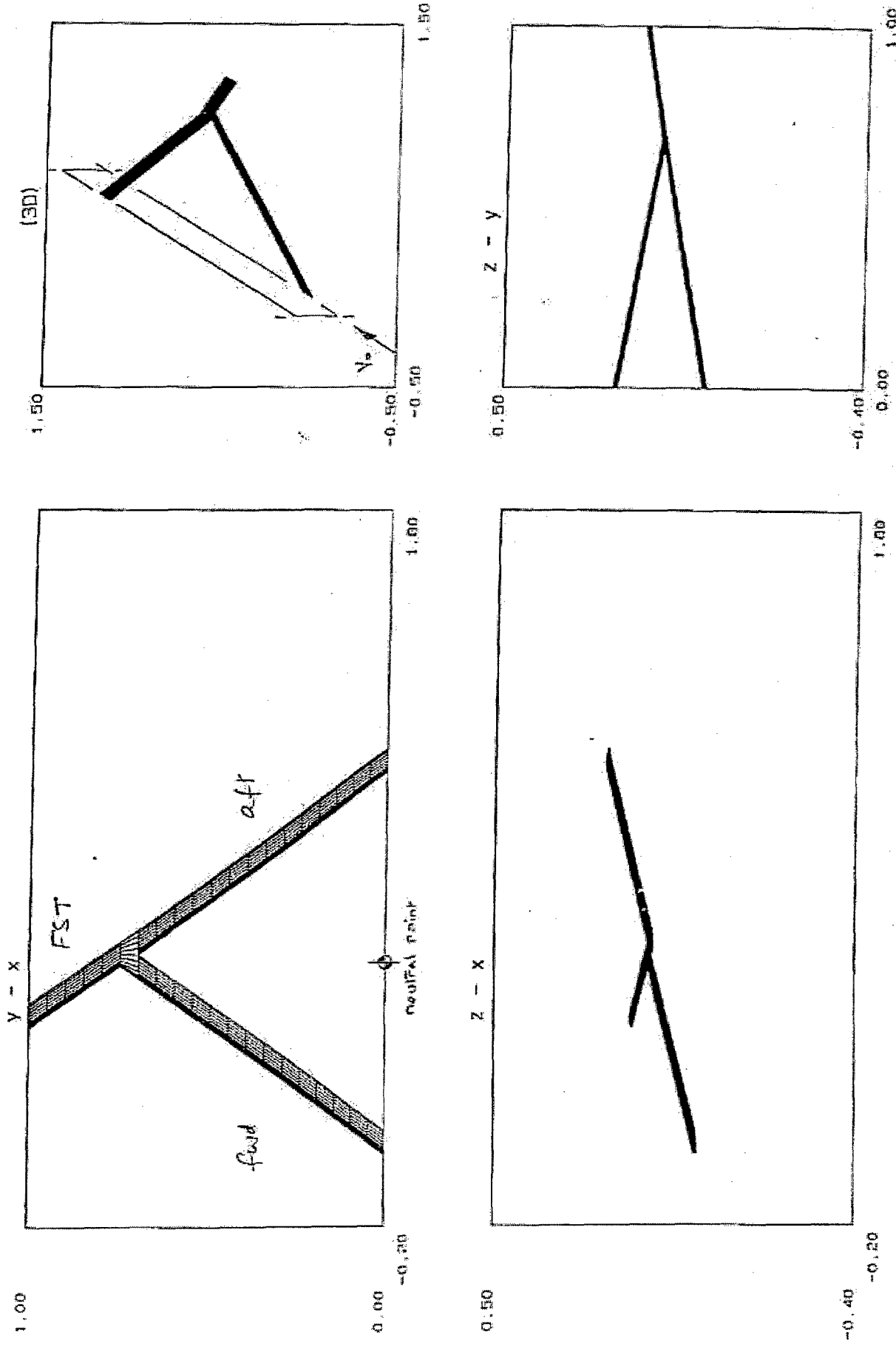
FIG. 5.1.1 CONFIG. FT1, GENERAL ARRANGEMENT (3 COMPONENTS)
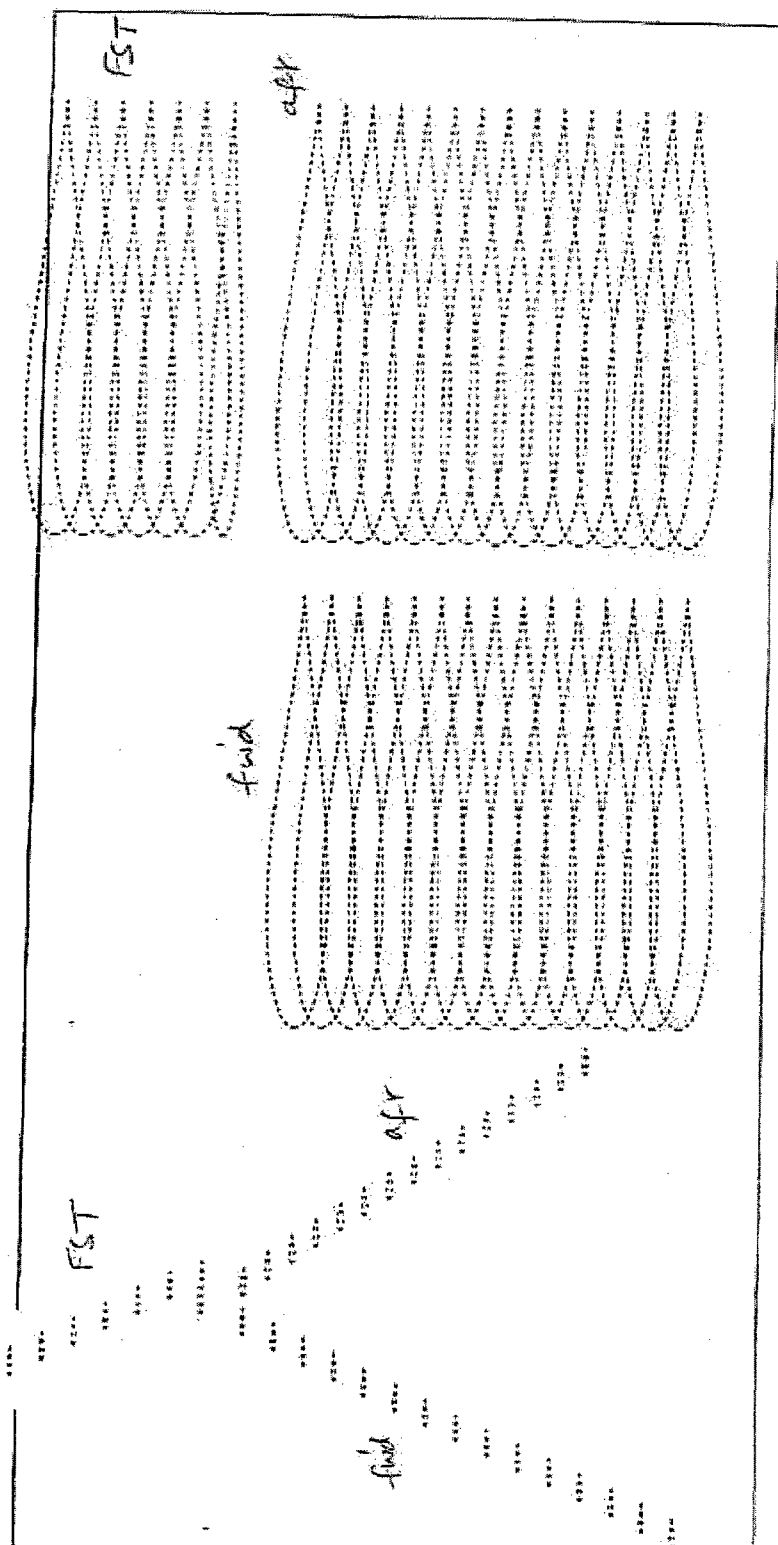
FIG. 5.1.2 CONFIG. FT1, UNCAMBERED AEROFOIL SHAPES
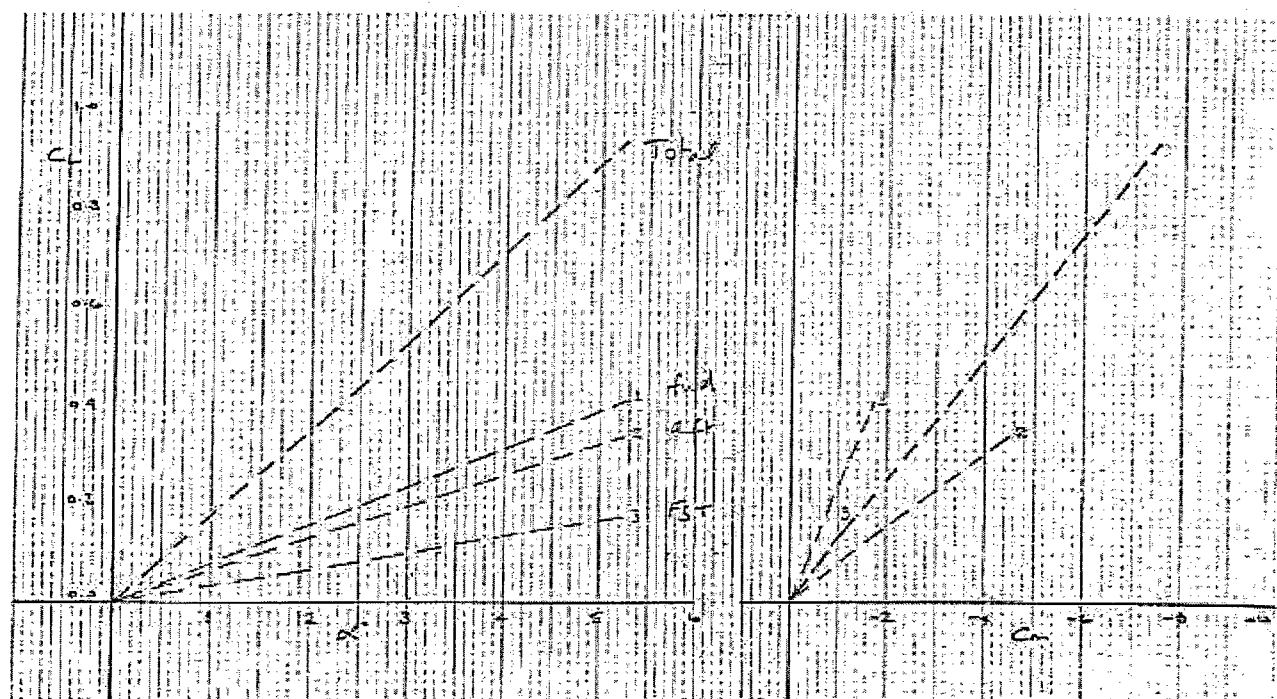
FIG. 5.1.3 CONFIG. FT1, UNCAMBERED WINGS, C_L & C_m CHARACTERISTICS & COMPONENT BREAKDOWN

$(\alpha, C_L) = (3.25°, 0.551)$

$(\alpha, C_L) = (4.25°, 0.760)$
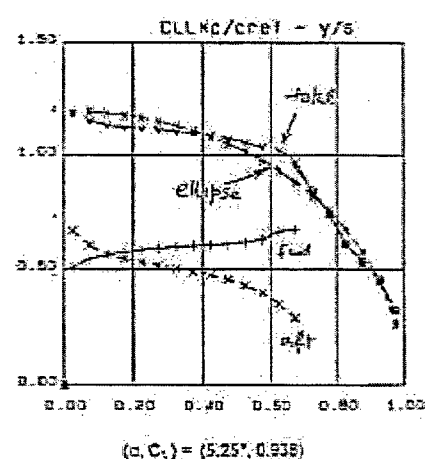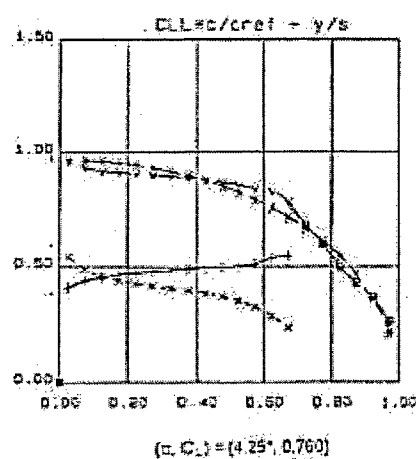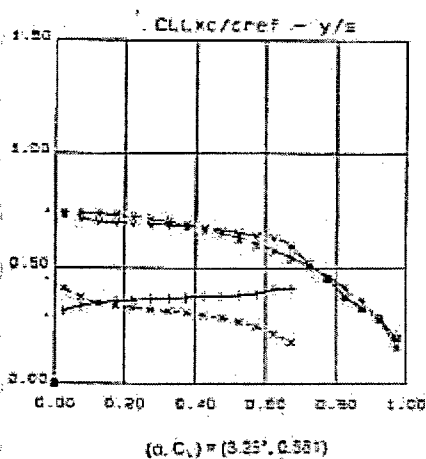
$(\alpha, C_L) = (5.25°, 0.938)$

FIG. 5.1.4 CONFIG. FT1, UNCAMBERED WINGS, C_{LL} SPANWISE LOADING

$(\alpha, C_L) = (3.25°, 0.551), \quad (4.25°, 0.760), \quad (5.25°, 0.938)$
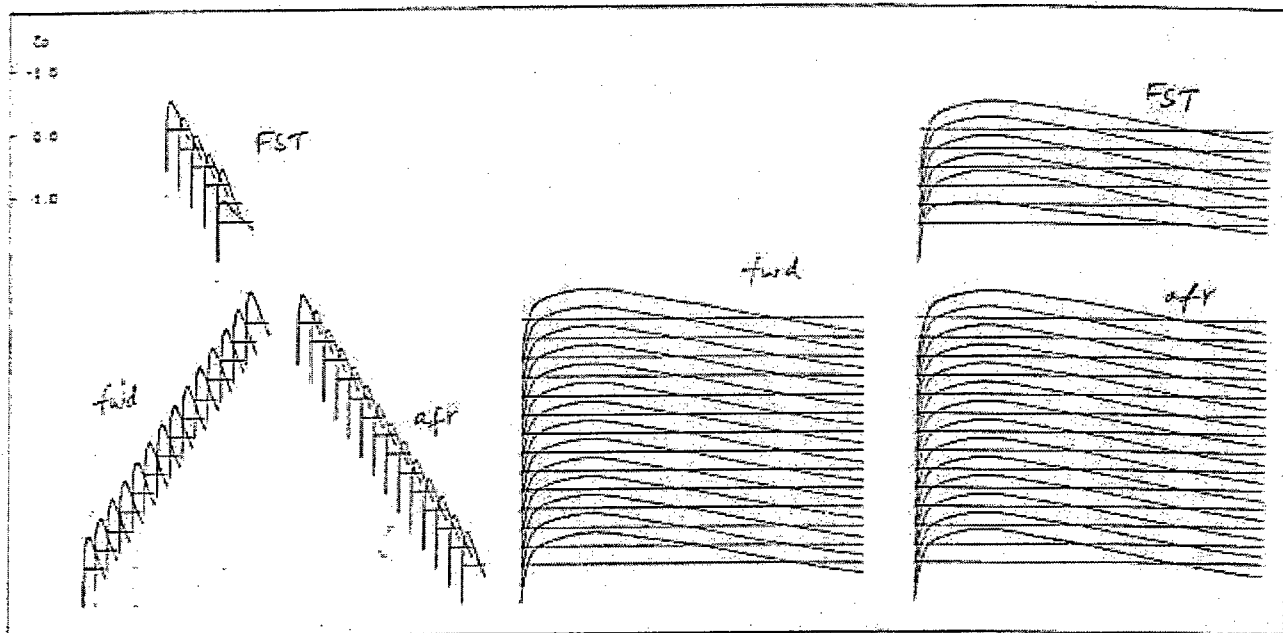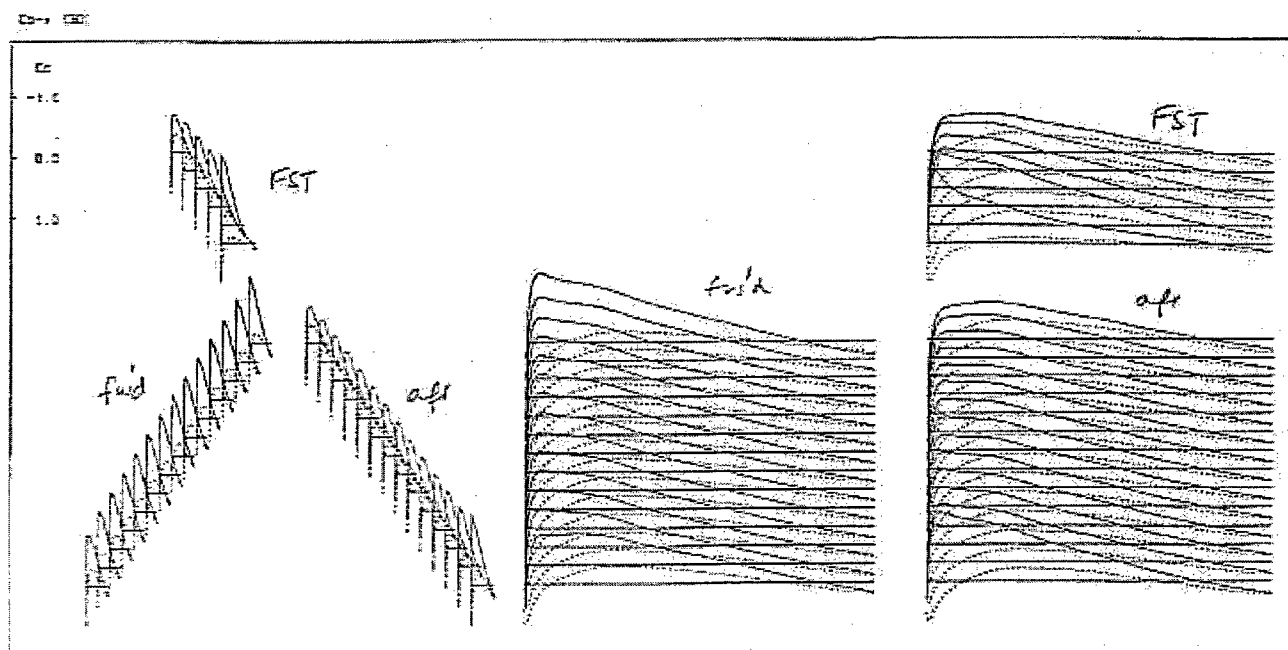
(a) $(\alpha, C_L) = (0.0°, 0.0)$

(b) $(\alpha, C_L) = (3.25°, 0.580)$

FIG. 5.1.5 CONFIG. FT1, UNCAMBERED WINGS, C_p DISTRIBUTIONS

$(\alpha, C_L) = (0.0°, 0.0)$, $(3.25°, 0.580)$, $(4.25°, 0.759)$, $(5.25°, 0.936)$
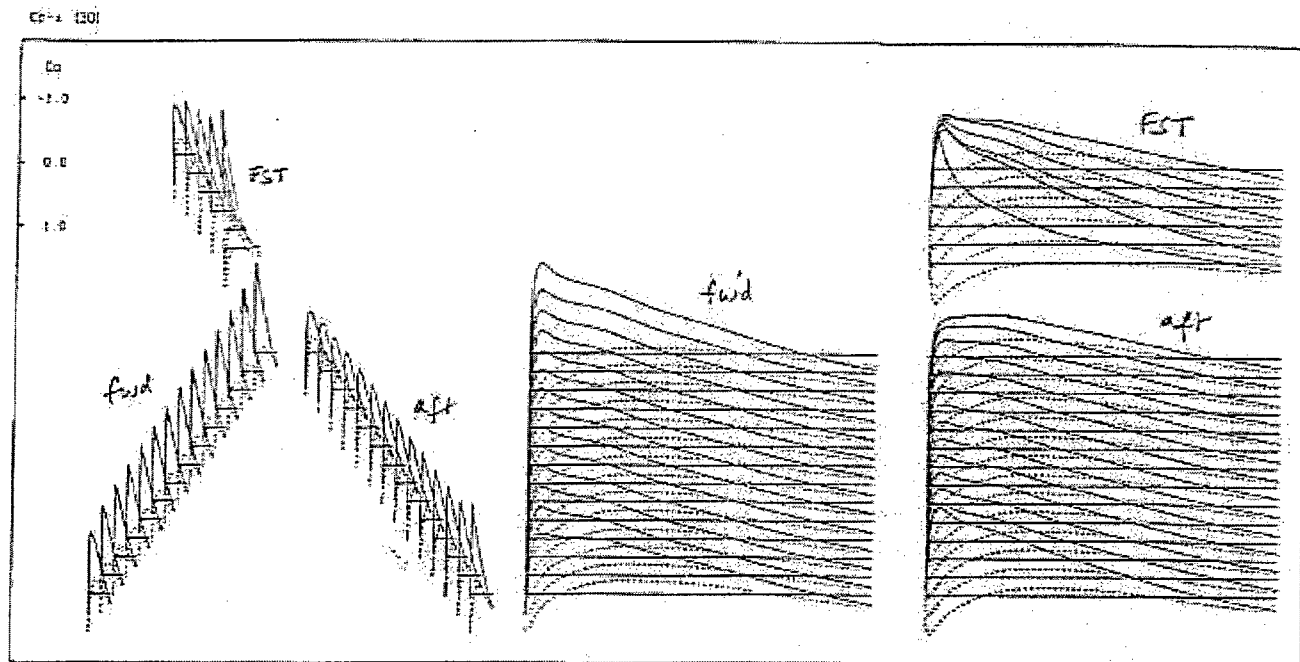
(c) $(\alpha, C_L) = (4.25°, 0.759)$
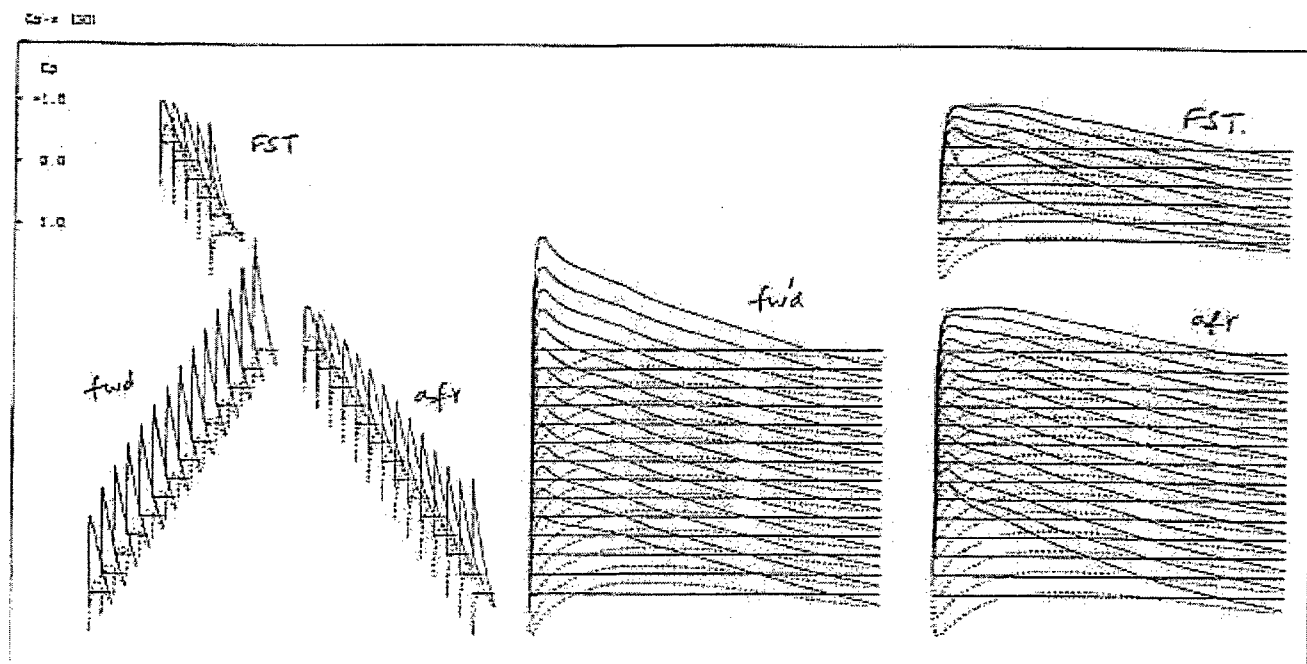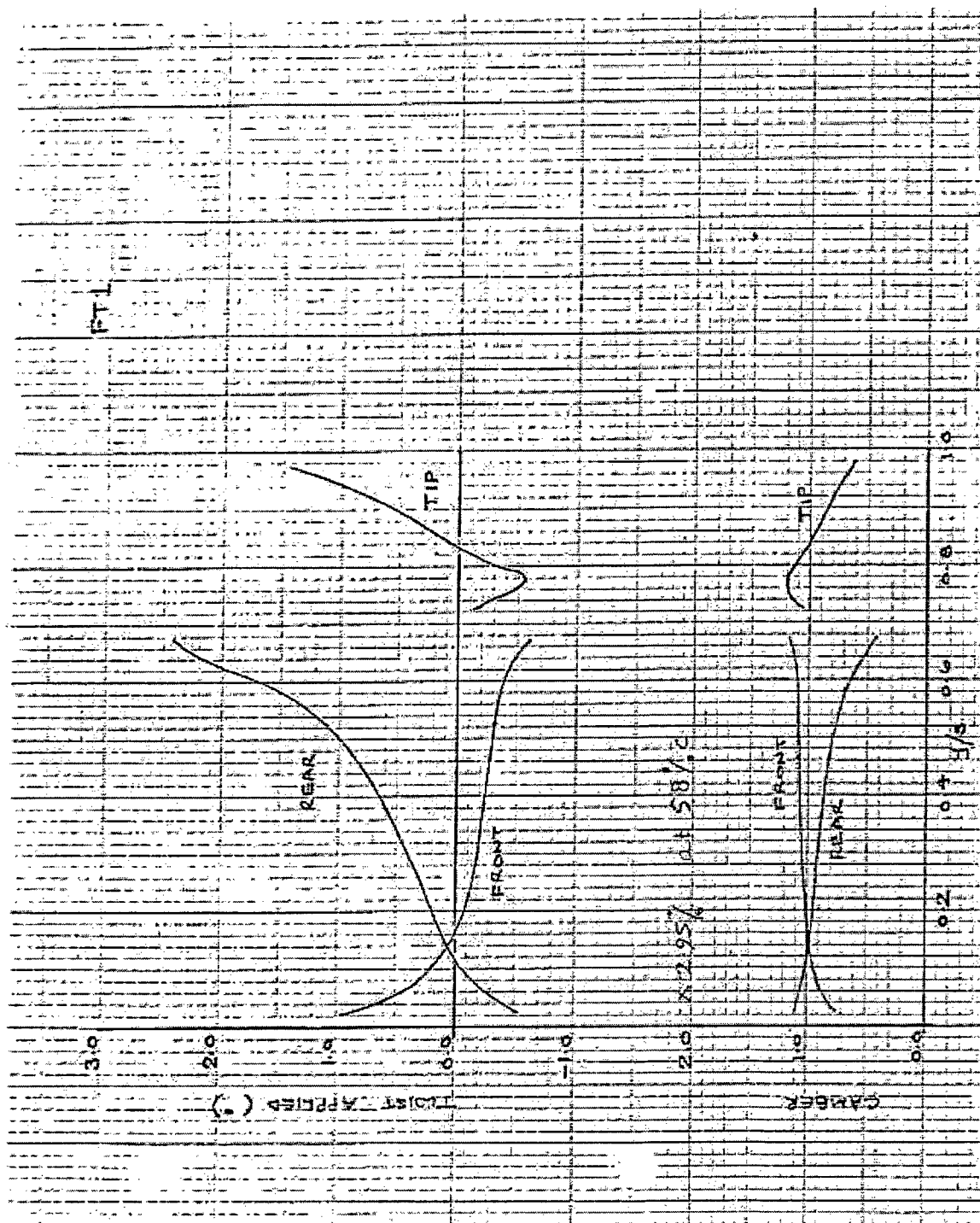

(d) $(\alpha, C_L) = (5.25°, 0.936)$

FIG. 5.1.5 (cont'd)
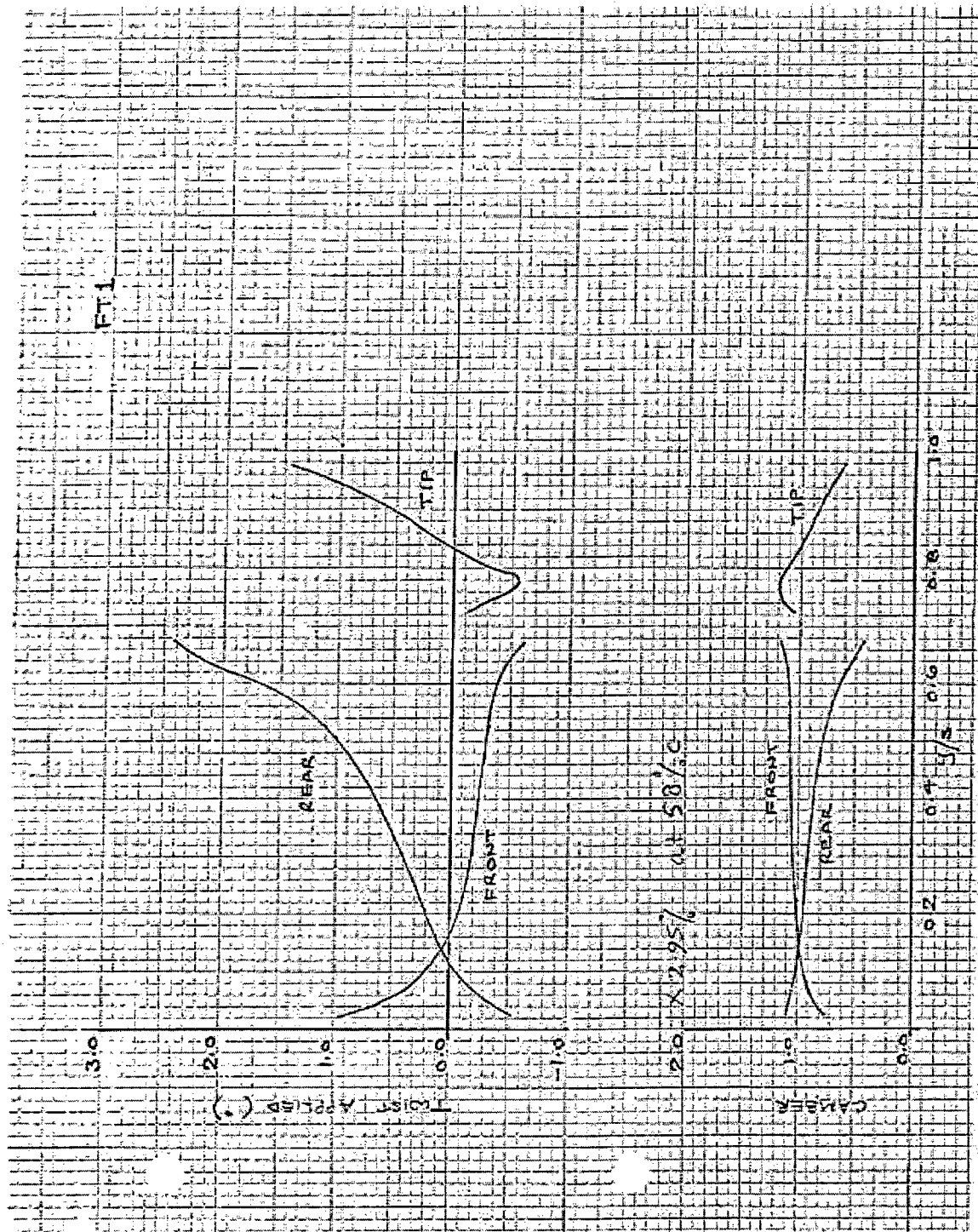
FIG. 5.2.1 CONFIG. FT1, DESIGNED CONFIGURATION, TWIST & CAMBER PARAMETERS ON ALL 3
COMPONENTS
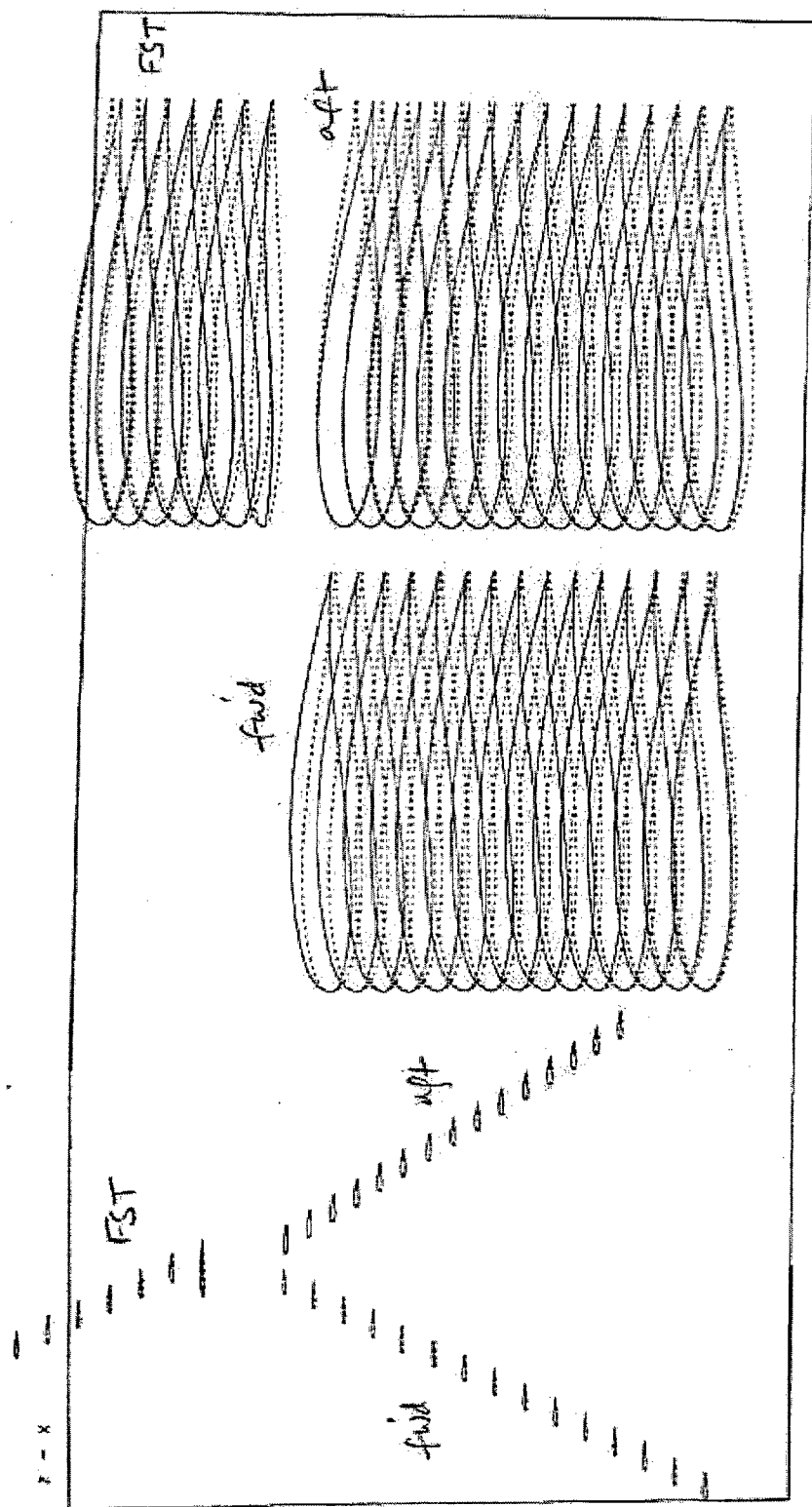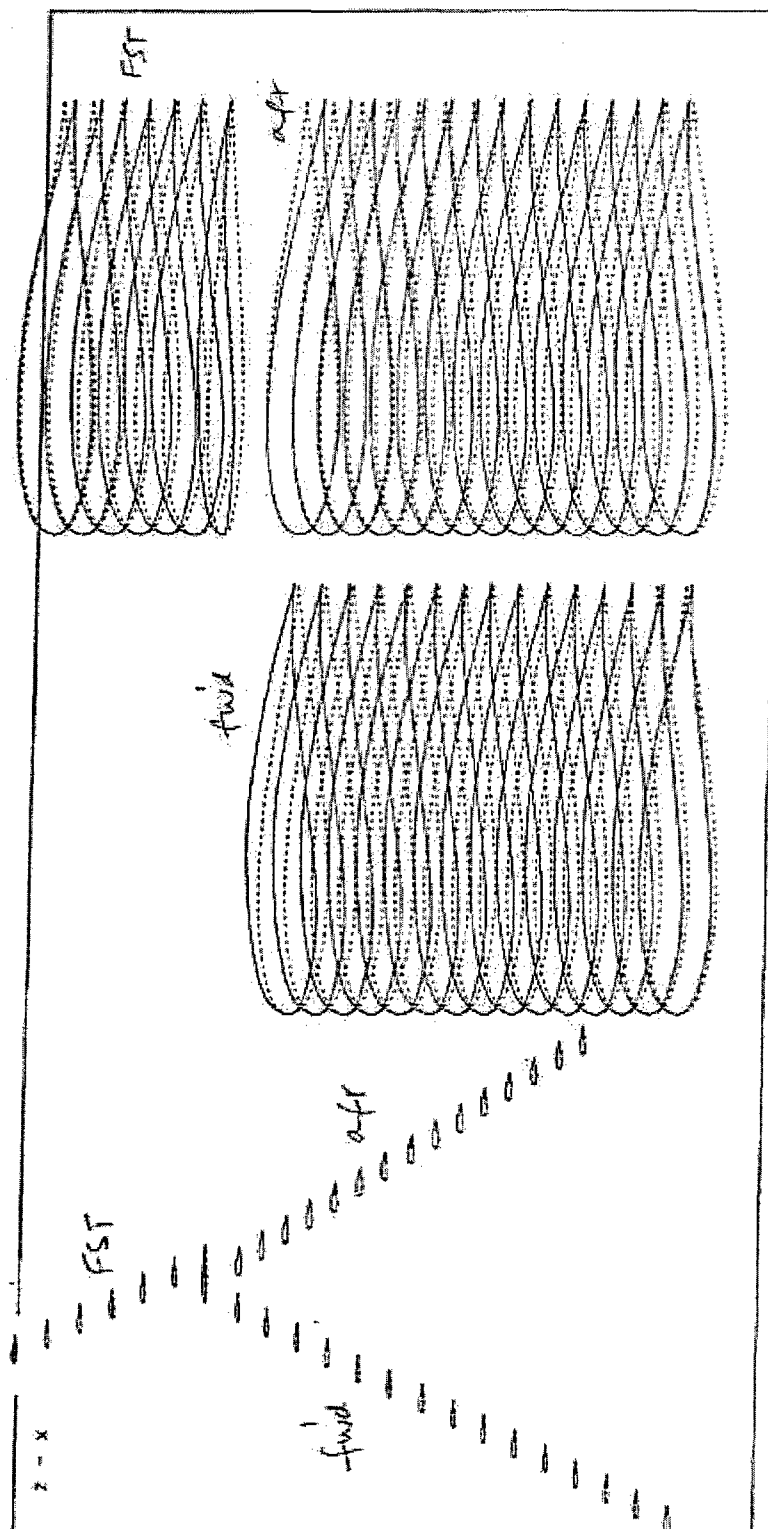
FIG. 5.2.2 CONFIG. FT1, DESIGNED CONFIGURATION, AEROFOIL SHAPES
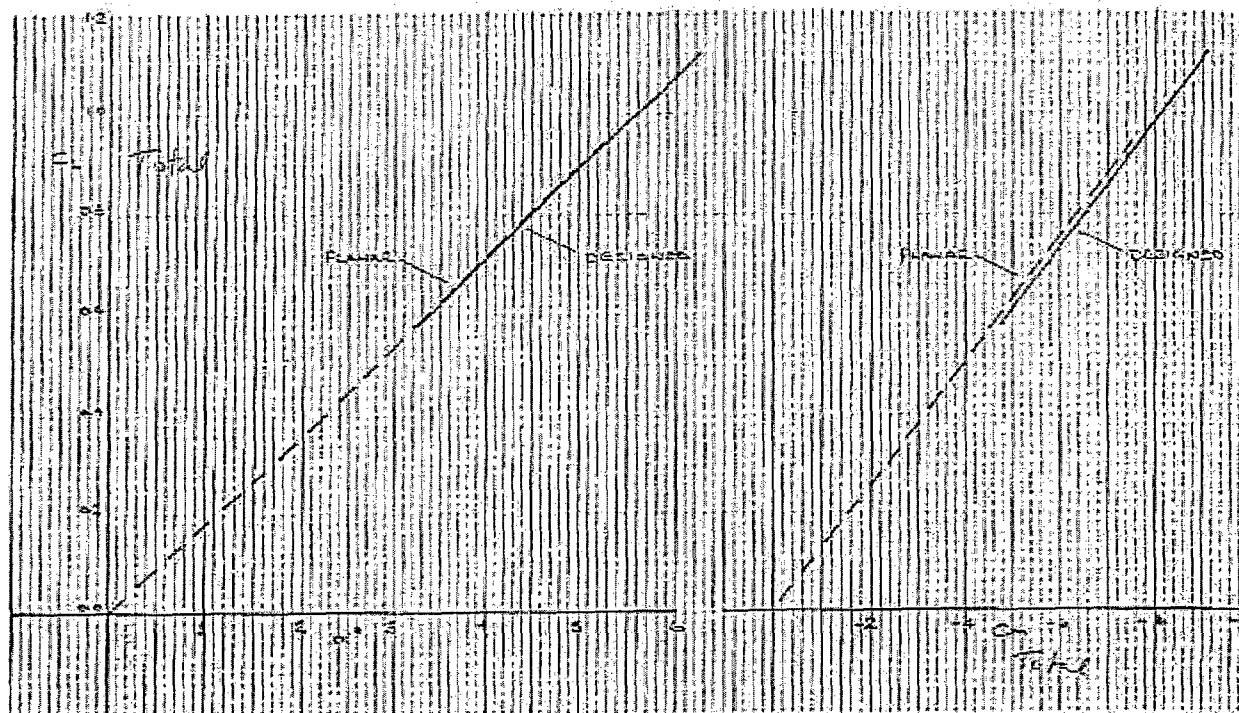
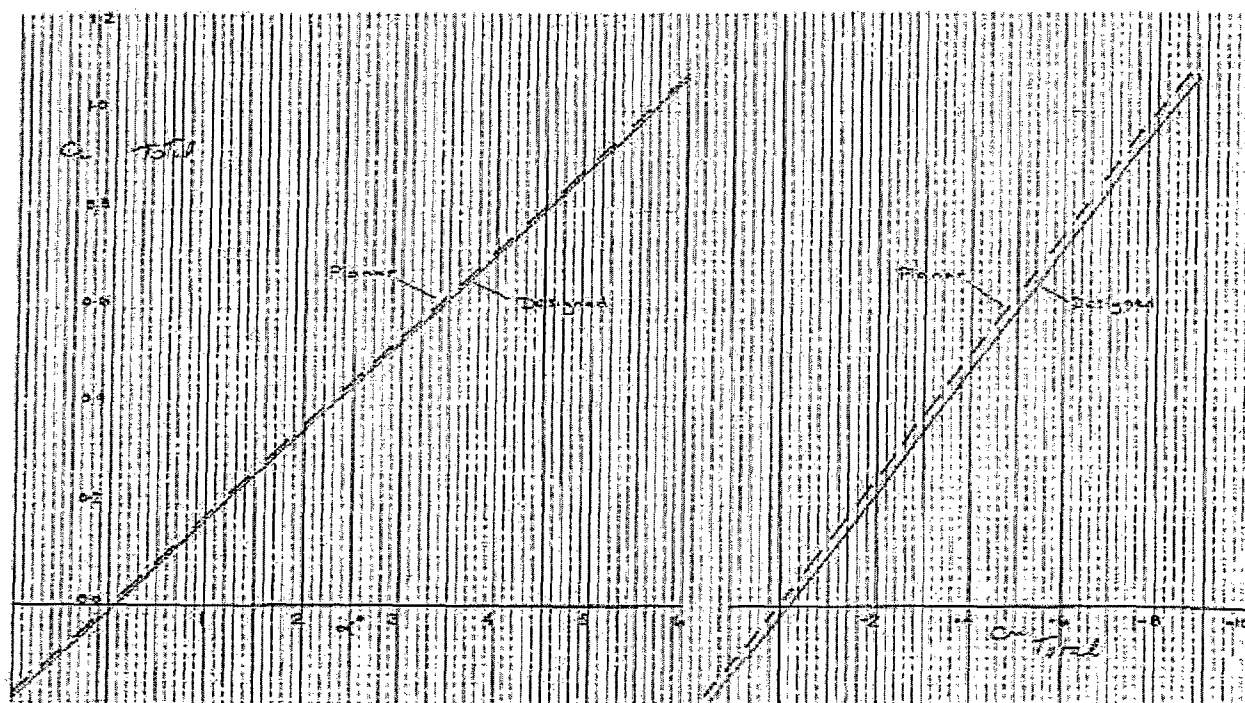FIG. 5.2.3 CONFIG. FT1, COMPARING CAMBERED & DESIGNED WINGS, C_L & C_m CHARACTERISTICS

$(\alpha, C_L) = (3.25°, 0.582)$ $(\alpha, C_L) = (4.25°, 0.781)$ $(\alpha, C_L) = (5.25°, 0.940)$
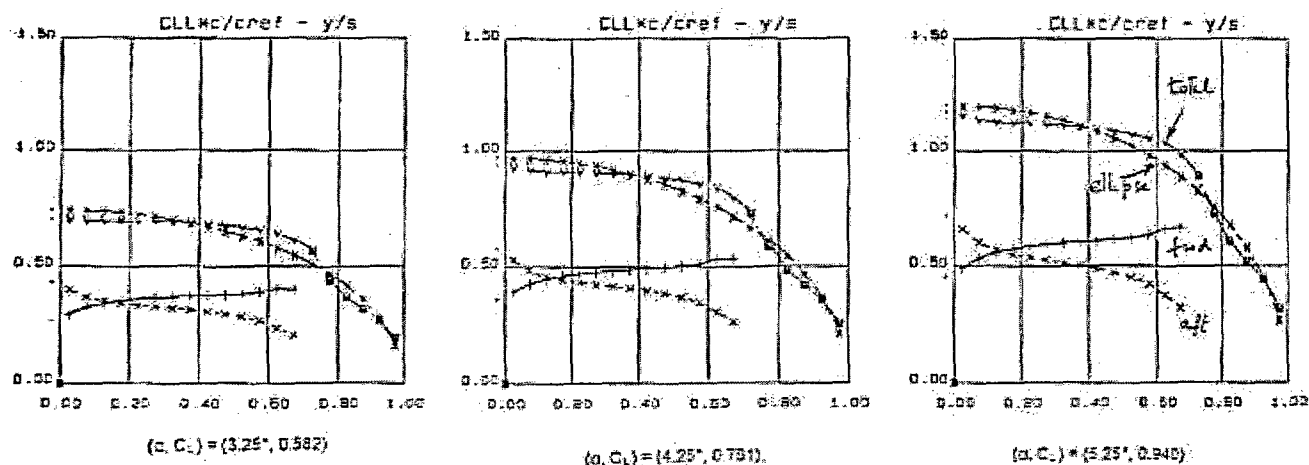
FIG. 5.2.4 CONFIG. FT1, DESIGNED WINGS, C_{LL} SPANWISE LOADING

$(\alpha, C_L) = (3.25°, 0.582)$, $(4.25°, 0.781)$, $(5.25°, 0.940)$

(a) $(\alpha, C_L) = (3.25°, 0.582)$
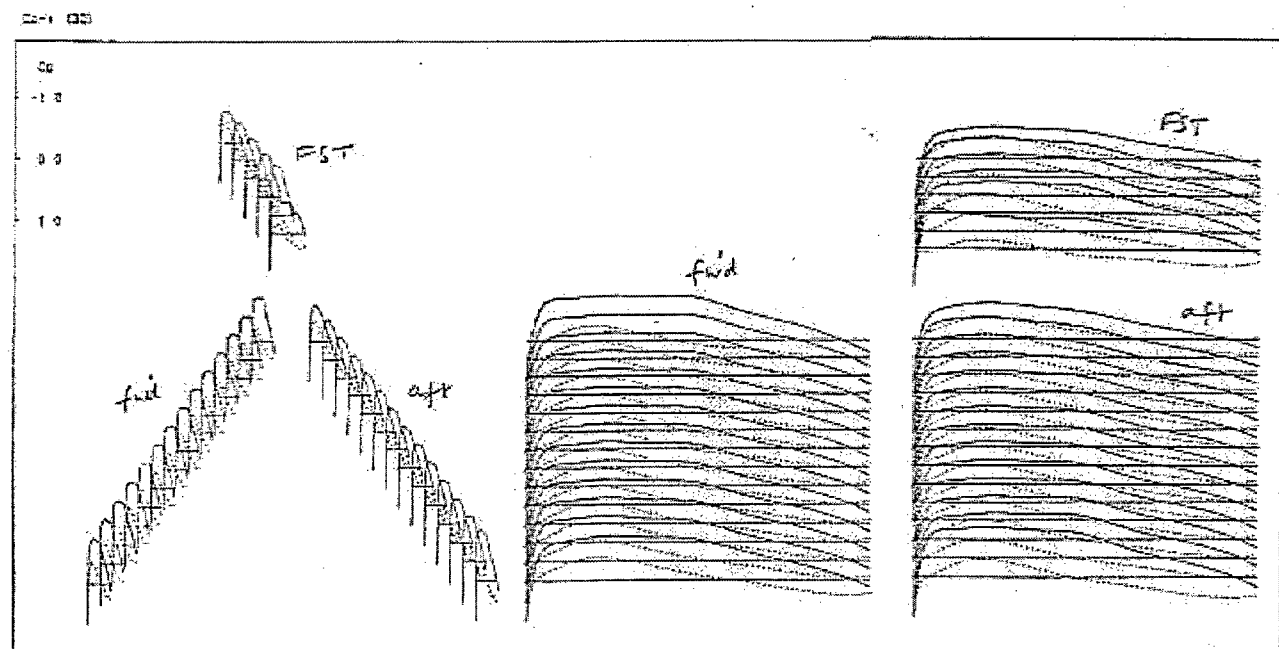
(b) $(\alpha, C_L) = (4.25°, 0.768)$

FIG. 5.2.5 CONFIG. FT1,   CAMBERED WINGS, C_p DISTRIBUTIONS

$(\alpha, C_L) =$.,   (3.25°, 0.582),   (4.25°, 0.761), (5.25°, 0.940)
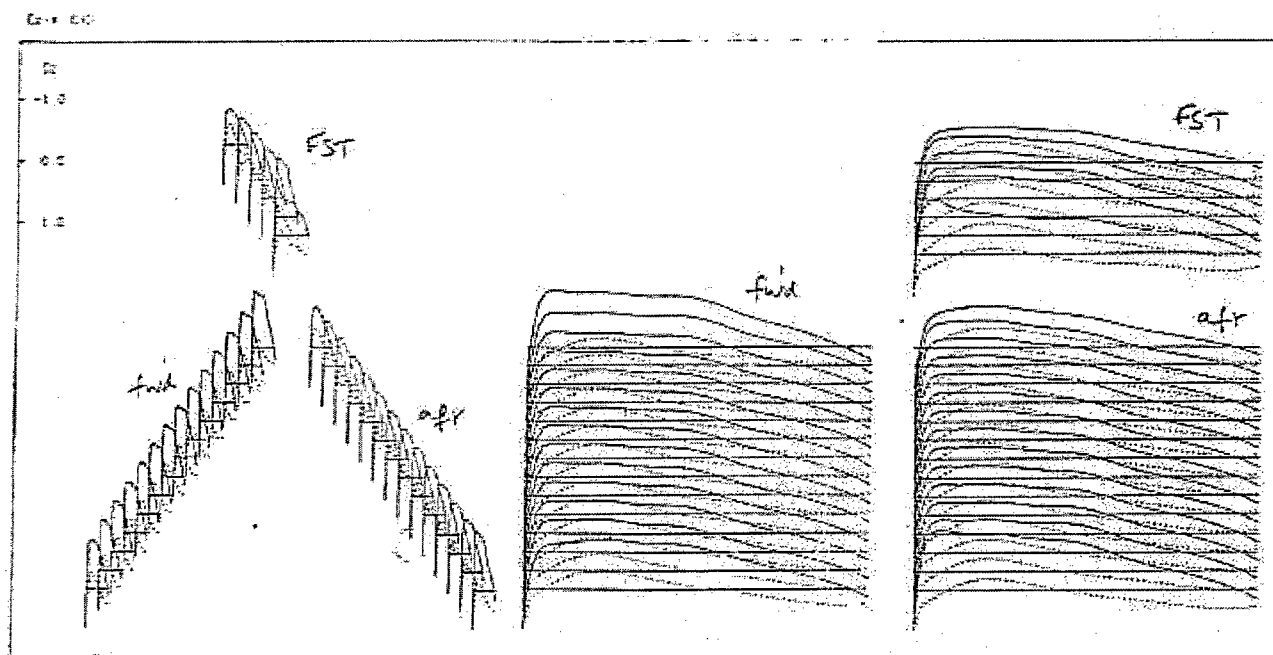
(c) $(\alpha, C_L) = (5.25°, 0.946)$

FIG. 5.2.5 (cont'd)
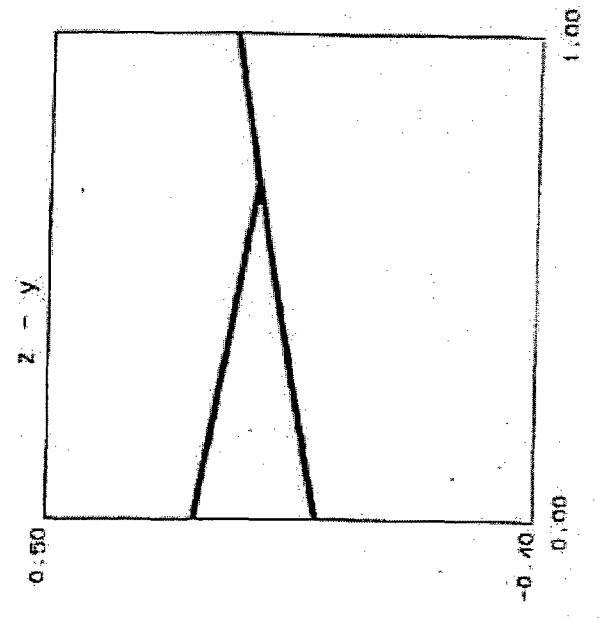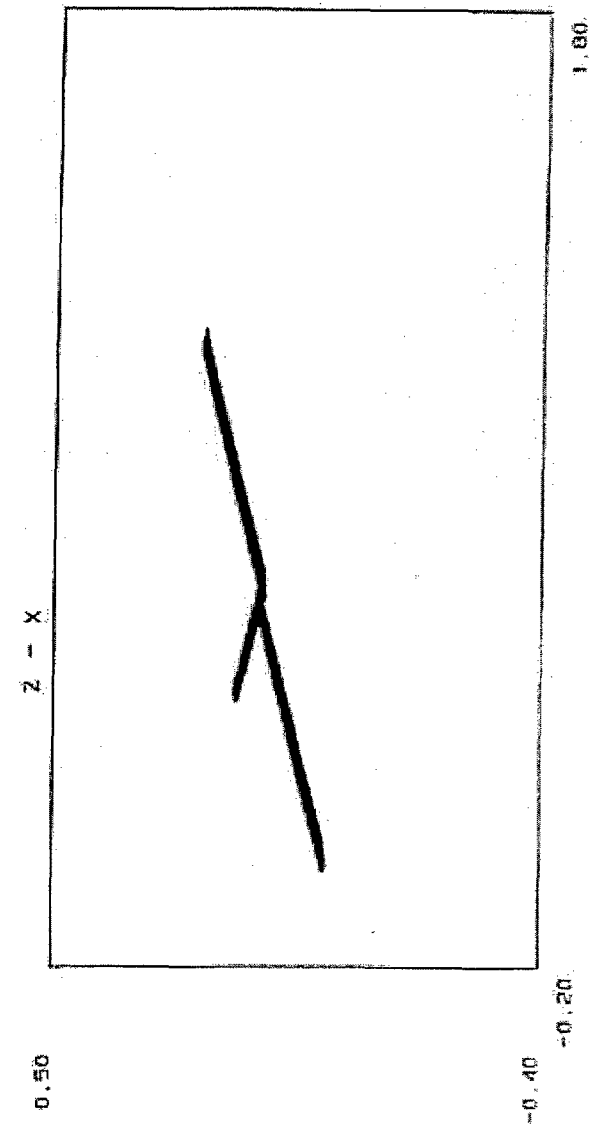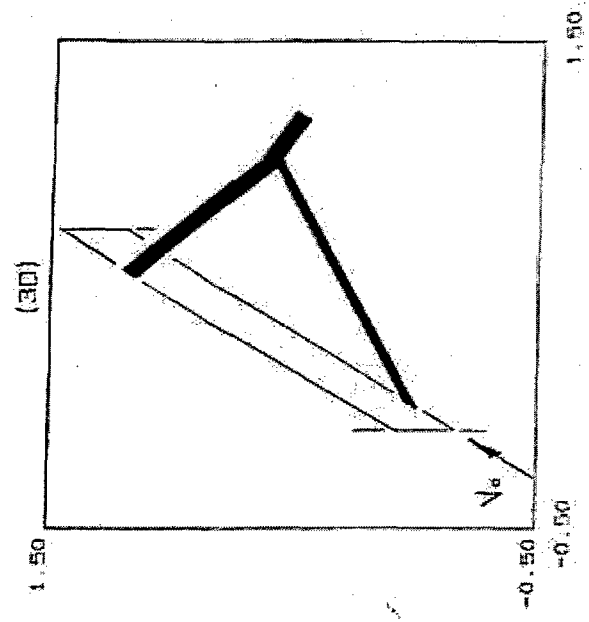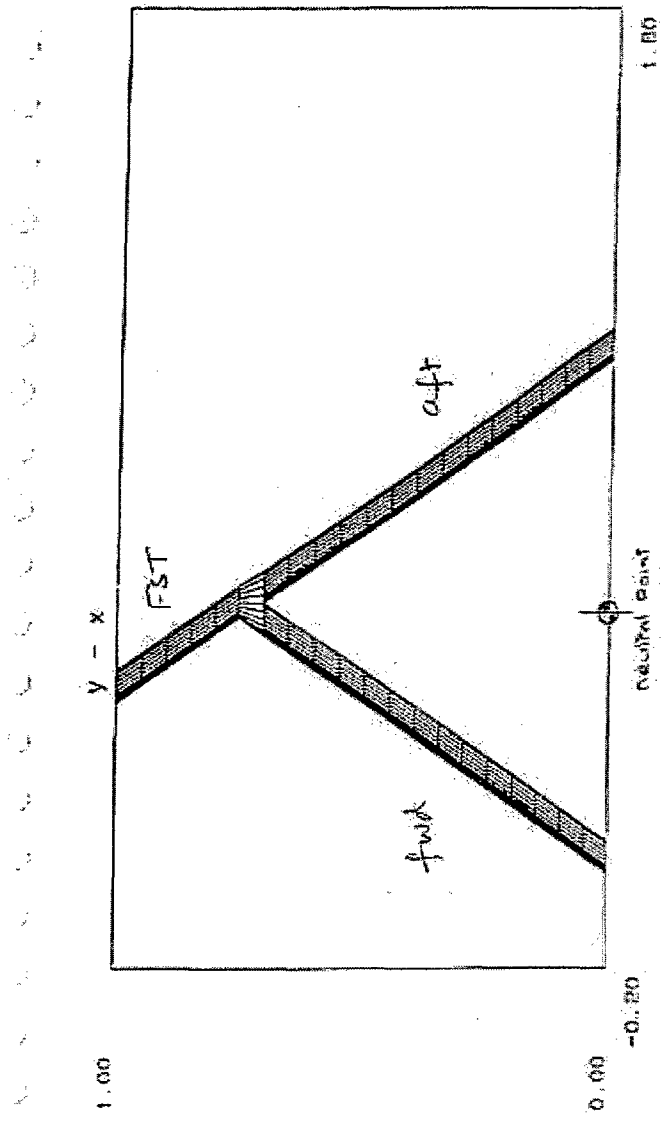
FIG. 5.3.1 CONFIG. FT1, GENERAL ARRANGEMENT (3 COMPONENTS), 17.2% l/c
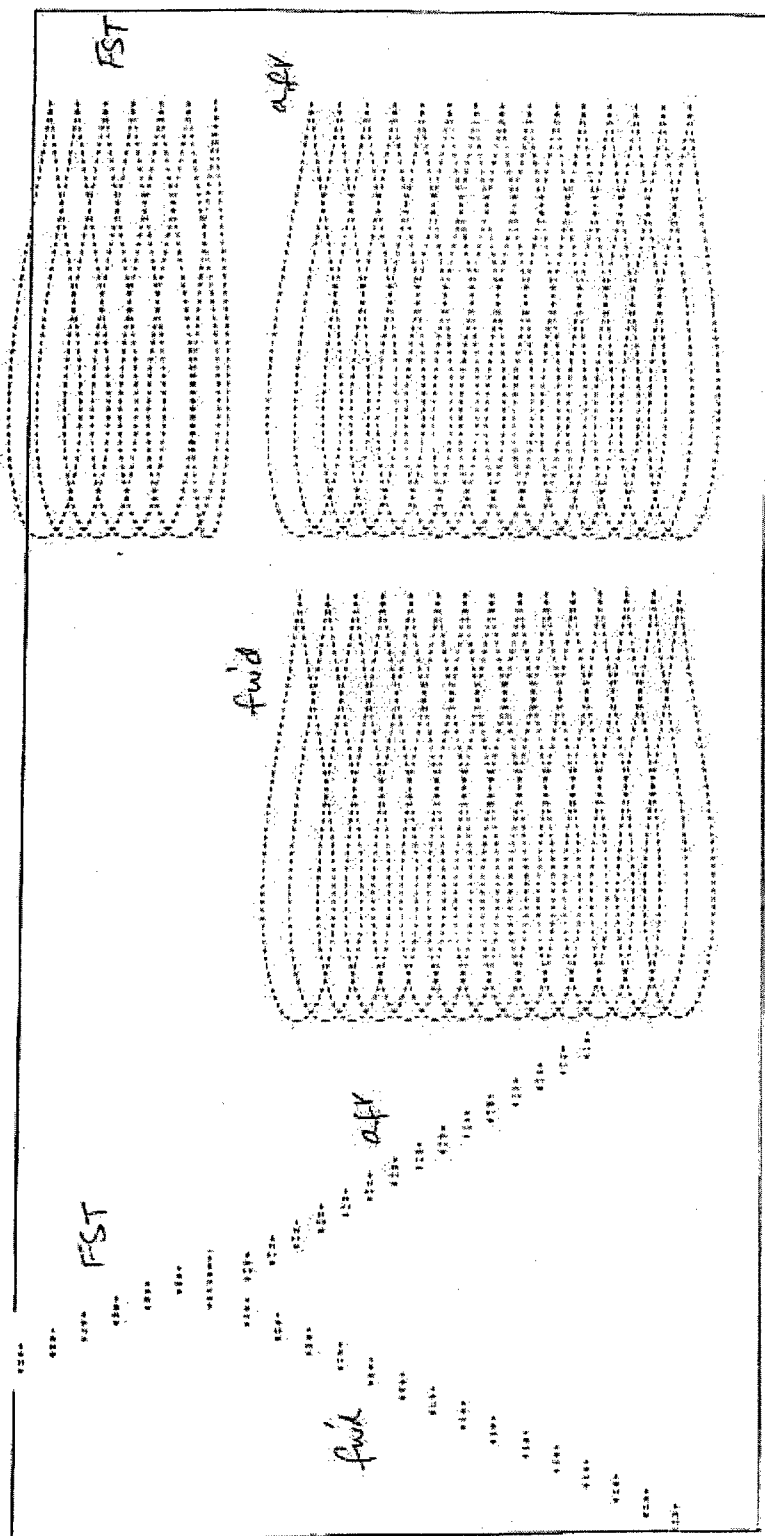
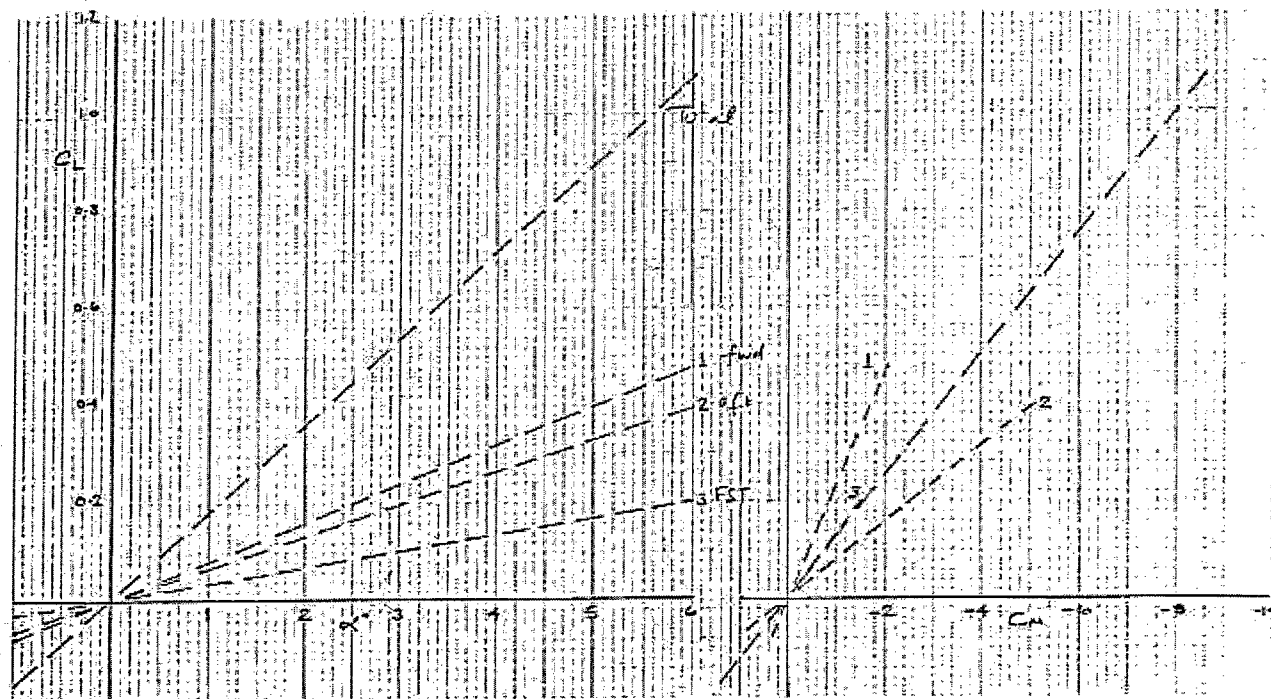FIG. 5.3.2. CONFIG. FT1, UNCAMBERED AEROFOIL SHAPES, 17.2% t/c
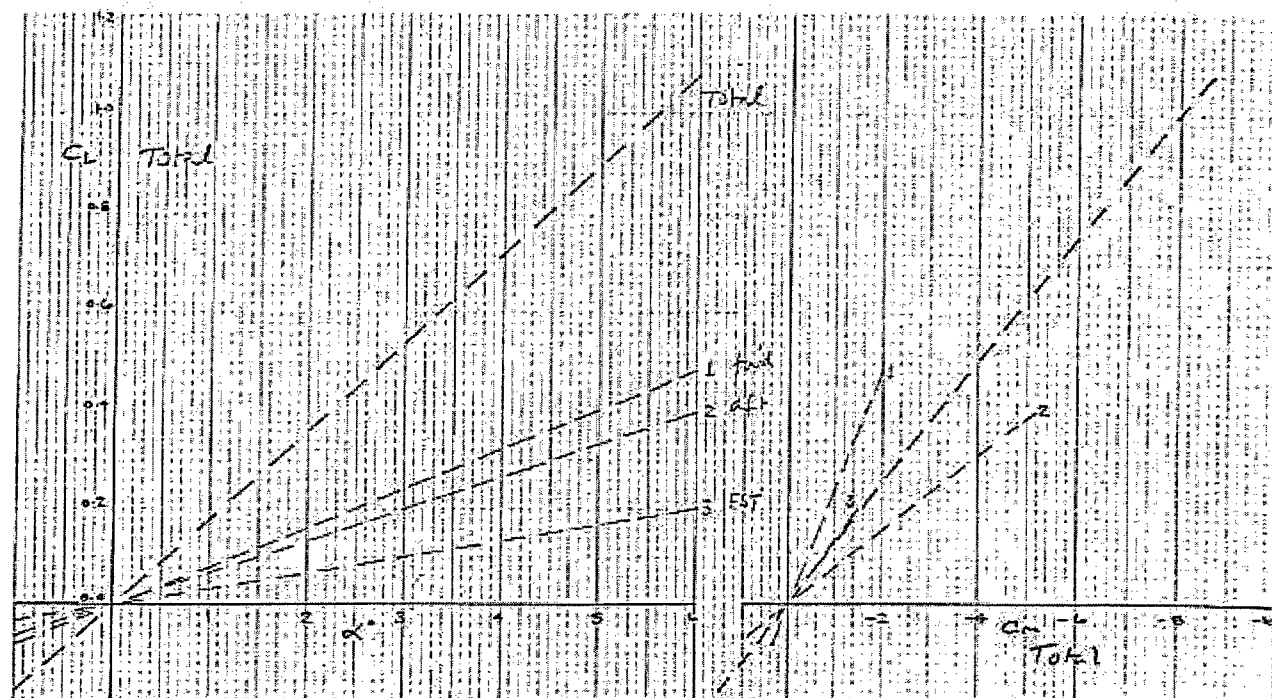
FIG. 5.3.3 CONFIG. FT1, UNCAMBERED WINGS, C_L & C_m CHARACTERISTICS & COMPONENT
BREAKDOWN, 17.2% t/c
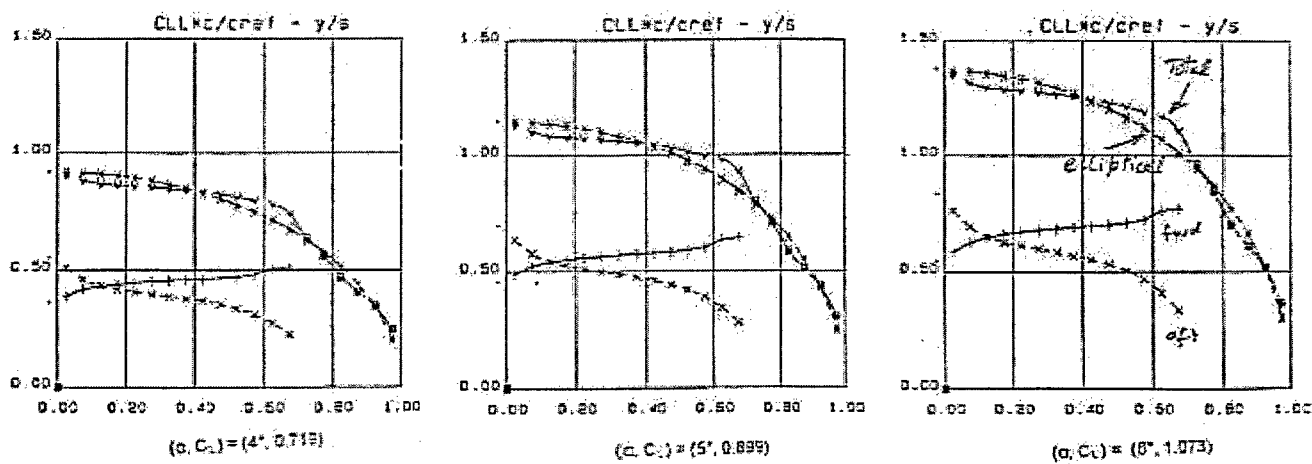
FIG. 5.3.4 CONFIG. FT1, UNCAMBERED WINGS, C_{LL} SPANWISE LOADING, 17.2% t/c

$(\alpha, C_L) = (4°, 0.719);\ (5°, 0.899),\ (6°, 1.073)$
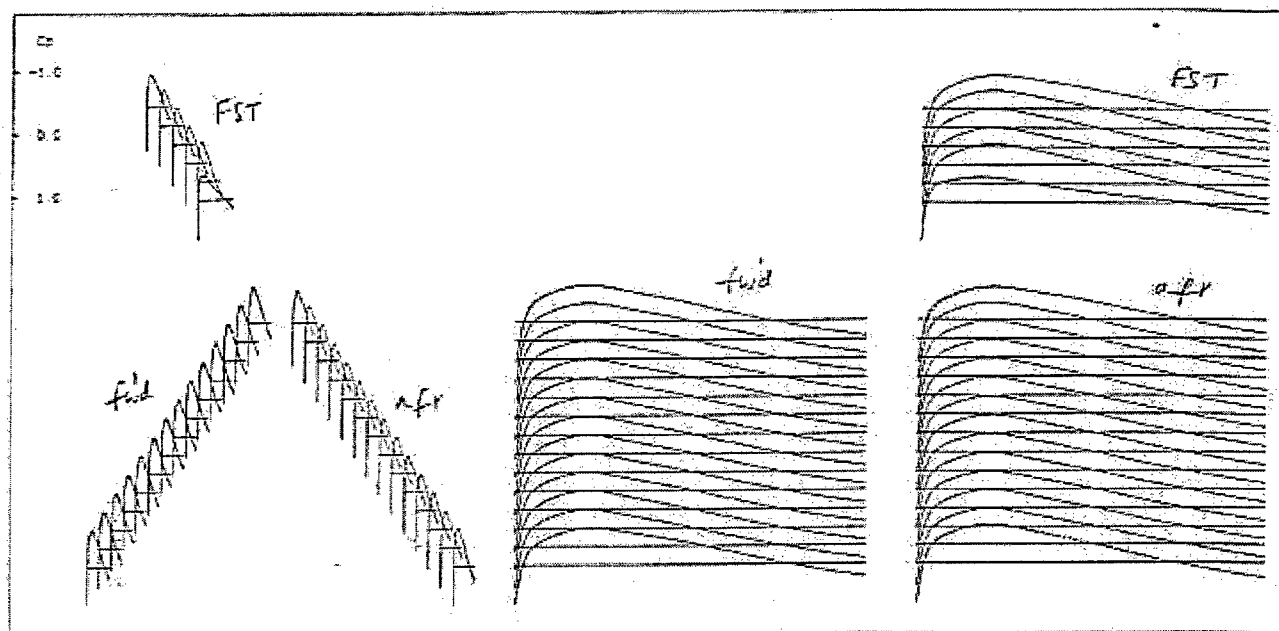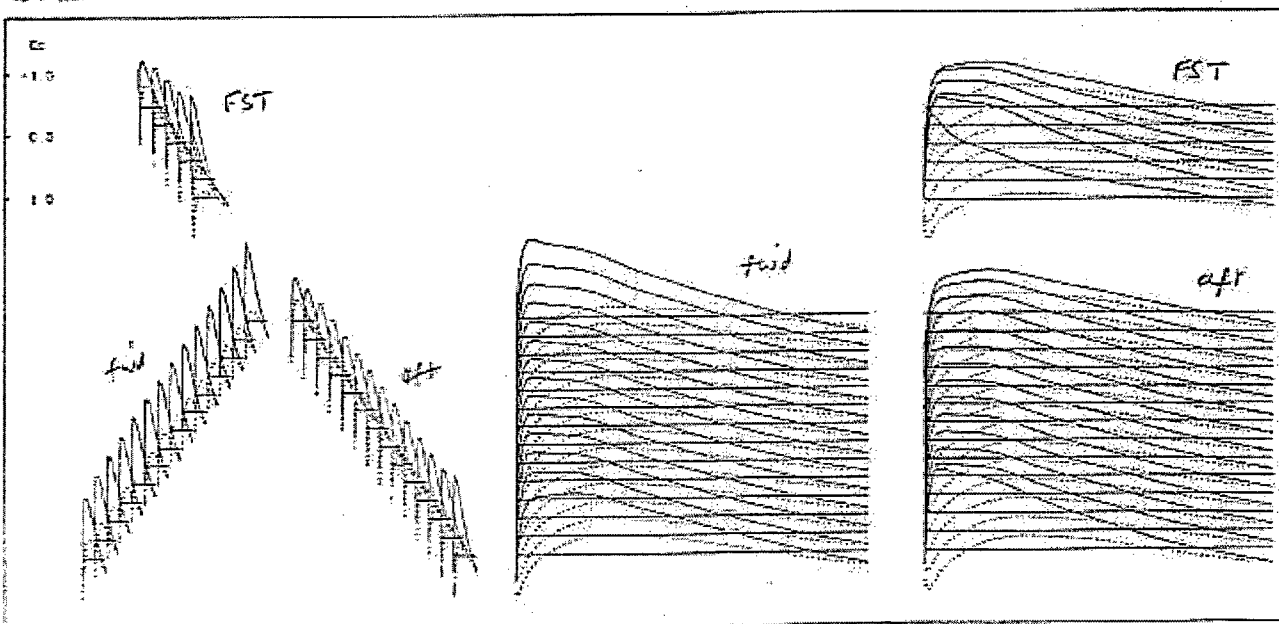
(a) $(\alpha, C_L) = (0.0°, 0.0)$

(b) $(\alpha, C_L) = (4°, 0.719)$

FIG. 5.3.5 CONFIG. FT1, UNCAMBERED WINGS, C_p DISTRIBUTIONS, 17.2% t/c

$(\alpha, C_L) = (0.0°, 0.0),\ \ (4°, 0.719),\ \ (5°, 0.899), (6°, 1.073)$

(c) $(\alpha, C_L) = (5°, 0.899)$
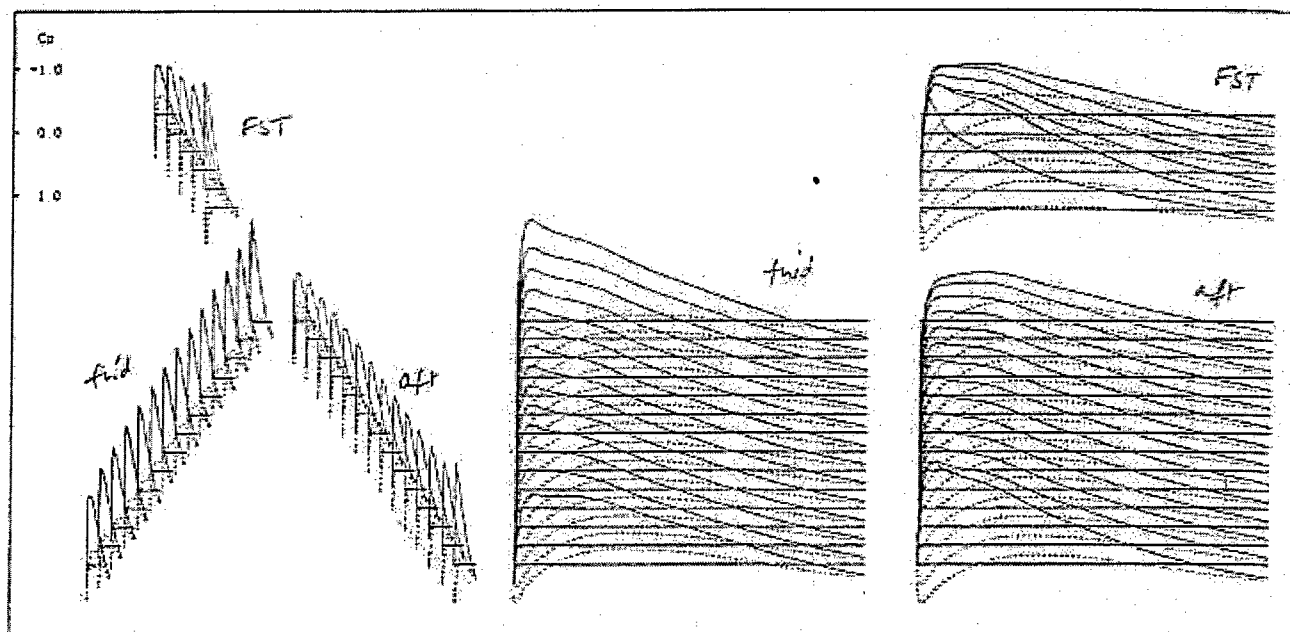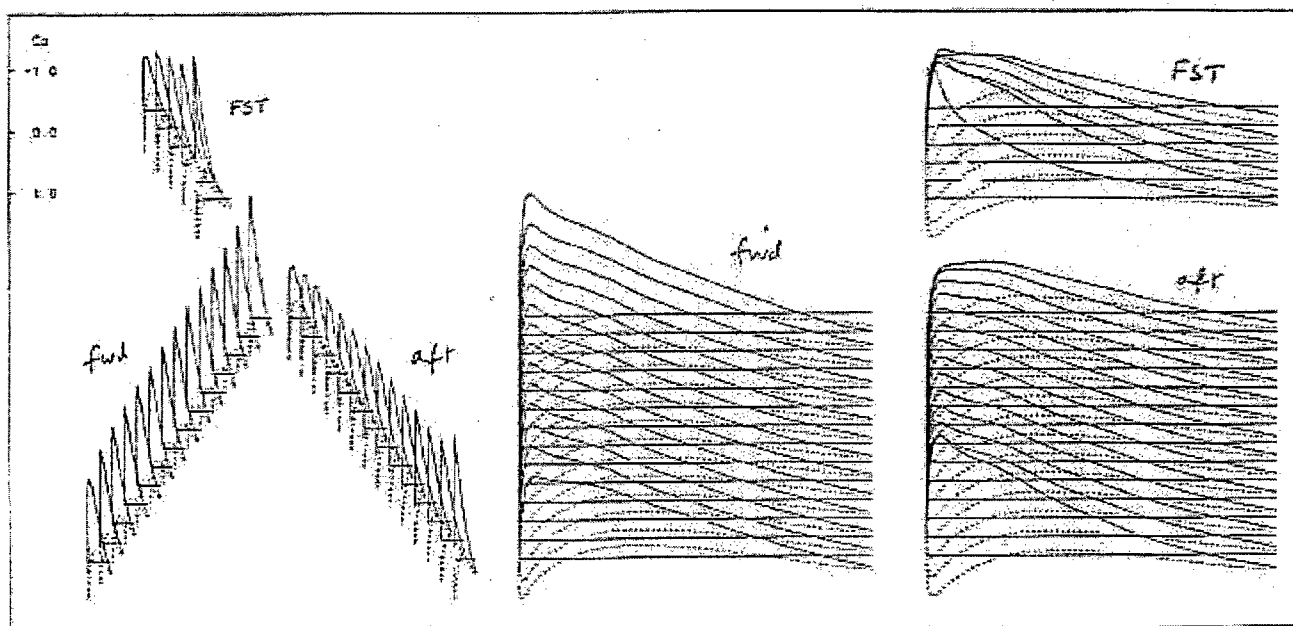
(d) $(\alpha, C_L) = (6°, 1.073)$

FIG. 5.3.5 (cont'd)

FIG. 5.4.1 CONFIG. FT1, DESIGNED CONFIGURATION, TWIST & CAMBER PARAMETERS ON ALL 3 COMPONENTS, 17.2% t/c

FIG. 5.4.2 CONFIG. FT1. DESIGNED CONFIGURATION, AEROFOIL SHAPES, 17.2% t/c

FIG. 5.4.3 CONFIG. FT1, COMPARING UNCAMBERED & DESIGNED WINGS, C_L & C_m
CHARACTERISTICS, 17.2% t/c

$(\alpha, C_L) = (4°, 0.711)$ $(\alpha, C_L) = (5°, 0.891)$ $(\alpha, C_L) = (6°, 1.071)$
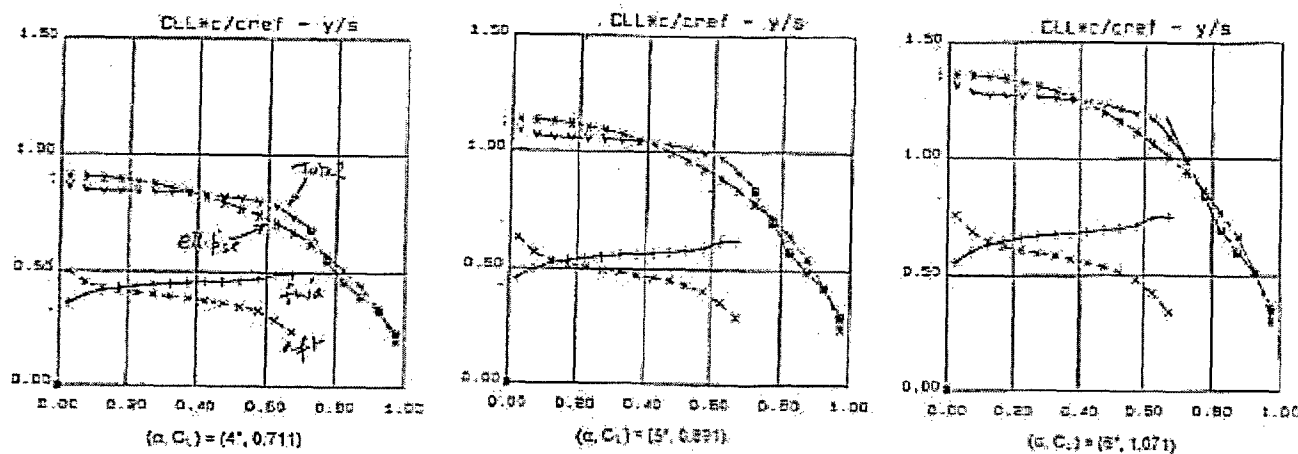
FIG. 5.4.4 CONFIG. FT1, DESIGNED WINGS, C_{LL} SPANWISE LOADING

$(\alpha, C_L) = (4°, 0.711)$, $(5°, 0.891)$, $(6°, 1.071)$
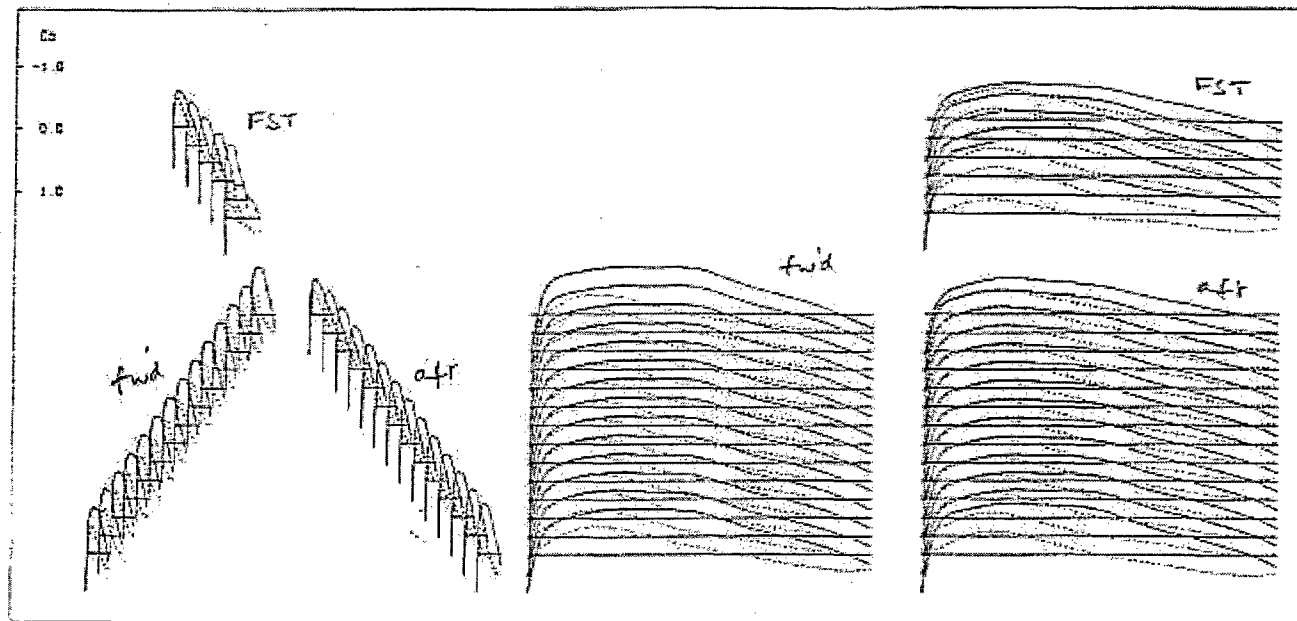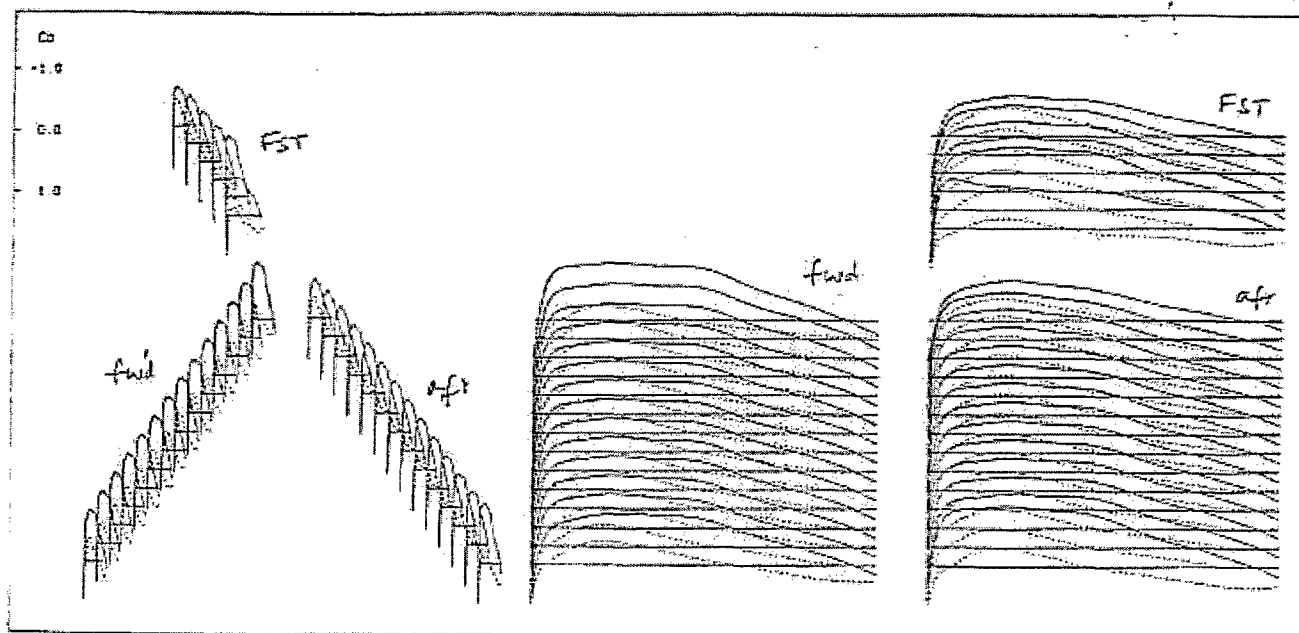
(a) $(\alpha, C_L) = (4°, 0.711)$

(b) $(\alpha, C_L) = (5°, 0.891)$

FIG. 5.4.5 CONFIG. FT1, CAMBERED WINGS, C_p DISTRIBUTIONS

$(\alpha, C_L) = (4°, 0.711), (5°, 0.891), (6°, 1.071)$

(c) $(\alpha, C_L) = (6^\circ, 1.07])$

FIG. 5.4.5 (cont'd)

(3D)

V_e

1.50

-0.50

1.50

-0.50

z – y

0.50

-0.40

1.00

0.00

FST

y – x

aft

fwd

neutral point

1.00

0.00

-0.20

1.80

z – x

0.50

-0.40

-0.20

1.80
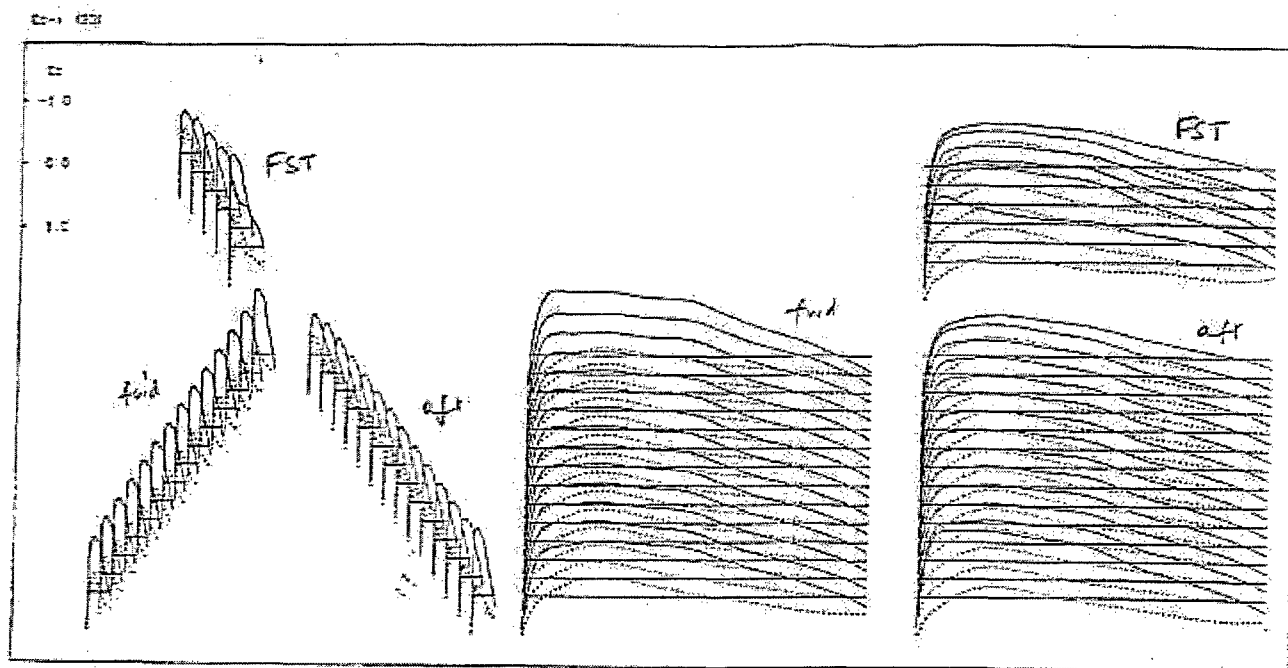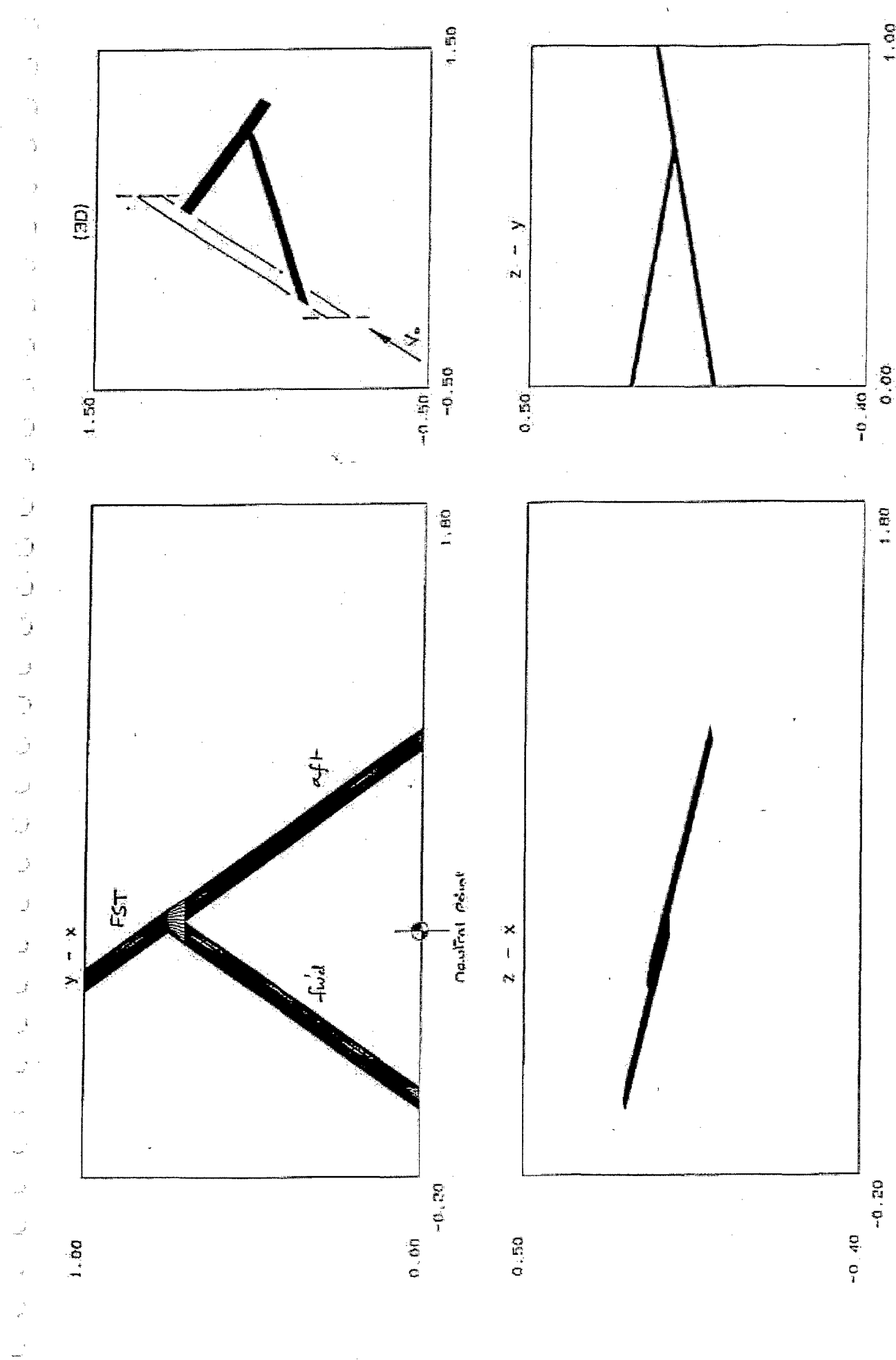
FIG. 6.1.1 CONFIG. FT2. GENERAL ARRANGEMENT (3 COMPONENTS)

FIG. 6.1.2 CONFIG. FT2. UNCAMBERED AEROFOIL SHAPES

FIG. 6.1.3 CONFIG. FT2, UNCAMBERED WINGS, C_L & C_m CHARACTERISTICS & COMPONENT BREAKDOWN
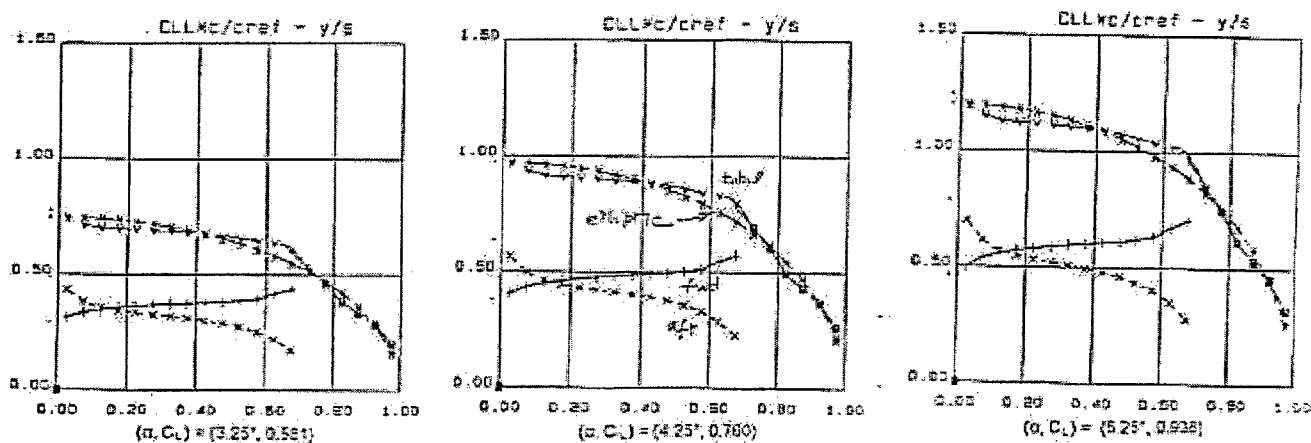
FIG. 6.1.4 CONFIG. FT2, UNCAMBERED WINGS, C_{LL} SPANWISE LOADING

$(\alpha, C_L) = (3.25°, 0.585)$, $(4.25°, 0.764)$, $(5.25°, 0.942)$
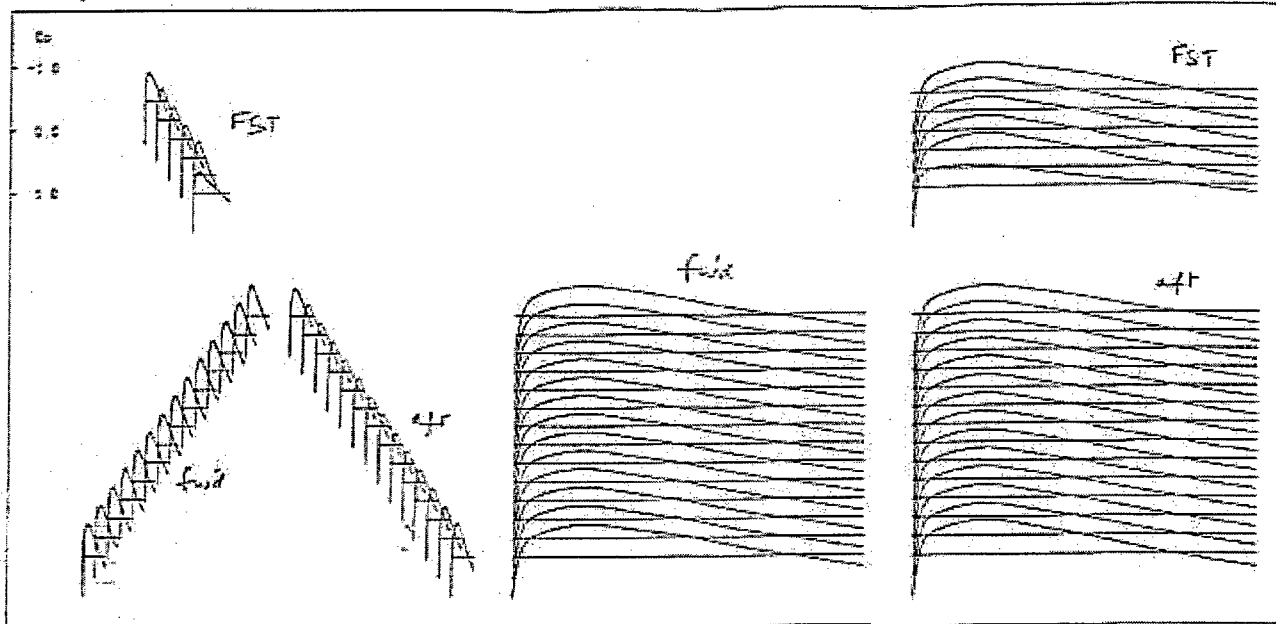
(a) $(\alpha, C_L) = (0.0°, 0.0)$
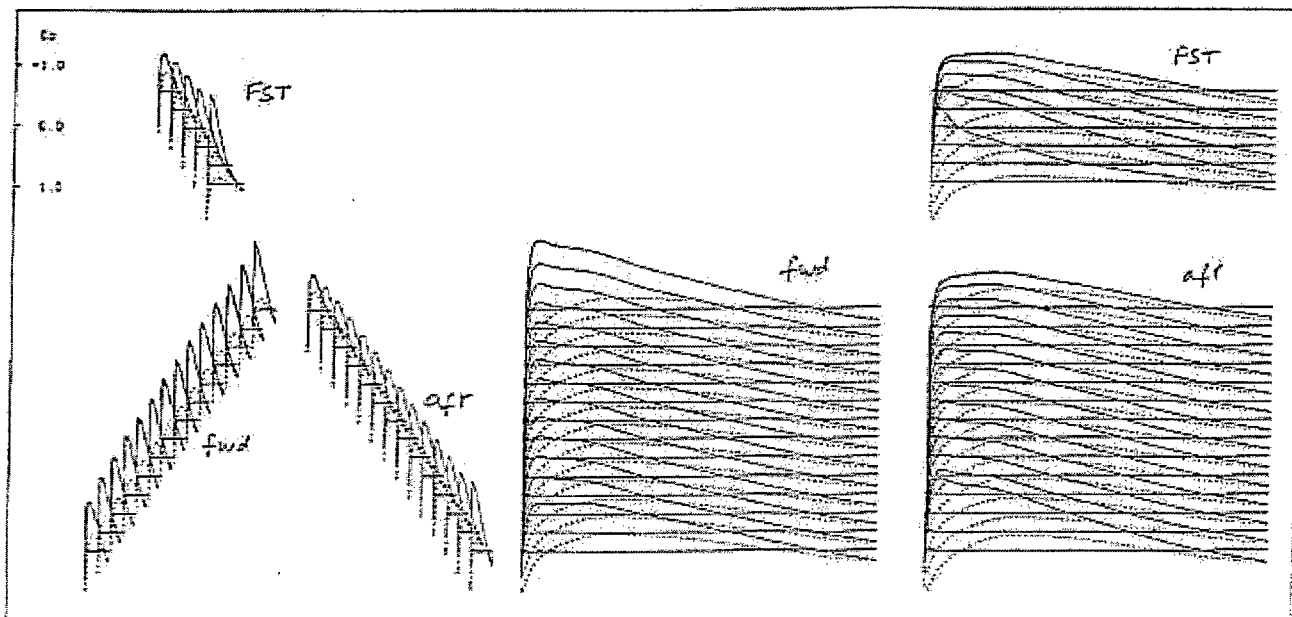
(b) $(\alpha, C_L) = (3.25°, 0.585)$

FIG. 6.1.5 CONFIG. FT2, UNCAMBERED WINGS, C_p DISTRIBUTIONS

$(\alpha, C_L) = (3.25°, 0.585),\ (4.25°, 0.764),\ (5.25°, 0.942)$

(c) $(\alpha, C_L) = (4.25°, 0.764)$
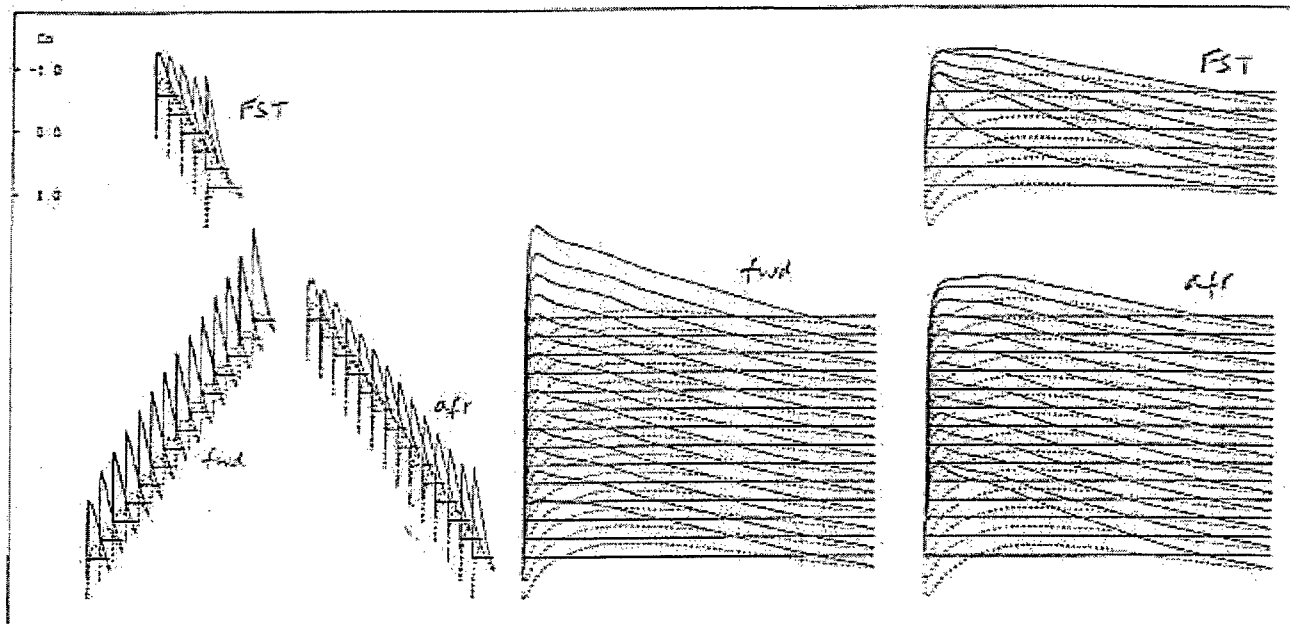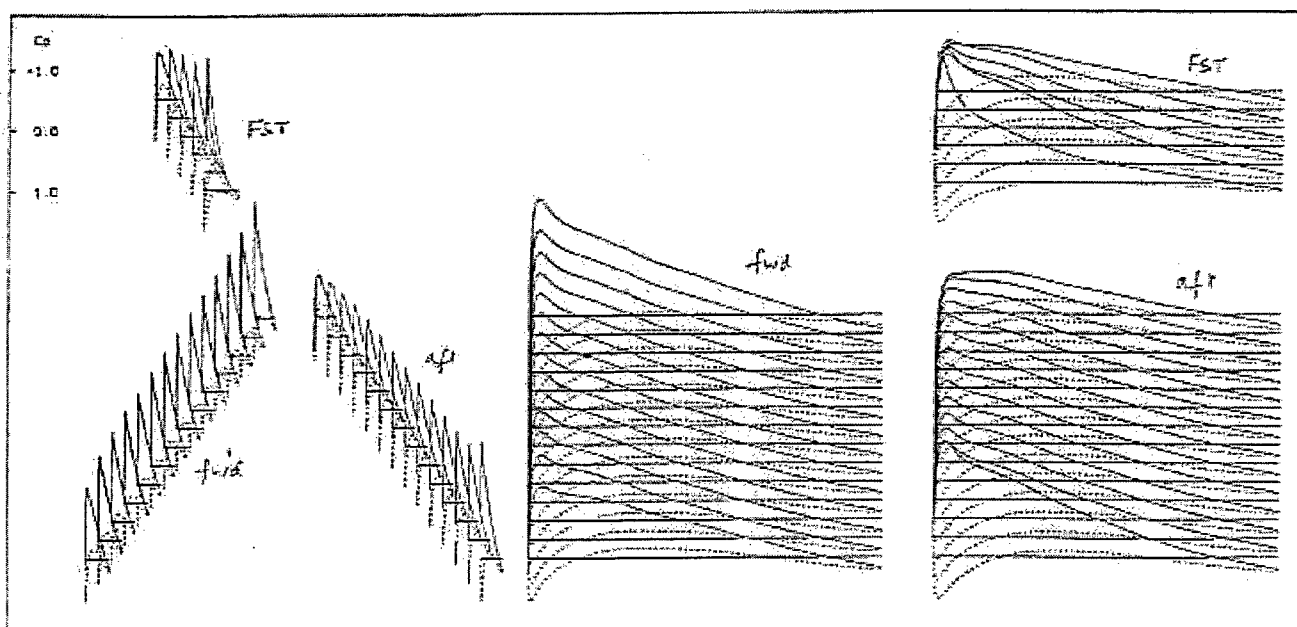
(d) $(\alpha, C_L) = (5.25°, 0.942)$

FIG. 6.1.5 (cont'd)
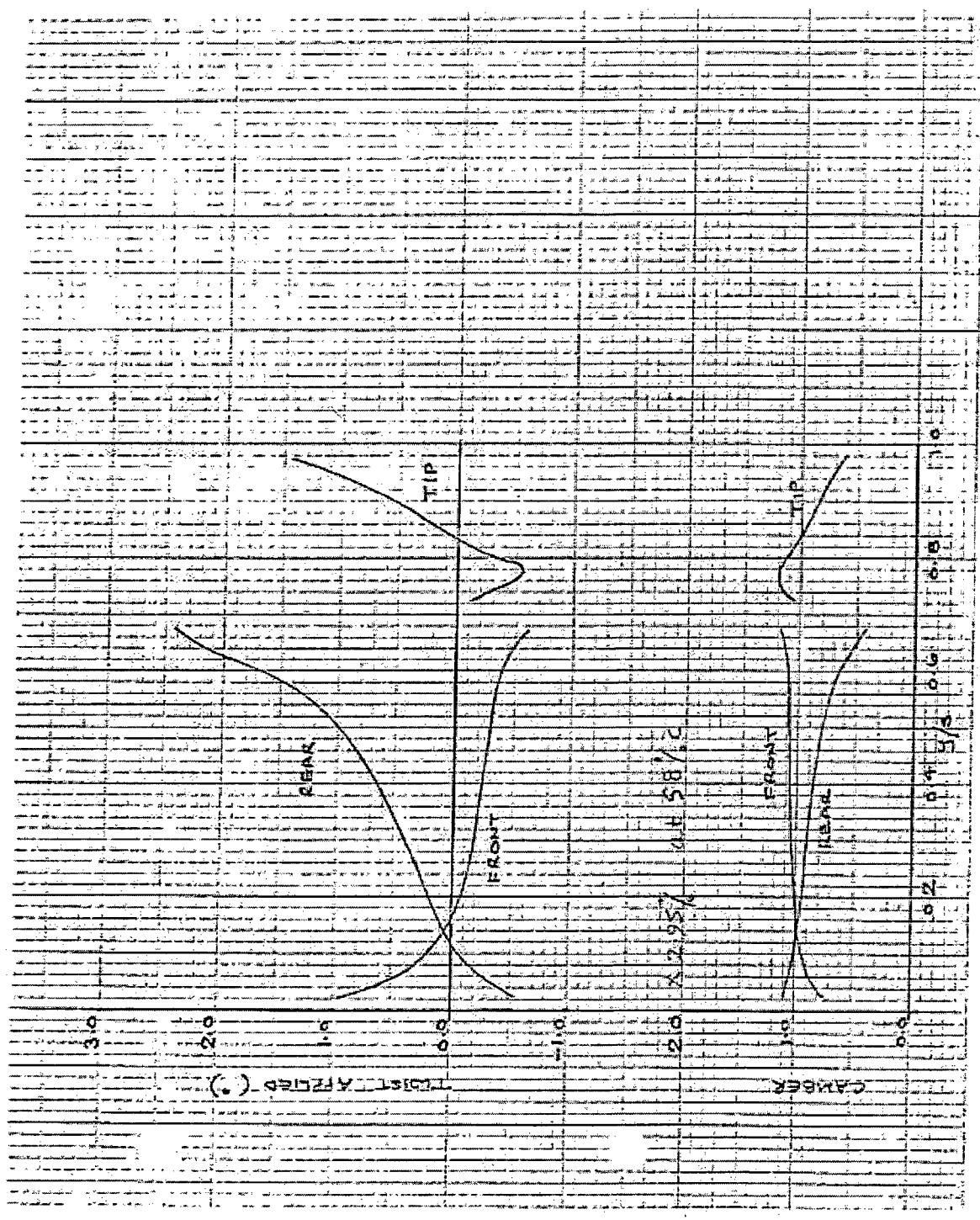
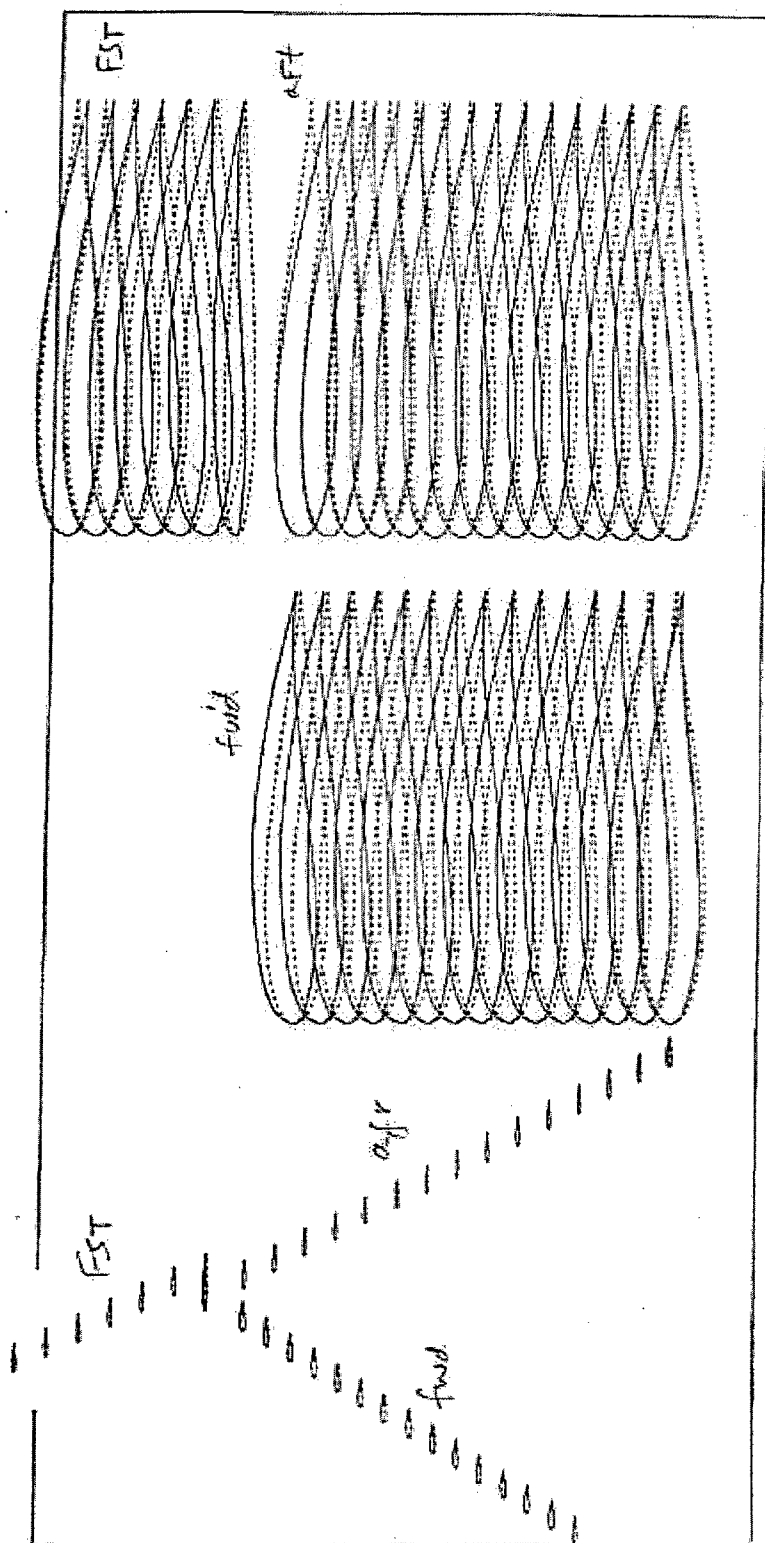FIG. 6.2.1 CONFIG. FT2, DESIGNED CONFIGURATION, TWIST & CAMBER PARAMETERS ON ALL 3 COMPONENTS

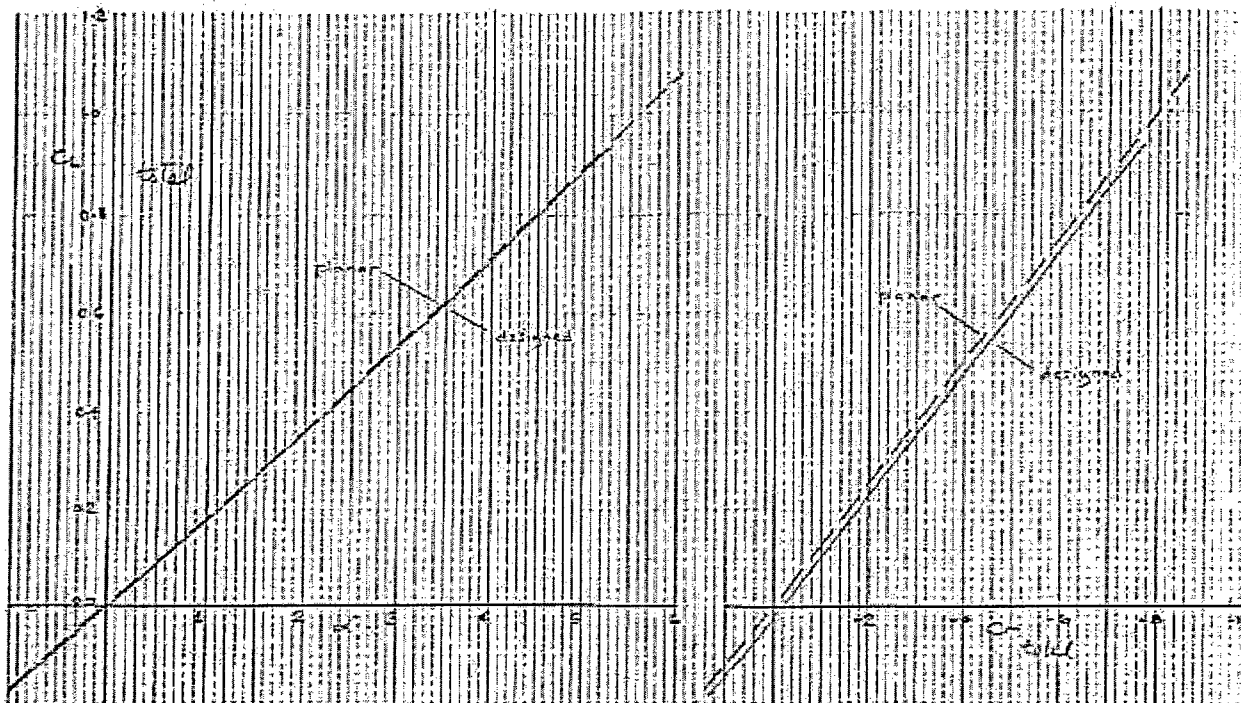FIG. 6.2.2 CONFIG. FT2, DESIGNED CONFIGURATION, AEROFOIL SHAPES

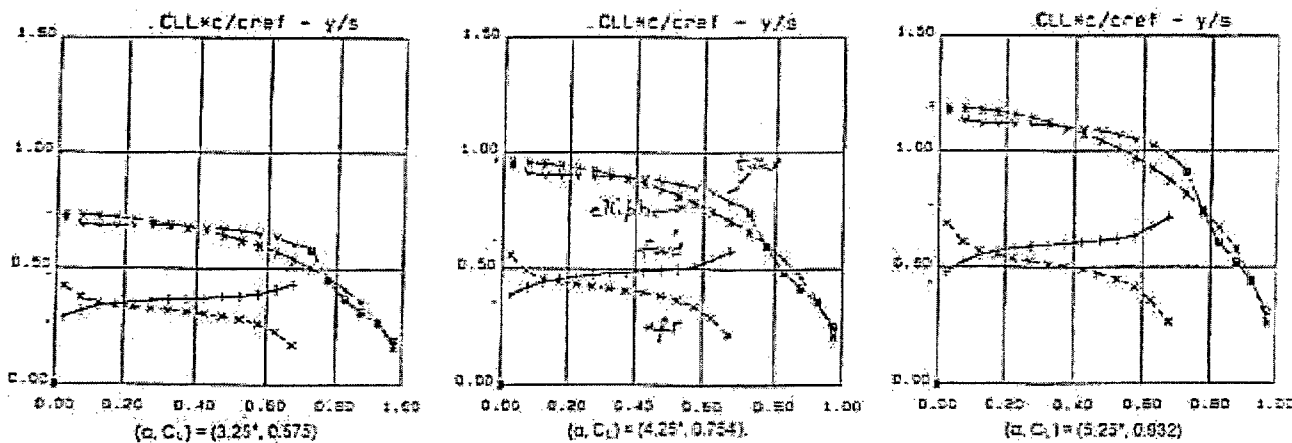FIG. 6.2.3 CONFIG. FT2. COMPARING UNCAMBERED & DESIGNED WINGS, C_L & C_m
CHARACTERISTICS

FIG. 6.2.4 CONFIG. FT2. DESIGNED WINGS, C_{LL} SPANWISE LOADING
$(\alpha, C_L) = (3.25°, 0.575),\quad (4.25°, 0.754),\quad (5.25°, 0.932)$

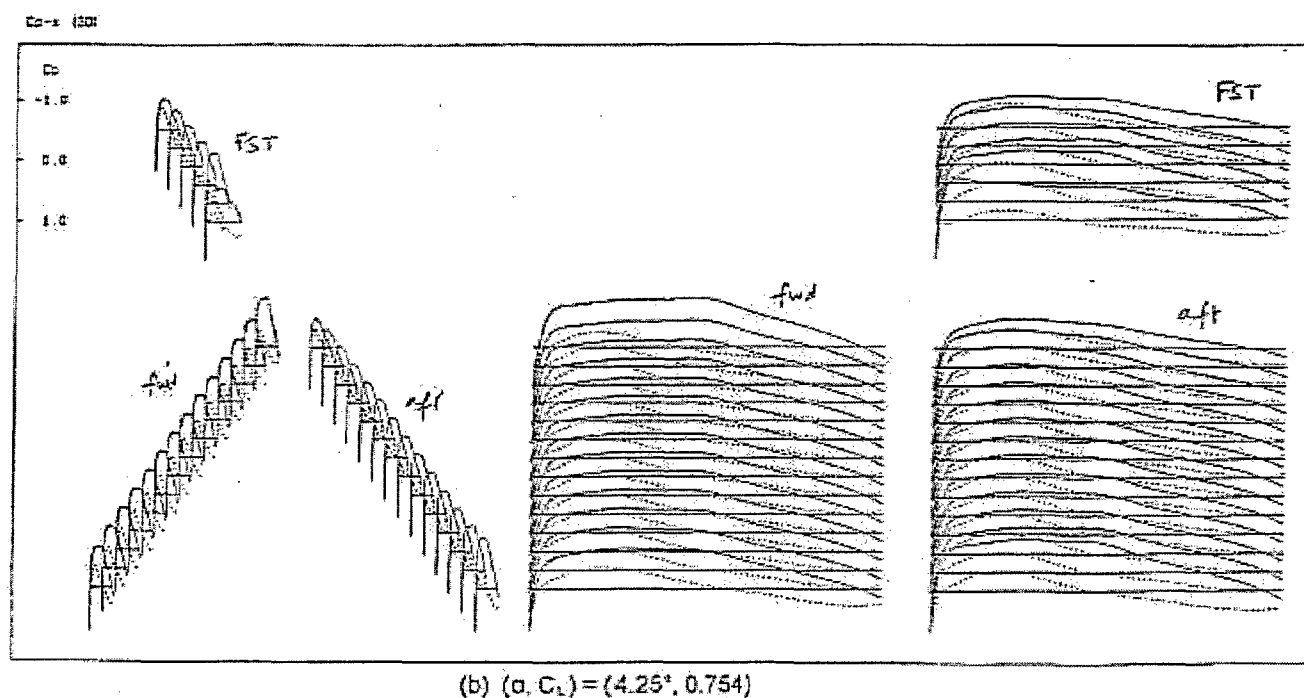(a) $(\alpha, C_L) = (3.25°, 0.575)$

(b) $(\alpha, C_L) = (4.25°, 0.754)$
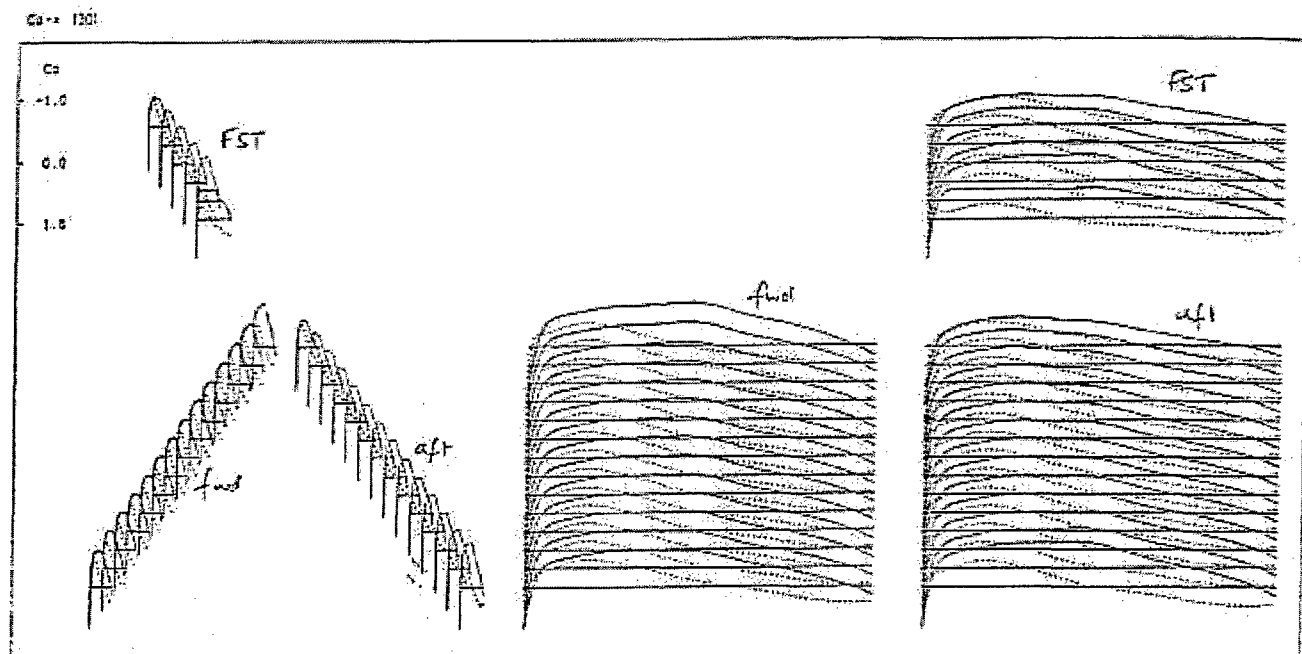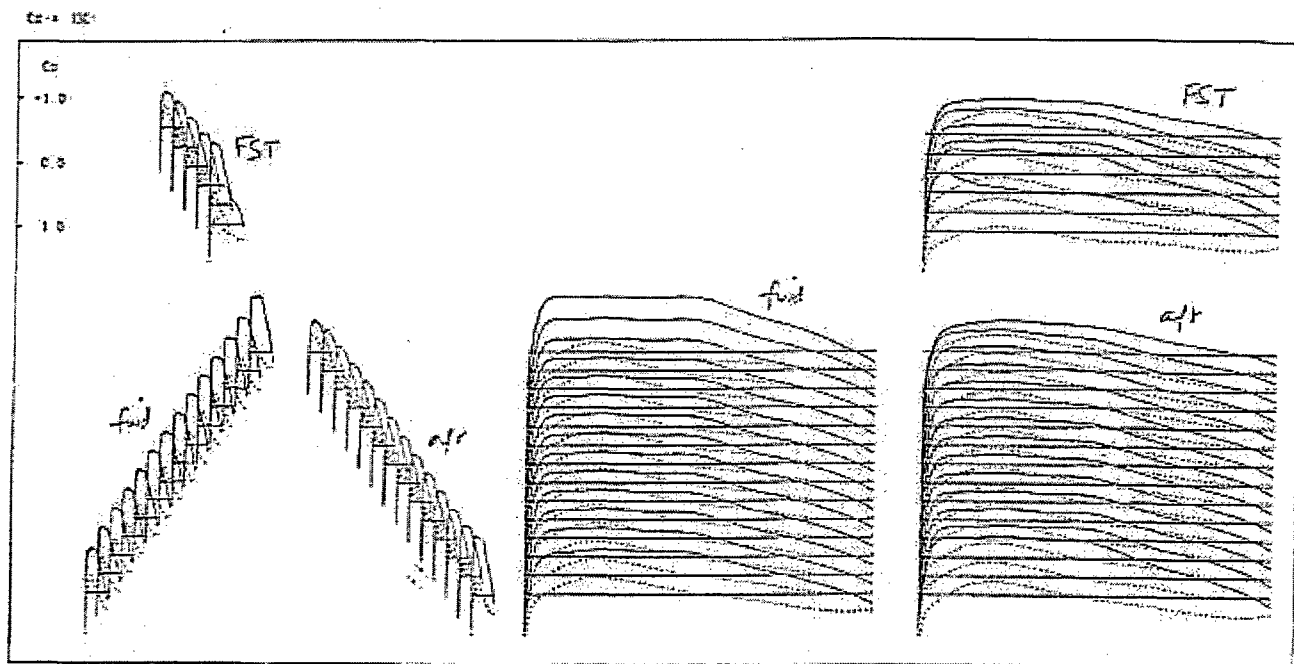
FIG. 6.2.5 CONFIG. FT2, CAMBERED WINGS, C_p DISTRIBUTIONS

$(\alpha, C_L) = (3.25°, 0.575), \quad (4.25°, 0.754), (5.25°, 0.932)$

(c) $(\alpha, C_L) = (5.25°, 0.932)$

FIG. 6.2.5 (cont'd)